University of CINCINNATI

# Climate Change Risk Assessment of the Upper Arun Hydroelectric Project in Nepal

Title: CLIMATE CHANGE RISK ASSESSMENT (CCRA) OF THE UPPER ARUN HYDROPOWER PROJECT IN NEPAL

Client: The World Bank

Contract No: 7193549

Pages: 104

Version: 1.0

Date: February 15, 2021

Author: Asphota Wasti & Patrick A. Ray, College of Engineering and Applied Science, University of Cincinnati

# Contents

# List of Figures

# List of Tables

# Abbreviation

| | |
|---|---|
| CMIP5 | Coupled Model Intercomparison Project 5 (CMIP5) |
| CORDEX | Coordinated Regional Downscaling Experiment |
| CRA | Climate Risk Analysis |
| CSPDR | Changjiang Institute of Survey, Planning, Design and Research |
| DTF | Decision Tree Framework |
| GCMs | General Circulation Models |
| GLOFs | Glacial Lake Outburst Floods |
| HYMOD-DS | Distributed version of HYMOD hydrologic model |
| IHA | International Hydropower Association |
| IPCC | Intergovernmental Panel on Climate Change |
| KGE | Kling-Gupta Efficiency |
| MCM | Million Cubic Meters |
| NPV | Net Present Value |
| NSE | Nash-Sutcliffe Efficiency |
| PMF | Probable Maximum Flood |
| PMP | Probable Maximum Precipitation |
| PPA | Power Purchase Agreement |
| PRoR | Peaking Run-of-River |
| RCP | Representative Concentration Pathway |
| UAHEP | Upper Arun Hydroelectric Project |
| UC | University of Cincinnati |
| USD | US Dollars |

# Executive Summary

The Upper Arun Hydroelectric Project (UAHEP) is a proposed peaking run-of-river hydropower facility with an installed capacity of 1040 MW, to be located approximately 200 km to the northeast of Kathmandu, where the upper reach of the Arun River drains into the Koshi basin. UAHEP has a catchment area of 26750 $km^2$, over 95% of which lies in the Tibetan plateau. With a rated net head of 508.26 m, UAHEP's average annual electrical output is projected to be approximately 4050 GWh/year. The electricity is expected to contribute to the national grid during evening peak hours (up to six hours), in addition to supplementing off-peak energy. The project is undergoing detailed design at this stage.

Because it is a run-of-river project, UAHEP has high dependency on consistency of riverine streamflow in a basin with extreme seasonal variability in precipitation (monsoon to non-monsoon). Snowmelt and glacier melt also contribute to streamflow, each in its own seasonal pattern. The economic lifetime of the project is 25 years, meaning that financial projections for the project must anticipate streamflow availability to the project through the year 2050 (assuming the project is in operation by 2025), at which point the climate of the Himalayan region is likely to be substantially different from the recent past. Additionally, the life duration of the project is 100 years, so the effect of climate change by the end of the century also warrants consideration.

The water systems analysis research group in the Department of Chemical and Environmental Engineering at the University of Cincinnati (UC) was hired to evaluate climate change risks to the performance of UAHEP, and to put those risks in context relative to risks of other kinds. The Project Team followed the methods laid out in the World Bank's Decision Tree Framework and adopted by the International Hydropower Association (IHA) in its Hydropower Sector Climate Resilience Guide (CRG). The methods are founded on bottom-up, robustness-based concepts that respond to deep uncertainty in future climate conditions not by designing for an unknowable "expected" set of conditions, but by ensuring the ability of the project to perform acceptably well over a wide range of conditions that might reasonably be expected to occur within the project's lifetime.

To do so, the research group conducted a detailed analysis of all available data regarding observed historical and projected future hydro-climatic conditions in the basin in order to understand trends, and climate drivers. The research group then developed a series of models (weather generator, hydrologic model, hydropower generation model, financial model) capable of confidently reproducing historical basin conditions, as well as projecting future UAHEP performance. The models were run using a systematically generated set of scenarios of possible future scenarios of climate (precipitation and temperature). Hydropower projects worldwide are vulnerable to a variety of climate risks such as unsustainable long-term flow (mean streamflow), changes in extreme events in terms of both magnitude as well as frequency (floods and droughts), changes in seasonality (early snowmelt, shifts in the precipitation timing), large scale disasters (glacial avalanches or glacial lake outburst floods, GLOF). In addition to the direct climate change effects, the hydropower sector is also vulnerable to secondary effects such as landslides or erosion, increased sediment load, and increased competition for water from other uses, though careful evaluation of those secondary effects was outside of the scope of the current analysis.

For the UAHEP project, the climate risks of greatest concern are: 1) long-term financial performance; 2) chances of increased sediment load; and 3) flood risks. Changjiang Institute of Survey, Planning, Design and Research (CSPDR) is responsible for the detailed financial analysis of the project. This assessment has closely collaborated with the CSPDR team and the World Bank panel of experts for project details such as capital costs, selling rate, discount rate etc. and operational details such as reservoir operation and sediment flushing regimes.

**Conclusion on Concerns Regarding Future Insufficiency of Flow:**
Increases in temperature increase evaporation, which has a negative impact on total annual streamflow, but also increase rates glacier melt, which increase streamflow. Glacier melt occurs mostly during summer months, concurrent with the Indian monsoon, when additions to streamflow contribute no financial value for hydropower generation. However, more-rapid snowmelt each year, while not changing the annual water balance, shifts the seasonality. Earlier snowmelt increases streamflow during the winter dry season and decreases streamflow during the summer wet season. Figure ES 1 illustrates the impact of this shift on total annual electricity generation and overall project finances. Increasing temperature, especially February and March, is likely to increase the dry season contribution to streamflow by snow and glacier melt (the figure on the left). Because the installed turbine capacity is sufficient to accommodate increased dry season streamflow, the current estimate of the annual energy generation of 4492 GWhr appears to be a safe estimate. Figure ES1 shows that, though the bulk of general circulation models (GCMs) project an increase in total annual precipitation by midcentury, some climate models predict a decrease in the precipitation by as much as 10%. Such a reduction in the precipitation would cause a decrease in average annual energy production of 1%-5%, an unlikely worst-case scenario.

As shown in Figure ES 1 (right), none of the explored climate change scenarios (significantly beyond the range of the extent of the full ensemble of the current generation of GCMs) results in a negative net present value for the project (there is no red area on the plot on the right). It should be made clear that Figure ES 1 accounts only for shifts in average annual conditions. Shifts in extremes are evaluated in the flood risk section but are not translated into financial losses. Shifts in precipitation seasonality (or seasonal-specific results) were not systematically evaluated, as the GCM outputs supporting the likelihood aspects of such evaluations are not available with high confidence.

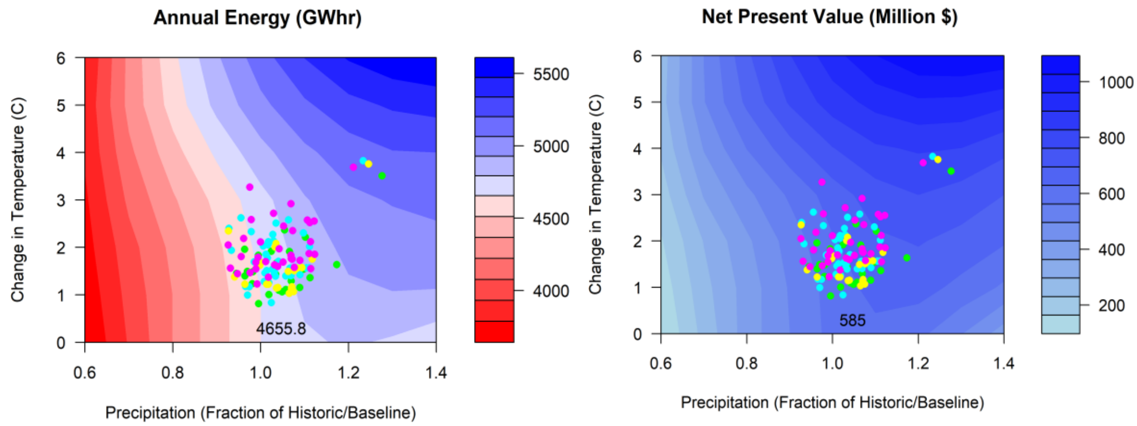


*ES 1 Response surface for Annual Energy and Net Present Value. The dots on the response surface represent the CMIP5 climate change projection (centered on year 2036). Representative concentration pathway (RCP) Green: RCP2.6; Cyan: RCP 4.5; Yellow: RCP 6.0; Magenta: RCP 8.5*

**Conclusion on Concerns Regarding High Sediment Load:**

Figure ES 2 shows that powerplant shutdown days are projected to increase 2-3 times with a 30-40% increase in precipitation, with the understanding that higher precipitation intensity is associated with larger suspended sediment loads. This translates to a loss of annual energy production of 438 GWHr to 876 GWHr due to power plant shutdown. Furthermore, most GCMs project an increase in precipitation by up to 20%. Such an increase in sediment could also increase the turbine abrasion. It is therefore recommended that a detailed cost-benefit analysis be conducted to evaluate the tradeoffs associated with investment in hard-coated turbines.

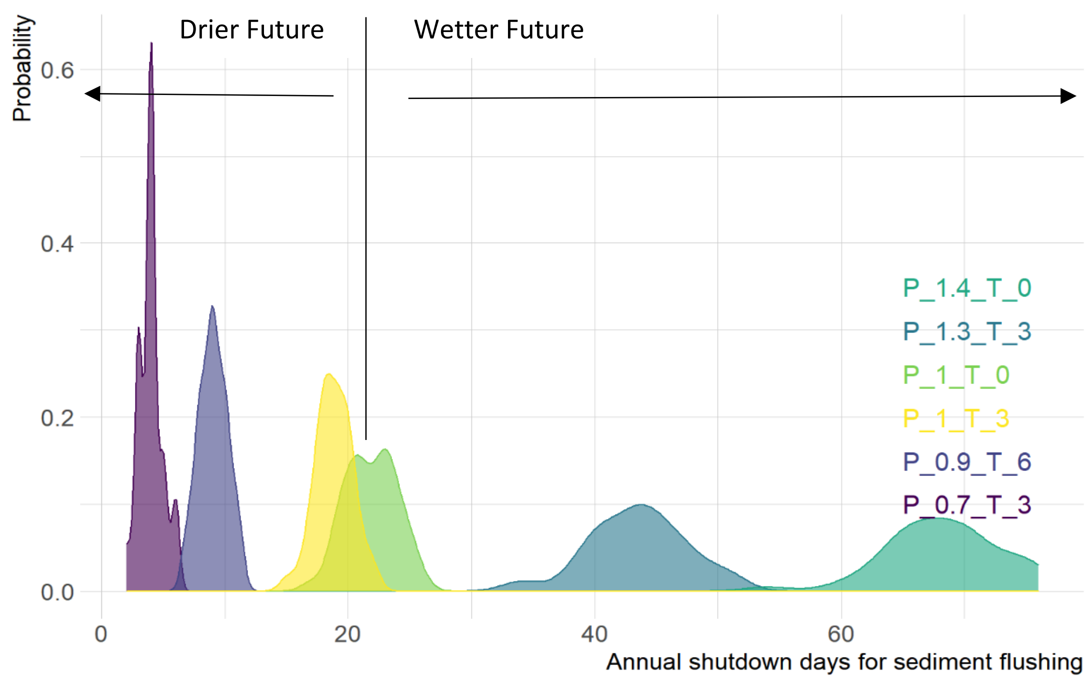


*ES 2 Frequency distribution of annual power plant shutdown days for sediment flushing. The distribution becomes flatter with increased mean as for a scenario that is wetter than the current climate. The distribution becomes sharper with lower mean for a scenario that is drier than the current climate. Only a few climate scenarios are presented here to prevent overcrowding.*

**Conclusion on Concerns Regarding Increasing Flood Risk:**

No statistically significant trends were detected in either the historical annual maximum precipitation or streamflow in the UAHEP basin. However, GCMs project an increase in temperature, relative humidity, dew point temperature, and the 3-day maximum precipitation (Figure ES 3). This indicates the likelihood of a future intensification of the extreme precipitation in the basin. The effect of changes in extreme precipitation on the flood were estimated using the Probable Maximum Flood (PMF) approach. Although the 3-day maximum precipitation in the basin is likely to increase by 12% on average by 2056-2085, the projected changes in the maximization ratio by the end of the century are erratic. Figure ES 4 illustrates the 12% increase in 3-day max precipitation corresponding to an increase in 3-day PMF by 13% in the basin and no change in the maximization ratio. Improvements to the existing approaches to estimation of the impact of climate warming on probable maximum precipitation (PMP) are an area of active study, and in need of improvement for refinement of the results presented here.

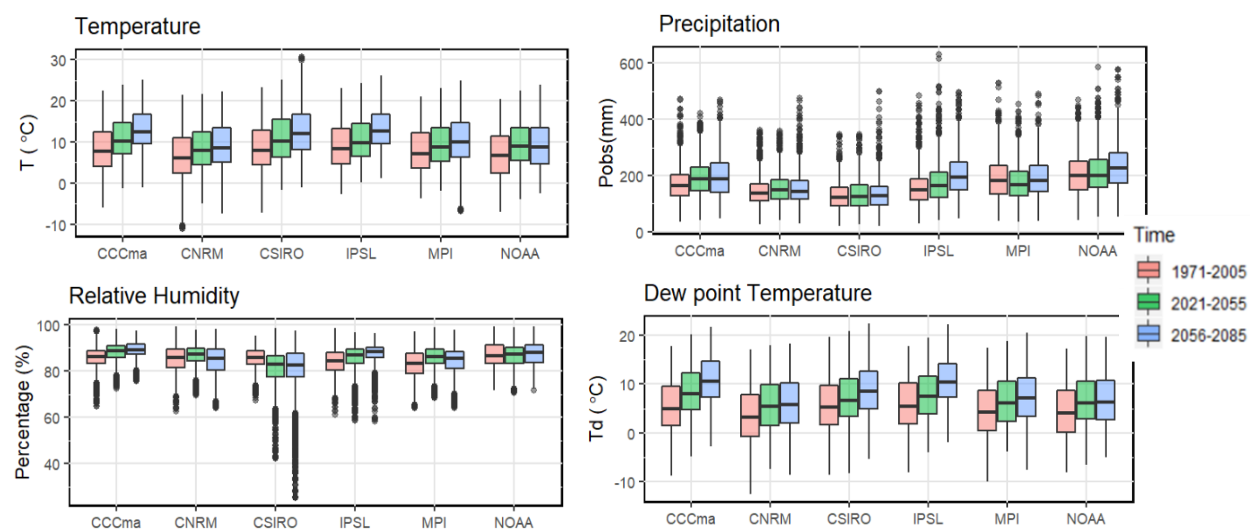


*ES 3 CORDEX results of the extremes from CORDEX dataset for temperature, precipitation, relative humidity and dew point temperature for historical (1971-2005), near future (2021-2055), and far future (2056-2085). The points in the boxplot are the values for CORDEX grids laying within the catchment area.*

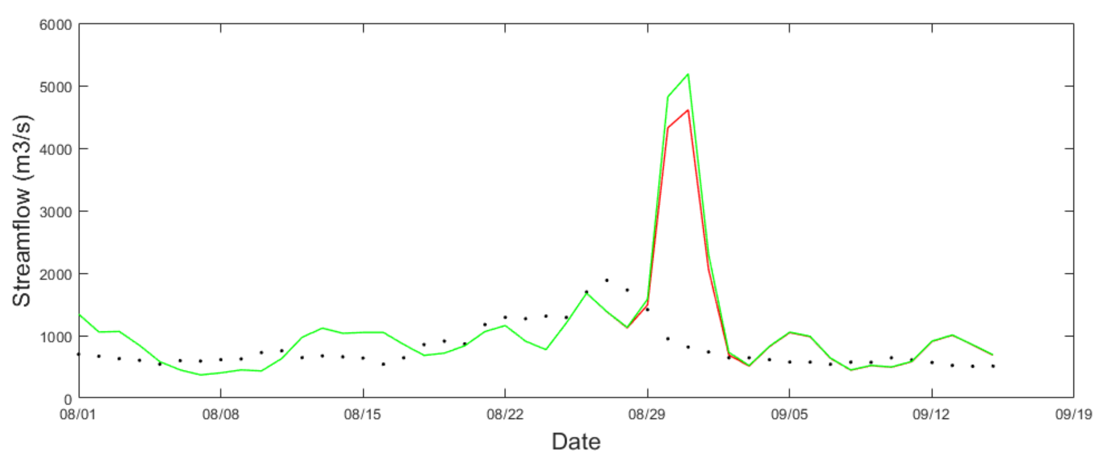


*ES 4 PMF estimation under climate change. The black dots are historical flow in the basin. The red is the PMF calculated with the historical data (4612 $m^3s^{-1}$). The green represents the projected PMF calculated by increasing the 3-day precipitation by 12% in the far future (5186 $m^3s^{-1}$).*

The current design of the UAHEP is based on GLOF risk. Both the 10,000-year flood estimate, and the climate-change-increased PMF are lower than the GLOF-derived design flood for the UAHEP, and therefore no change to project design flood is recommended.

**Recommendations for Climate Change Adaptation:**
No climate change adaptation measures are recommended to manage risks associated with low flows.

For flood risk, since the current design is based on the GLOFs, regular monitoring of the glacial lake and establishment of early warning system is recommended. Furthermore, it is recommended to perform a detailed geo-hazard analysis and disaster risk assessment to quantify the flood risk associated with landslides, avalanches, and earthquakes.

In response to the risk of increased sediment load, this report proposes installation of coated turbines. A detailed cost-benefit analysis is recommended to the design team to consider investing in coated turbines.

# 1 Introduction

**Background**

The Upper Arun Hydroelectric Project is a proposed peaking run-of-river project in Eastern Nepal (Figure 1) with a rated net head of 508.26 m, and a catchment area of 26750 km$^2$. With an installed capacity of 1040 MW, the project is expected to generate nearly 4500 GWh of electricity per year. The energy generated will serve domestic usage in Nepal and may be exported to the neighbouring countries.

The catchment of the UAHEP stretches from the Tibetan plains in the north to the Himalayas in Nepal in the south. It is glacier-fed, with the bulk of its area above the elevation of 4500 m (refer Figure 2). The climate, topography, and hydrologic characteristics of the two regions – Tibet on the north side of the Himalayan ridge and Nepal on the south side – is heterogeneous, making the hydrology of the catchment complex. The north side in Tibet is cold and arid with an average precipitation of approximately 300 mm, and the topography is imbedded with many glaciers and glacial lakes. The south side of the Himalayan range in Nepal belongs to a mild climatic zone with an average annual precipitation in excess of 1000 mm, receiving most of the precipitation (both rain and snow) from the Indian monsoon. More than 10 major tributaries in Tibet and Nepal contribute to the runoff upstream of the proposed power plant intake.

Climate change is expected to affect the hydrology of the project location. The increasing temperature is likely to affect the timing and amount of glacier melt, and potentially shift the likelihoods of the occurrence of Glacier Lake Outburst Floods (GLOFs) (mainly in the Tibetan plains). Changes in atmospheric processes may change the monsoon precipitation pattern (mainly in the catchment in Nepal). The combined effects of these two processes influence the seasonality, low flow, and high floods of the Upper Arun River, affecting the performance of UAHEP. Additionally, the sediment load is likely to increase with increasing precipitation intensity or riverine discharge, which would affect the project performance.

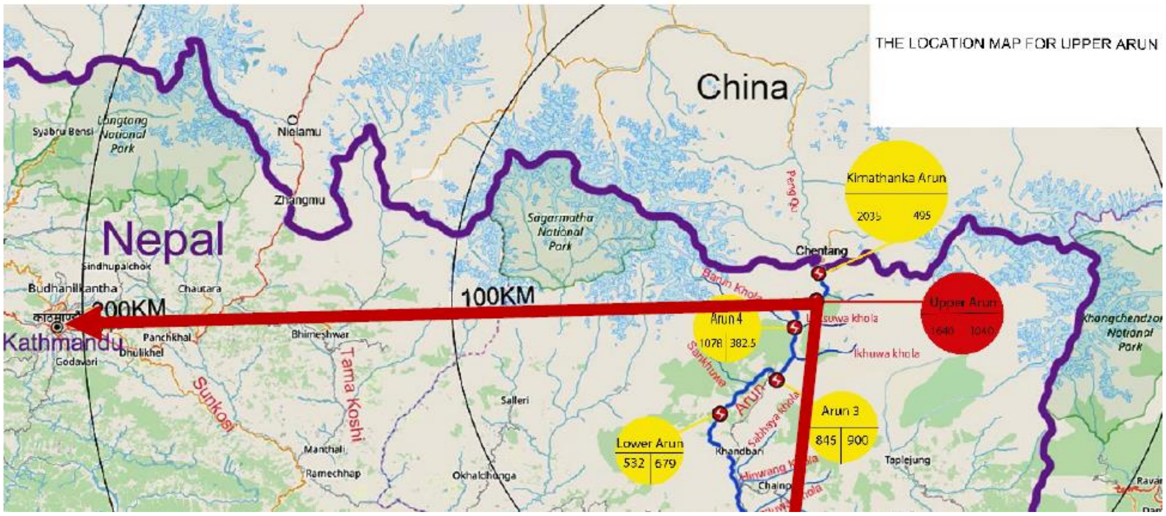


Figure 1 Geographical location Map of Upper Arun Hydroelectric Project (Adapted from CSPDR report)

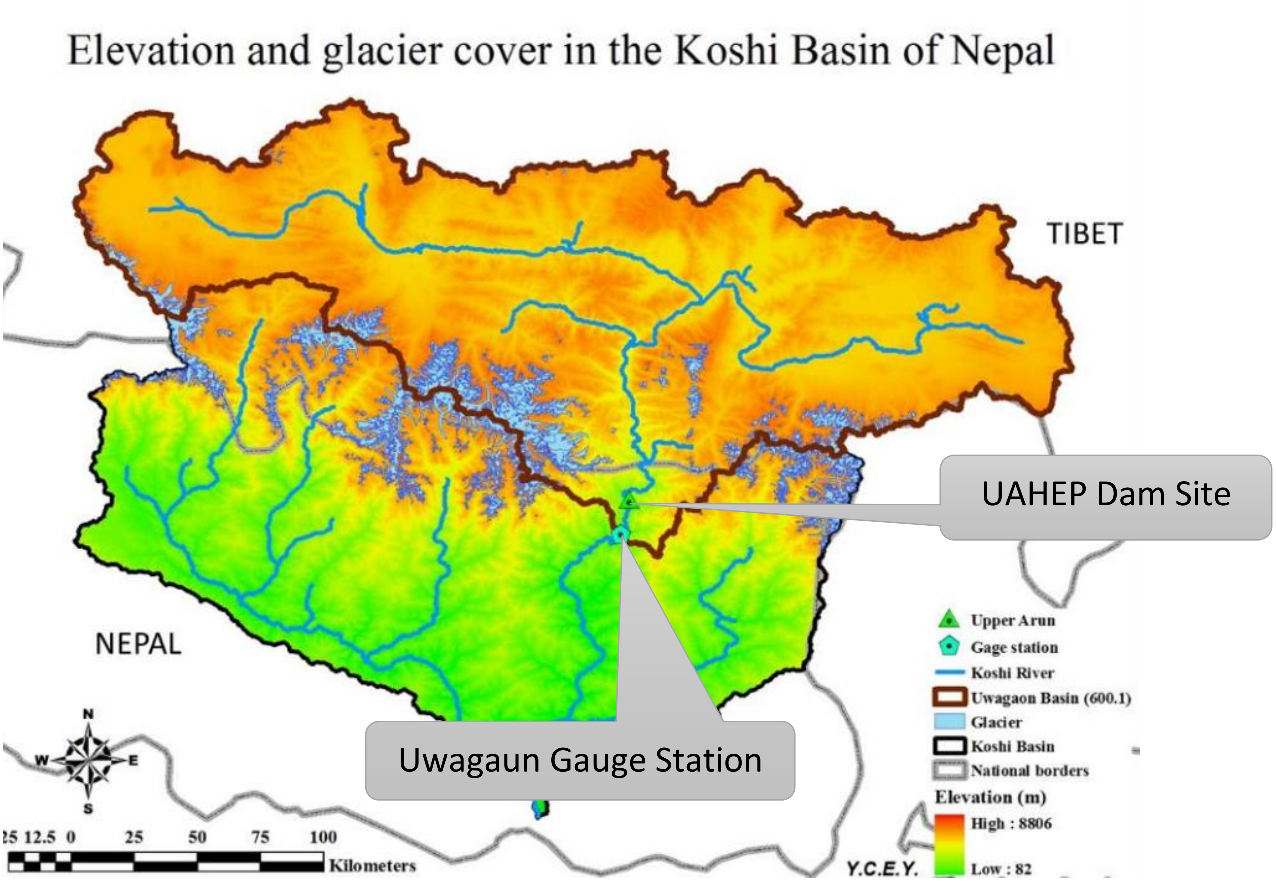


Figure 2 Elevation and Glacier coverage in the Koshi River Basin of Nepal. The catchment are above the dam site is 25,700 km$^2$. (Adapted form AUS11077)

**Previous Work Related to Climate Risks on the UAHEP**

To understand the climate change risks to UAHEP performance, the World Bank carried out an intensive study with a bottom-up approach as a pilot project of the Decision Tree Framework in 2015. The report is available for free download as Report No: AUS11077, *South Asia Investment decision making in hydropower: Decision Tree Case Study of the Upper Arun Hydropower Project and Koshi Basin Hydropower Development in Nepal.* The report was prepared in the Feasibility Study stage of the project. It assessed the long-term performance of the project with the then project design of 335 MW and found it to be robust to climate change. The analysis identified an opportunity to harness additional energy due to melting glaciers by mid-century and recommended an update of the project design from 335 MW to between 750 MW-1350 MW to maximize the project benefits.

Currently, the project is undergoing detailed re-design with a capacity of 1040 MW, along with additional updates in the design of the settling basin. The climate change risk assessment in the updated feasibility study was based on historical trend analysis and a single downscaled GCM projection evaluated under (Intergovernmental Panel on Climate Change Representative Concentration Pathway) IPCC RCP 2.6 scenario. Using a single GCM with a lower representative concentration pathway potentially underestimates the risks to the system. The International Hydropower Association Climate Resilience Guide (IHA 2019) includes five well-defined stages for management of climate change risks to hydropower projects. It recommends the following as a minimum requirement for hydropower risk assessment:

a) *"As a minimum, look at two different Representative Concentration Pathways (RCPs) (e.g., 4.5 and 8.5) and a minimum of two future 30-year time periods …."*
b) *"It is important to consider at least the full range of the current ensemble of climate projection…"*

This study fills the gap in the Climate Risk Assessment (CRA) of UAHEP, with the new project design of 1040 MW and updated data available since AUS11077. Additionally, it also evaluates the risks to the project with potential changes in a) flood, and b) sediment (within the scope of available data), to augment the risks on the long-term project performance evaluated previously. The assessment is based on the bottom-up, robustness-based decision support method following the International Hydropower Association (IHA) Hydropower Sector Climate Resilience Guide (https://www.hydropower.org/publications/hydropower-sector-climate-resilience-guide). The methodology of the IHA guide is illustrated in Figure 3.

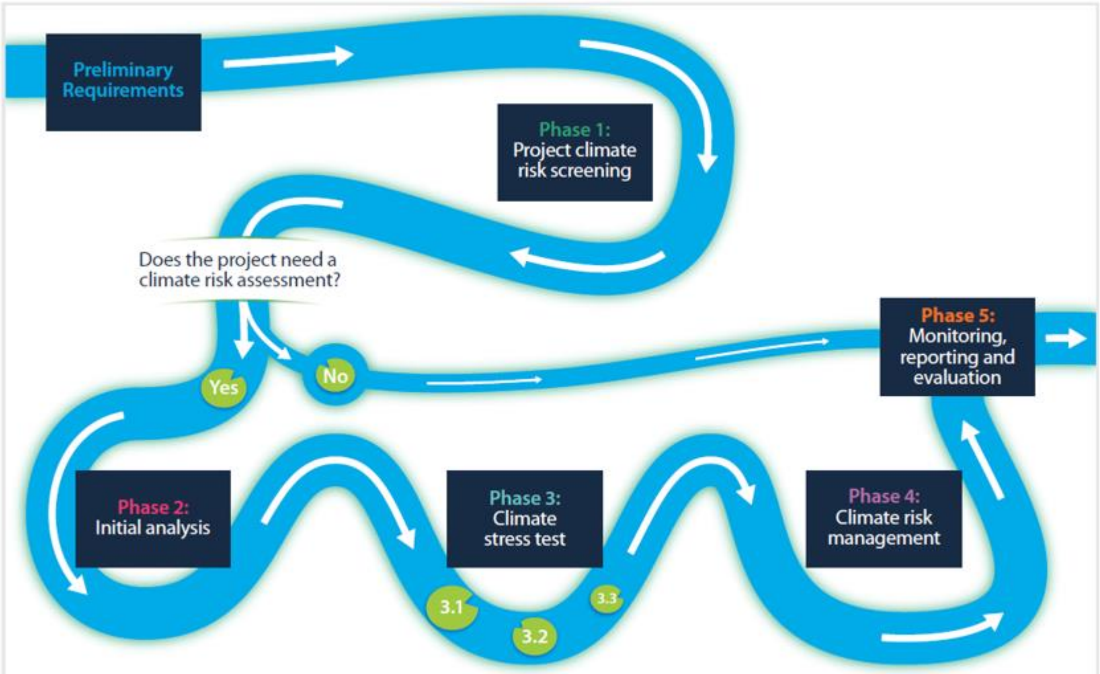


Figure 3 Decision "river" framework in IHA guide (IHA, 2019)

# 2 Updates since the Interim Report

This is the draft final report of the Climate Change Risk Assessment of the UAHEP project. Several changes and updates since the submission of the interim report have occurred, and are presented below:

a) The hydrologic model was updated to capture the long-term flow process in close consultation with Dr. Nick Mandeville.

b) An alternate calibration of the hydrologic model was made that captures the major storms and the floods. This version of the calibration was used for PMF estimation in the basin.

c) An energy model was introduced that accounts for reservoir operation regimes and turbine operation and associated head loss. An excel version of the model was provided by Dr. Peter Meier, which was translated into an R script and used in the analysis.

d) A sediment flushing schedule was incorporated into the analysis. The number of annual power plant shutdown days required for regular sediment flushing was estimated. An excel version of the model was provided by Dr. Peter Meier, which was translated into R and used in the analysis.

e) The Probable Maximum Precipitation (PMP) and the Probable Maximum Flood (PMF) were estimated for historical and future climate projection. UC consulted the World Bank Panel of Experts for guidance on the process of estimation of PMP and PMF.

f) In addition to the tasks and agreement in the ToR, UC provided the hydrologic model and weather generator perturbed climate traces to CSPDR. The research team at UC also provided training on how to use the model to generate perturbed streamflow traces and use it for further analysis.

# 3 Phase 1 of the Climate Change Risk Assessment

## 3.1 Introduction

Phase 1 of the IHA guide is the Inception Phase. It is a qualitative assessment of the climate change related risks to the hydropower project. The initial part of Phase 1 consists of desktop study of previous works and gathering of available data. The major risk factors to the project and uncertainty range around the risk factors are discussed with the stakeholders in this phase. If the project is identified to be vulnerable to climate risks, an assessment framework is laid out. The performance metrics and threshold for the success of the project is defined by the end of Phase 1.

A UC team consisting of Dr. Patrick Ray and two graduate students conducted an inception workshop on 21-25 October 2019 at the CSPDR headquarters in Wuhan, China. The first goal of this visit was to provide a workshop with hands-on-training to the trainees (CSPDR, World Bank team and other participants) on the bottom-up climate change impact assessment along with demonstration of an example application. The second goal of the visit was to establish point of contact for knowledge exchange to collect information (data, models, reports etc.) required for the CRA of the UAHEP. The inception visit was successful in the completion of both the goals. The meeting minutes of the inception visit is presented in Annex 2: Inception Visit of this report.

## 3.2 Data Review

**Data and reports collected:**

Since the publication of the World Bank Report AUS11077 in 2015, there has been an update in the availability of hydro-meteorological data. The streamflow record has been updated from 1986-2005 to 1976-2014 at Uwagaon Station. The meteorological data is now available for station **Num** from 1959-2015 and Station **Chepuwa** from 1959-2015. The installed capacity of the project has been updated from 335MW to 1040MW. The cost and other economic parameters of the project have also been updated. New sediment data is now available for the project. The major reports, data, and models collected relevant to CRA are listed in Table 1.

*Table 1 Summary of reports, models, and data received for CRA of Upper Arun Hydroelectric Project*

| S/No. | Reports, Data, Model Collected | Dates Received and Notes |
|---|---|---|
| 1 | Record of hydrologic and meteorological data used by CSPDR in the preparation of the Updated feasibility report | 2019/10/21<br>Received form Dr. Li in CSPDR headquarters, Wuhan |
| 2 | UAHEP Updated Feasibility Study Report - pdf of a PowerPoint presentation (105 pages summarizing the major findings) | 2019/10/23<br>Sent by: Dr. Li via email |
| 3 | GLOF Report (101 pages)<br>Updated Feasibility Report - Annex B: Hydrology and Sediment Investigation Report (138 pages)<br>World Bank Comments on the Hydrology (July 2019) | 2019/11/01<br>Sent by: Dr. Li via email |
| 4 | South Asia Investment decision making in Hydropower: Decision Tree Case Study of the Upper Arun Hydropower Project and Koshi Basin Hydropower Development in Nepal (AUS11077) | 2019/10/18<br>Retrieved from the internet |
| 5 | Results, R-codes, figures from the previous analysis (developed for AUS11077) | Available at UC |
| 6 | Modules for HyMOD-DS hydrologic model<br>(developed for AUS11077) | 2019/11/04<br>Sent by: Dr. Wi via email |
| 7 | Updates on the hydrologic model | In close consultation with Dr. Nick Mandeville |
| 8 | Updates on the economic parameters used (cost, selling price, rate etc.) | Provided by CSPDR |
| 9 | Reservoir and turbine operation regime | Provided by Dr. Peter Meier |
| 10 | Sediment flushing regime | Provided by Dr. Peter Meier |

## 3.3 Stakeholder-Defined Categories of Concern

The stakeholders who are affected by the project (owners of the project, population utilizing the generated electricity, and the population inhabiting the Upper Arun Basin), and the Client (the World Bank) are concerned about climate and non-climate risks to the project.

**Climate Risks:** The climate change concern related to the project is on the long-term performance with possible shifts in precipitation and temperature mean. Additional concern related to the ancillary effects of climate change such as changes to flood peak, drought, seasonal shift, glacier melt, and GLOFs, which expands the scope of previous Decision Tree (and IHA CRG) applications, were also identified by the client and stakeholders.

**Non-Climate Risks:** Examples include changes to the selling price, increase in capital costs, uncertainty in estimation of sediment load, and seismic hazards. The research team at University of Cincinnati does not intend to perform a detailed analysis of these non-climate risks.

Besides the stakeholders meeting during the inception visit, there has been regular communication with the client by email. On March 25, 2020, we presented in a webinar entitled, "Climate change, melting glaciers and hydropower in the Himalayas" moderated by the World Bank. The focus of the webinar was the discussion of the unique challenges and opportunities associated with developing hydropower under uncertainty and climate volatility in the Himalayan region. One of the key objectives of the webinar was to inform the Government of Nepal's multi-stakeholder dialogue, called the Mt Everest Dialogue, forum originally scheduled from April 2-4, 2020. Global experts in monsoon dynamics, Himalayan glaciers, GLOF events, and representative of the Government of Nepal were amongst the other key speakers. The major factors identified to be of concern in the webinar were changes in the monsoon rainfall with climate change, increasing glacier melt with warming and the possibility of an increase in GLOF events.

In this CRA of the Upper Arun project, we address all climate related risks (some in greater depth than the others). Additionally, other non-climate risks (or their surrogates) are also explicitly addressed.

## 3.4 Definition of performance metrics

The performance metrics are the project performance characteristics that could potentially be affected by changes in climate as well as non-climate risk factors. Typically, these metrics are related to the hydropower generation, and monetary value of the project. For some projects, the performance metrics might have a much wider scope incorporating societal well-being or other non-tangible measure of success. The threshold set for these metrics determines the success or failure of the project in an alternate future scenario. For instance, in terms of financial performance, the performance metrics is the Net Present Value (NPV), and the project is successful if the NPV is positive. Similarly, in terms of long-term performance, the performance metrics is annual energy generation and the threshold for success is the estimate of annual energy based on historical observation. The stakeholders' concerns (both climate and non-climate) identified in Phase 1 defines the performance metrics and its threshold for success of the project. In Phase 2, we design a framework for the sensitivity analysis of the project performance metrics around the plausible ranges of uncertainty in the risk factors (both climate and non-climate). In Phase 3, we perform the sensitivity analysis and evaluate the likelihood of success of the project in future.

For CRA of the UAHEP, the performance metrics and thresholds are defined in Table 2.

*Table 2 Definition of the performance metrics and its threshold in the response surface*

| S/No. | Performance Metrics | Units | Threshold | Risk/Opportunity |
|---|---|---|---|---|
| 1 | Streamflow Volume (Annual, Wet Season, Dry Season) | Million Cubic Meters (MCM) | Estimates based on historical observations | Opportunity: Blue<br>Risk: Red |
| 2 | Annual Energy Generation | GWhr | Estimates based on historical observations | Opportunity: Blue<br>Risk: Red |
| 3 | Net Present Value | Million USD$ | 0 | Opportunity: Blue<br>Risk: Red |
| 4 | Annual Sediment Load | Million Tons | Estimates based on historical observations | Risk: Red |

In addition to the response surface, other changes are also presented in this report. The shift in the distribution of the annual power plant shutdown days to account for sediment flushing with climate change is presented.

The changes in PMP and PMF under future projection is analyzed with Coordinated Regional Downscaling Experiment (CORDEX) regional downscaling. The flood future PMF design is compared against GLOF as well. The design flood is selected as the maximum of the different flood estimates in the future.

# 4 Phase 2 of the Climate Change Risk Assessment

## 4.1 Introduction

The main objectives of Phase 2 of the IHA guideline are data analysis, definition of the baseline scenario, and laying out the framework for Phase 3 analysis. In this phase, uncertainties bound of the climate and non-climate risk factors are quantified to define a plausible range for sensitivity analysis in Phase 3. The ranges/uncertainty in the non-climate risk factors (e.g., capital costs, discount rate, selling price etc.) are generally defined in consultation with the client and the stakeholders. The ranges/uncertainty in the climate risk factors is defined by both historical observation and future projections. At the end of Phase 2, the underlying assumptions and the required features in the model that captures the project performance under a different future are identified. The model development and execution along with the sensitivity analysis is performed in Phase 3.

## 4.2 Data Analysis

For the Climate Change Risk Assessment of the Upper Arun Hydropower project, data (climate and non-climate) collected from different sources are listed in Table 3.

### 4.2.1 Historical Observations

The historical records of precipitation, temperature and streamflow stations were explored in this analysis. The closest streamflow station to the project dam location is Uwagaon Station and the other streamflow stations further downstream along the same river includes the flow from other tributaries. The available ground stations for precipitation data are location in Nepal further downstream of the project location and outside the catchment area at lower elevation. No temperature station is available in the project location. To estimate the local climate in the project catchment area and develop a hydrologic model, the gridded datasets of precipitation as well as temperature were further explored. For the estimation of glacier extent and depth in the basin global datasets were explored. Additionally, the data related to sediment concentration and properties in the basin was also explored.

*Table 3 Datasets Explored in this analysis.*

| | Datasets | Spatial Resolution / Station Location | Time Step | Temporal Resolution |
|---|---|---|---|---|
| | **Streamflow Data Ground Stations** | | | |
| 1 | Uwagaon (Station 600.1) | ($87^0$20’22”, $27^0$35’21”) | Daily | 1976-2014 |
| 2 | Tumlingtar (Station 602) | ($87^0$12’45”, $27^0$18’36”) | Daily | 1976-2014 |
| 3 | Simle (Station 606) | ($87^0$09’16”, $26^0$55’42”) | Daily | 1976-2014 |
| 4 | Turkighat (Station 604.5) | ($87^0$11’30”, $27^0$20’00”) | Daily | 1975-2008 |
| | **Precipitation Data Ground Stations** | | | |
| 5 | Chepuwa Station | - | Daily | 1959-2015 |
| 6 | Num Station | - | Daily | 1959-2015 |

| | | | | |
|---|---|---|---|---|
| | **Gridded Precipitation Datasets** | | | |
| 7 | TRMM[1] 3B42 v7 | $0.25^0$ x $0.25^0$ | Daily | 1998- 2019 |
| 8 | GPCC[2] V2018 | $0.5^0$x$0.5^0$ | Monthly | 1891-2016 |
| 9 | WFDEI[3] | $0.25^0$ x $0.25^0$ | Daily | 1979-2019 |
| 10 | APHRODITE[4] | $0.25^0$ x $0.25^0$ | Daily | 1961-2007 |
| 11 | IMERG[5] | | Daily | 2000-2019 |
| | **Gridded Temperature Datasets** | | | |
| 11 | UDelware[6] | $0.25^0$ x $0.25^0$ | Monthly | 1891-2016 |
| 12 | WFDEI | $0.25^0$ x $0.25^0$ | Daily | 1979-2019 |
| 13 | APHRODITE | $0.25^0$ x $0.25^0$ | Daily | 1951-2007 |
| | **Glacier Data** | | | |
| 14 | RGI 3.2[7] | Glacier Area: 1413 $km^2$ | | |
| 15 | ICIMOD[8] | Glacier Area: 1276 $km^2$ | | |
| 16 | NRC[9] | Glacier Area in Ganges: 6,677 $km^2$ | | |
| | **Sediment Data** | | | |
| 17 | FSR 1991[10] | | Sediment sampling dates | 1990-1991 |
| 18 | UAHEP[11] | Intake site UAHEP | | 2018-2019 |
| 19 | Arun-4[12] | Downstream UAHEP | | April-Dec, 2018 |

*Data Sources:*

TRMM[1] : Tropical Rainfall Measuring Mission 3B42 v7 (Huffman et al. 2014)

GPCC[2] : Global Precipitation Climatology Centre (Schneider et al. 2011)

WFDEI[3] : WATCH Forcing Data methodology applied to ERA-Interim reanalysis data (Weedon et al. 2014) Rain and snowfall corrected with GPCC.

APHORDITE[4] : Asian Precipitation- Highly- Resolved Observational Data Integration Towards Evaluation of Water Resources (Yatagai et al. 2012; Yasutomi et al. 2011; Kamiguchi et al. 2010)

IMERG[5] : Integrated Multi satellite Retrievals for GPM (IMERG) data product (Huffman et al. 2014)

UDelware[6] : University of Delaware (Willmott and Matsuura 2001)

RGI 3.2[7] : Randolph Glacier Inventory 3.2 (Pfeffer et al. 2014)

ICIMOD[8] : International Centre for Integrated Mountain Development Glacier Map

NRC[9] : National Research Council (Eriksson et al. 2009)

FSR 1991[10] : Estimates from Feasibility Report, 1991

UAHEP[11] : Sediment sampling carried out in the Upper Arun Project intake site

Arun-4[12] : Estimates from Arun-4 project further downstream of the UAHEP

The climate estimates form the different sources vary quite a lot in this basin. Amongst the climate data sources, TRMM and IMERG data are satellite-based data.

### 1. Streamflow observations

The streamflow in the Upper Arun River is measured at gaging stations established near the project intake, Station Uwagaon (Station 600.1), and further downstream along the same river (Station Tumlingtar). The rest of the stations further downstream of the basin with major contributions from other tributaries are not included in the development of hydrologic model in this analysis.

*Table 4 Annual Maximum Streamflow Series for Stations Tumlingtar, Uwagaon and extracted for Dam Site. None of the series indicates a significant increasing trend. (Further details on Table 4)*

| Stations | Uwagaon | Upper Arun Dam Site | Tumlingtar |
|---|---|---|---|
| Increase in discharge ($m^3s^{-1}$ /year) | 1.67 | 1.85 | 7.73 |
| P-value | 0.611 | 0.498 | 0.352 |
| Is the trend significant? | No | No | No |

As presented in Table 4, the trends of the annual maximum streamflow time series in Upper Arun Basin are not significant. Further details on the data used and additional analysis are presented in Annex 3: Data Analysis of this report. **Uwagaon (Station 600.1)** was chosen for the calibration and validation of the hydrologic model as it is situated closest to the project dam site (refer Figure 2).

### 2. Precipitation observations

The APHRODITE data captures the daily precipitation and temperature pattern of the catchment very well but underestimates the total monthly precipitation. The monthly estimates of precipitation from the GPCC data, is the closest to the estimates of TRMM data and is considered representative of the basin climate. In the previous report AUS11077, the daily APHRODITE data bias corrected with monthly GPCC totals was used for the development of hydrologic model, and the dataset was named APHRO_GPCC. The APHRODITE data ends in 2007, so for this analysis, other sources of gridded data were further explored.

WFDEI is the WATCH Forcing Data methodology applied to ERA-Interim reanalysis data. These daily gridded datasets have separate estimates of rainfall and snowfall which when added together gives the total precipitation estimates. Among different versions of WFDEI data, the one bias corrected with GPCC data closely follows the daily precipitation pattern of the APHRO_GPCC and preserves the monthly precipitation balance. The sum of the estimates form 'Rainf_WFDEI_GPCC_' and 'Snowf_WFDEI_GPCC_' was used as an estimate of the daily precipitation in the basin.

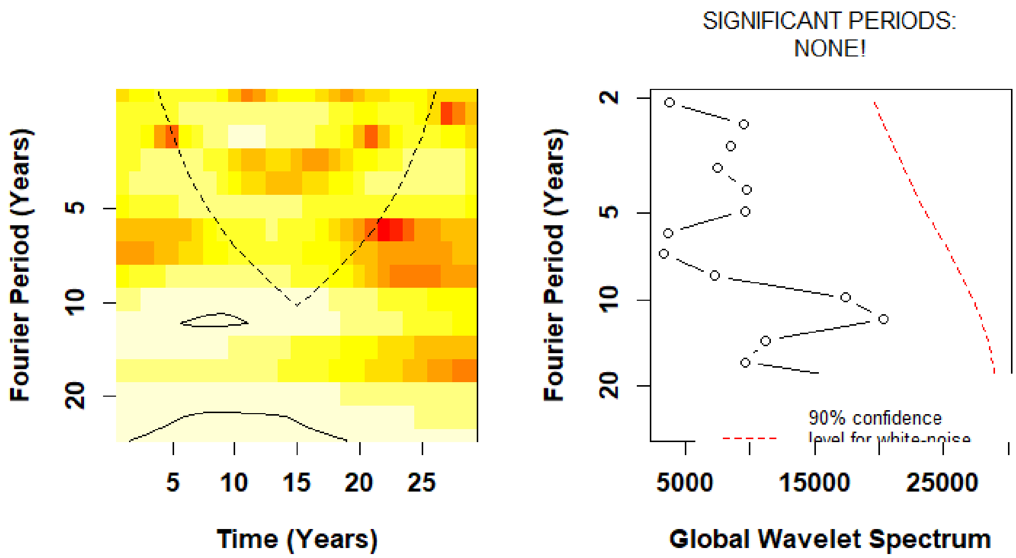


*Figure 4 Wavelet analysis of the WFDEI precipitation dataset (1979-2014) in Upper Arun Basin.*

It is noted that there is no significant change in the basin precipitation since 2007 (based on the analysis of WFDEI dataset). So, the **APHRODITE_GPCC data (1979-2007) precipitation estimate** is used in this analysis to calibrate and validate the hydrologic model. The daily APHRODITE_GPCC precipitation estimates is used for the development of the weather generator and the climate traces. Please refer to Annex 3: Data Analysis for further details.

### 3. Temperature data

The APHRODITE dataset, which best represents the temperature in the basin, ends in 2007. Thus, other sources of gridded data were explored. Although WFDEI data estimates the precipitation pattern of the basin pretty well, it fails to capture the daily temperature pattern of the basin.

UDelaware is the monthly global gridded high-resolution station (land) data for air temperature from 1900-2014. This data captures the annual pattern of temperature variation in the basin and closely matches the pattern of the APHRODITE temperature dataset. However, since the data was available only on a monthly time scale it was not very useful for the development of hydrologic model.

It is noted that there is no significant change in the basin temperature since 2007 (based on the analysis of UDelaware dataset). So, the **APHRODITE data (1979-2007) temperature estimate** is used in this analysis to calibrate and validate the hydrologic model. The daily APHRODITE temperature estimates are used for the development of the weather generator and the climate traces. Please refer to Annex 3: Data Analysis for further details.

### 4. Glacier data

Several sources of glacier data are available with disagreeing estimates (Figure 36). The uncertainties pertaining to glacier is associated with the estimate of its initial dimension (area and depth), its melting temperature, and movement rate. Randolph Glacier Inventory (**RGI) 3.2 was used in this analysis** and glacier volume was estimated using the multivariate glacier area-volume scaling relationships proposed by Grinsted (2013).

### 5. Sediment data

The sediment data collected from various studies over time in the basin is fitted to a rating curve seasonally to derive empirical relationship between river discharge and sediment concentration. **An annual rating curve fitted to the data is used for analysis in this study.**

**Major characteristics of historical data:** Figure 4 indicates that there is no significant multi-year periodicity in the precipitation pattern in the Upper Arun basin. The historical data averaged over the basin has a mean of 1225 mm with a standard deviation of 110 mm. The data has a slight negative skew of -.09. The temperature in the basin varies with widely with altitude. On average, the maximum basin temperature is between 8 to 10 degrees during the summer months of July-August, dropping to below freezing in the winter months of November-March. These properties of the data are preserved by the traces of the weather generator that captures its natural variability. The historical precipitation and temperature data do not have any significant trends. Table 4 indicates that the trends of the annual maximum streamflow time series in Upper Arun Basin are not significant.

### 4.2.2 Future climate projections in the basin

#### a) Changes in Mean:

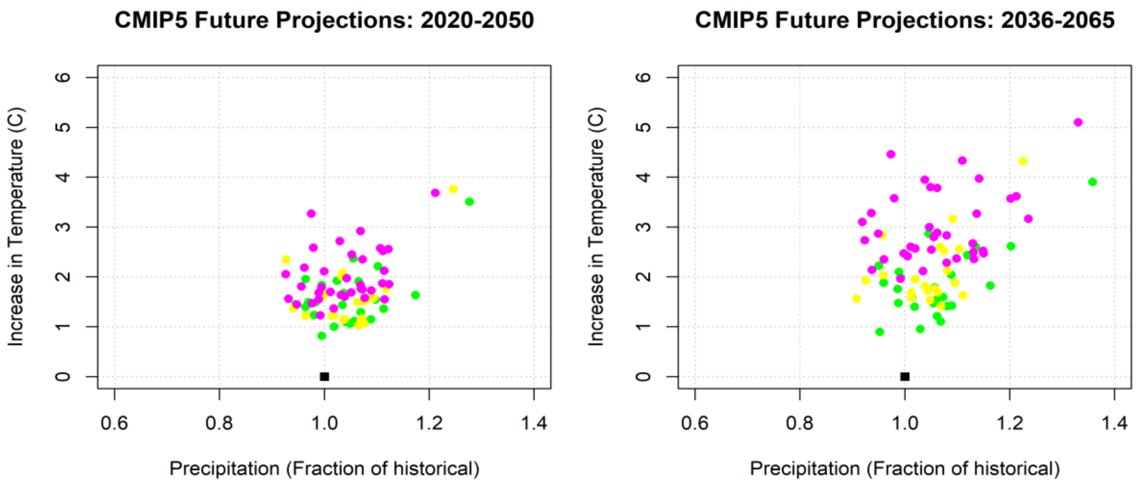


*Figure 5 Future climate for the Upper Arun Basin for near future (2020-2050) and far future (2035-2065) expressed with respect to the historical observation (1970-1999). The colors of the dots represent different representative concentration pathway (RCP) scenario defined in the CMIP5 climate projection. Green: RCP 2.6; Cyan: RCP 4.5; Yellow: RCP 6.0; Magenta: RCP 8.5. The black rectangle at the mid-bottom of the graph represents the historical observation i.e., no change in precipitation or temperature.*

Figure 5 represents the long-term changes in the mean precipitation and temperature in the basin for near-future and far-future. In the near future (2020-2050) the projections cluster around an increase in temperature by 2-3 degrees with about 10% increase in precipitation. In the far future (2036-2065) the future projections are dispersed anywhere between 2-5 degrees of warming and -10% to +35% variations in precipitation. The median of the ensemble of climate projections indicates a warmer and a wetter future for Upper Arun Basin, with higher warming under RCP 8.5 climate scenario.

#### b) Changes in Extremes:

For understanding the changes in extreme precipitation events in the future, we used Coordinated Regional Climate Downscaling Experiment (CORDEX) data over South Asia. We presented our analysis on both historical simulation and future projection under Representative Concentration Pathway 8.5 (RCP8.5) scenario. These models are regional downscaled versions of the General Circulation Models (GCM) downloaded from http://cccr.tropmet.res.in/home/esgf_node.jsp. Evaluation of the RCM results from the CORDEX data (including the ones used in this study) demonstrates a good consensus amongst the ensemble members, and lower uncertainty in the high mountains compared to the sub-hills in Central Himalayas (Sanjay et al., 2017). The analysis of the models used in this study shows an increase in the extreme precipitation over south Asia (Suman & Maity, 2020) although local variations are seen. The Driving GCMs used in this study are CCCma-CanESM2, CNRM-CM5, CSIRO-Mk3.6.0, IPSL-CM5A-LR, MPI-ESM-MR, and NOAA-GFDL-ESM2M. These models were downscaled using the RegCM4 downscaling experiment and are available at 50 km x 50 km grid resolution.

To understand the changes in the extremes in future, we analyzed air surface temperature (T), and 3-day maximum precipitation ($P_{obs}$). Boxplot of the values of temperature and precipitation for all the grids within the catchment area for three different time-period (Figure 6) indicates that the temperature and precipitation is increasing in the basin.

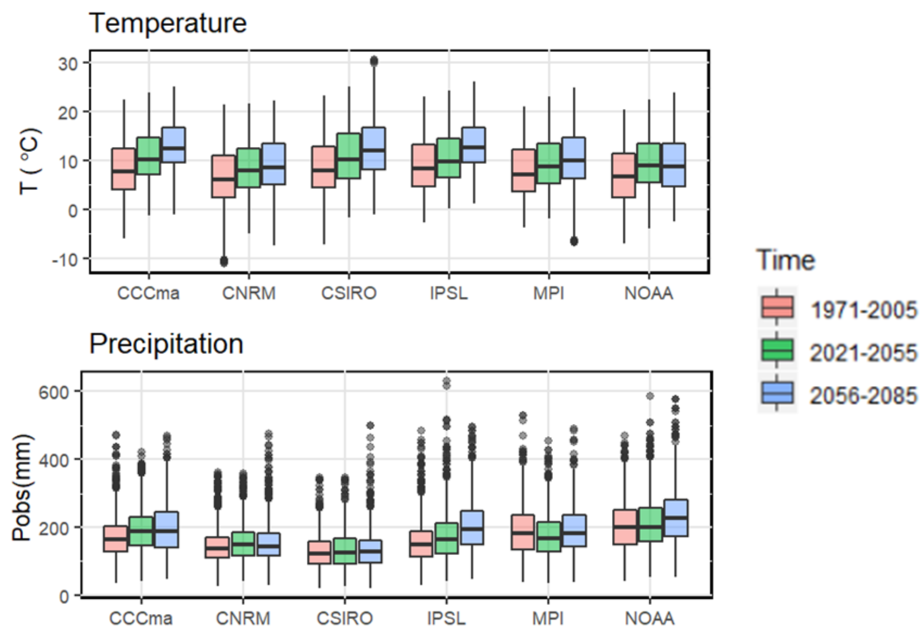


*Figure 6 Boxplot of daily temperature and 3-day precipitation ($P_{obs}$) in the project catchment area from different downscaling experiment with the CORDEX model.*

### 4.2.3 Non-Climate Data

Other data required for analysis such as project capital cost, electricity selling price, discount rate, project economic life, reservoir, and turbine operation regime, sediment-flushing schedule, and environmental release required to support downstream aquatic life were obtained from previous reports and via communication with the client.

The reservoir and turbine operation regime are described in 5.2.3.1, and the sediment flushing schedule is described in 5.2.3.2. The data associated with the costs of the project is described in 5.2.4.

## 4.3 Rapid Scoping

Rapid scoping is the process of identifying the variables of concern and their ranges of uncertainty to set plausible boundaries in the sensitivity analysis of the performance metrics. The risk and opportunity register defined at the end of Phase 1 (Table 2) is refined based on the data analysis, availability, and relative impact of various risks to the project. Rapid scoping consists of a qualitative or semi-quantitative analysis. The outcome of the scoping exercise is a clear and well-defined range of climate and non-climate risk factors for the stress test analysis in Phase 3.

### 4.3.1 Future climate uncertainty

**1. Shifts in mean climate:**

The future projections of climate in the Upper Arun basin indicate a warmer future (Figure 5) with higher warming under RCP 8.5 climate scenario. The uncertainty increases as we project into the far-future with dispersion in the results of the climate projections. To evaluate project robustness to climate change, we perform a sensitivity analysis of the hydrologic model and other project performance metrics under changed climate. We apply mean changes to precipitation between -40% and 40 % and between 0 to 6 degrees of warming. This range is chosen to evaluate the project performance beyond the uncertainty cloud defined by future climate projections. We superimpose the future climate projections centered in 2035, i.e., depicting the near future climate (2020-2050) over the response surfaces in Phase 3 analysis. This period of near future (2020-2050) is more relevant to the project life in the next 30 years.

**2. Shifts in Extremes: (floods and droughts)**

The Indian Summer Monsoon Rainfall (ISMR) is the primary source of precipitation and flood events in the project area. The ISMR is also known for its high interannual variability, which is often linked with the Southern Oscillation Index (SOI). Generally, the El Nino phase is associated with less than normal precipitation while the La Nina phase is associated with more than normal precipitation in ISMR (Kumar et al., 1999; Sigdel & Ikeda, 2012). The seasonal precipitation in Nepal exhibits similar relationship, but the relationship disappears as the analysis is performed on higher precipitation quantiles (over 90%) (Bohlinger & Sorteberg, 2018). However, in the past 40 years, changes in the magnitude and behavior of extreme precipitation have been observed (Baidya et al., 2008; Shrestha et al., 2017) suggesting the effect of climate change.

The initial plan was to perform a flood frequency estimate and analyze the effect of climate change on the flood estimates. For the design of the UAHEP project, the probable maximum flood (PMF) approach based on a 3-day PMP was chosen over the estimate from a flood frequency analysis. In this assessment we look at the changes in extremes (Precipitation, Temperature, Relative Humidity, and Dew Point Temperature) to predict the changes in the PMP estimates in the future. We then use the expected changes in PMP to predict the PMF under climate change. Further details are presented in Phase 3 of the analysis.

**3. Shift in likelihood and magnitude of GLOF event:**

Rapid glacier-melt and GLOF risks are among the biggest climate change concerns to the UAHEP stakeholders. The increased temperature is causing rapid shrinking of majority of glaciers in Nepal (Shrestha and Aryal 2011). The catchment area of UAHEP is embedded with many glaciers along the Himalayan ranges and Tibetan plateau. The increased glacier retreat and increase in glacier meltwater contributes to the areal expansion of the downstream glacial lake (Zhang et al. 2015). Glacial lakes in the Central Himalayas have expanded by up to 17% between 1990 and 2000 (Nie et al. 2018). If these lakes are not monitored for its continued expansion and structural stability, they could result in sudden outbreaks known as GLOFs. The detailed GLOF risk study of the UAHEP has identified 49 glacial lakes in the catchment, 4 that has been marked with the probability of outburst. The study has further identified Lower Barun Glacial Lake (originating from Mount

Makalu in Nepal) and Qiangzongke Tsho Glacier Lake (originating in Tibetan Plains) to be of biggest concern to UAHEP. GLOF risks of these two lakes are modelled in detail with MIKE-11, a hydrodynamic model. Based on the modeling exercise, the GLOF magnitude is estimated as 7,576 $m^3s^{-1}$ and 8,478 $m^3s^{-1}$ at the dam and tailrace respectively.

The current flood design is based on GLOFs. We have modelled the future flood risk to UAHEP with focus on the potential changes to the monsoon flood and found that the future flood (under a large uncertainty) is lower than the GLOF risks.

### 4.3.2 Future non-climate uncertainty

**1. Sediment Load**

The abrasion of electromechanical components including turbine due to suspended load is one the risk to UAHEP. In this analysis, the changes in the annual sediment load with climate change are presented. Additionally, the shift in the distribution of annual power plant shutdown days required for sediment flushing with climate change is also evaluated.

**2. Upstream or downstream changes to socio-economic conditions manifested in competition for limited water resources:**

Based on the Socio-Economic Report and the Social Action Plan Report, no immediate growth of population or economy in the region is expected. Current uses of the Upper Arun River for drinking water, religious ceremony, and recreational fishing are assumed to be uniform in the future. **Potential future upstream diversions and other risks of competition for the available water for hydropower generation are not considered in this present analysis.** The Arun Valley is also known for its cardamom plantation. The effect of climate change on the agricultural production in the valley is outside the scope of this study. However, the agricultural activities close to the river might be affected by the project particularly due to daily fluctuation in the river water levels downstream of the intake site as well as downstream of the tailrace the powerhouse location. The 6-hour peaking pond reserves about 20 MCM (235 $m^3/s$ of design discharge accumulated over six hours). When this volume of water is released, the water level in the river fluctuates. This volume of water does not make much of a difference during the wet season. However, in the dry season when the average daily flow falls to 75-100 $m^3/s$, the sudden release of water could increase the river volume to twice its value in the duration of the day. Such variation could be detrimental to the agricultural activities in the riverbank. Thus, crop plantation in the flood plains in not recommended in the vicinity of the project intake site or the tailrace.

**3. Electricity Selling Prices**

The selling rate of electricity in Nepal for wet season (June-Nov) is NPR 4.80/KWhr, and for dry season (Dec-May) is NPR 8.40/KWhr. During the peak hours, the selling rate of electricity for dry season is 10.55/KWhr. The conversion rate is taken as 110 NPR/USD.

**4. Project Costs**

The initial cost of the project is taken 1337 Million USD. The operation and maintenance cost is 1.5% of capital costs per annum. The construction period is 6 years.

## 5. Seismic Risks

For seismic risk, to the best of the knowledge of the consultants, no hydropower facility built in Nepal in the last 50 years has yet been destroyed by a seismic event. However, earthquakes and landslides have damaged (and temporarily taken off-line) hydropower facilities in Nepal (see for example Sun Koshi). The eastern Nepali Himalayan region is seismically active with risk of catastrophic earthquake during the lifetime of the planned project (Bollinger et al., 2014). We therefore consider the possibility that the UAHEP project could fail due to earthquake within the next 30 years, but model that failure as a low-probability event.

# 5 Phase 3 of the Climate Change Risk Assessment

## 5.1 Introduction

Phase 3 of the IHA guidelines is the climate stress test. The outcome of this phase is the understanding of the project performance under different possible climate futures and identification of the conditions under which the project is vulnerable. A sensitivity analysis of the performance metrics is evaluated under a wide range of climate scenarios. The likelihood of failure or success of the project is identified based on either historical trends or future climate projections or a combination of both. Phase 3 addresses the risks factors identified in Phase 1 and the perturbation ranges defined in Phase 2. By the end of Phase 3, the potential risks and opportunities under future climate scenarios are quantified. If the project is found to be vulnerable to climate change, adaptations measures are designed in the Phase 4 of the analysis. Stress to the project with other non-climate risk factors might be performed in addition to climate stress test, as an additional risk assessment although it is not a requirement of the Climate Risk Assessment.

In the CRA of UAHEP, based upon the results of the Phase 2 analysis we proceed with Phase 3. Given the reasonably high quality of data available, and the interest of the stakeholders in a thorough stress test, a comprehensive version of the CRG Phase 3 stress test is developed here. The Phase 3 analysis consists of evaluation of the following performance metrics: 1) low (insufficient in the long term) flow (resulting in low financial performance); 2) high (flood) flow (resulting in damage to the structure, and potentially putting at risk the safety of those downstream); and 3) sediment load greater than that for which the project was designed. Climate response surfaces are developed for low flow analysis (streamflow, annual energy, financial performance) and sediment risks with changes in mean shifts in precipitation and temperature. In this report, we present a) low flow risks; and b) sediment risks through the development of climate response surfaces.

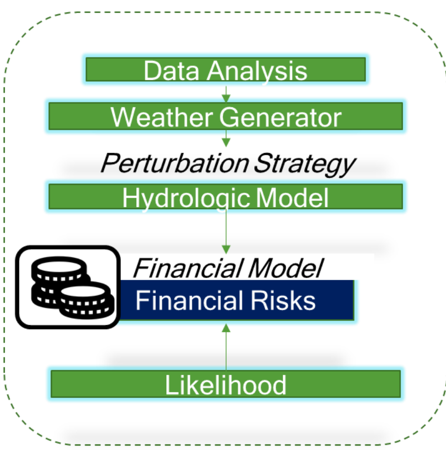


***Perturbation Strategy***

a) Percentage changes in Precipitation
-40% to +40%
b) Degree increase in Temperature
$0^{0}$C to $6^{0}$C

***Financial Model***

Net Present Value Estimation

*Figure 7 Flowchart showing the modeling chains in the development of response surface for long-term performance.*

The workflow for Phase 3 analysis is presented in Figure 7. The section 5.2 and the section 5.3 is organized as follow: 1) Weather generator; 2) Hydrologic model; 3) Energy Model; 4) Financial Model, 5) Sediment-Discharge Relationship, and 6) Response Surface.

## 5.2 Models Developed

### 5.2.1 Weather Generator

A stochastic weather generator is used to generate a daily time series of climate data (precipitation, and mean temperature) with similar characteristics as the original time series. The APHRODITE (1961-2007) is reshuffled by preserving the intra-annual and inter-annual variability to generate 50 years of synthetic data. A combination of autoregressive moving average (ARMA) model with K-nearest neighbor (KNN) resampling on daily and annual values was used to generate the synthetic data. The model consists of three state Markov chain to simulate the daily precipitation and its transition from one state to the other. The threshold that distinguishes dry days, wet days and extremely wet days are 10$^{th}$ percentile and 80$^{th}$ percentile respectively categorized for each month. Further details of the procedure followed can be found in Steinschneider and Brown (2013).

Fifteen traces of such time series were generated to capture the historical variability and the long-term processes. Once the traces were generated, mean changes to precipitation (expressed as a percentage increase/decrease) and temperature (degree increase) was applied to represent the perturbed climate scenarios. The generated climate traces have similar statistical properties but have marginally different mean, standard deviation and skew around the historical observations that represents the natural variability of climate in the basin (see Figure 8).

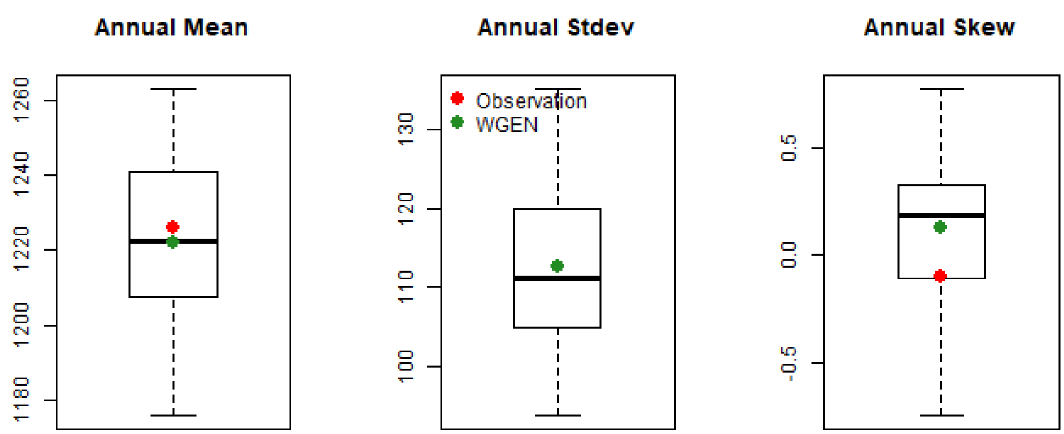


*Figure 8 Boxplots indicating the mean, standard deviation, and skew of the Properties of the climate traces compared to the observed value (15 trials and 50-years of APHRODITE precipitation). The red dot indicates the historical observation while the green dot represents the mean value for the weather-generated traces.*

### 5.2.2 Hydrologic Model

**Model Description**

The streamflow in the Upper Arun Basin consists of the contribution of summer monsoon precipitation, snowmelt, glacier melt, and base flow during the dry season. The hydrologic processes in the Upper Arun Basin are highly dependent on the temperature and its variation on a daily scale. The timing and peak of the snowmelt during spring and the contribution of the glacier melt to the flow in the basin is dependent on the temperature variation in the basin. Moreover, the basin has a high variation in the elevation consisting of all-year snowcapped mountains to terrain with high groundwater holding capacity. Thus, a suitable hydrologic model that can capture these processes well and at the same time is not very computationally expensive to do multiple runs under different climate scenarios and a range of internal variability at a daily time scale was required.

The distributed version of the HYMOD model (HYMOD-DS) was identified to be suitable for the modeling of the basin. This is a vector-based model that can work at either monthly or daily time scale and is relatively fast. It was implemented in MATLAB programming environment. The calibration of the model was performed using the Ohio Supercomputing facilities with parallel processing to speed the run time. The basin is divided into 23 Hydrologic Research Units (HRU's) based on their grid location. Each HRU is calibrated with a set of 15 parameters that were optimized using the genetic algorithm to search for the best combination of parameters that minimizes the Nash-Sutcliffe Efficiency (NSE) of the model. The model consists of the following five modules:

a) PET Hamon: The potential evapotranspiration (PET) using the Hamon method is estimated in mm as a function of daily mean temperature and hours of daylight.

b) Snow Module: The change in the snow volume is modeled by the ice accumulation and ablation rate governed by the snow degree day factor (DDFs) mass balance model (Moore, 1993; Stahl et al., 2008).

c) Glacier Module: The melting of glacier is modeled in a similar manner as the snow module. The glacier degree day factor ($DDF_g$) is a product of r and DDFs where $r > 1$ is a factor that accounts for faster melting rate of glacier compared to snow.

d) HYMOD Soil Moisture Accounting Module: Within each grid or unit, the direct runoff is routed with an instantaneous unit hydrograph (IUH) which is expressed by a gamma probability distribution function modeled as a linear series of N reservoirs with storage coefficient ($K_q$). The baseflow is estimated by a lumped reservoir with storage recession coefficient ($K_s$).

e) Lohman Routing Model: The runoff is routed into the channels using the diffusive wave approximation of the Saint-Venant equation (Lohmann et al. 1998) governed by the parameters wave velocity (Velo) and the diffusivity (Diff).

The modules were organized and run at a daily time scale with the input climate data. For further description on the modules, their parameters and their ranges, please refer to Wi et al. (2015).

**Updates on the hydrologic model since the submission of the interim report:** The hydrologic model was updated since the interim report in close consultation with the World Bank Panel of Experts. The recalibrated hydrologic model is presented in Figure 9 and Figure 10. This calibration captures the flow in the basin and is used for calculations related to the long-term flow (for economic and other analysis). A different calibration is presented in Figure 23 , that captures the peaks flows better (for PMF estimation).

**A) Long-term: Model Inputs, Calibration, and Validation Results**

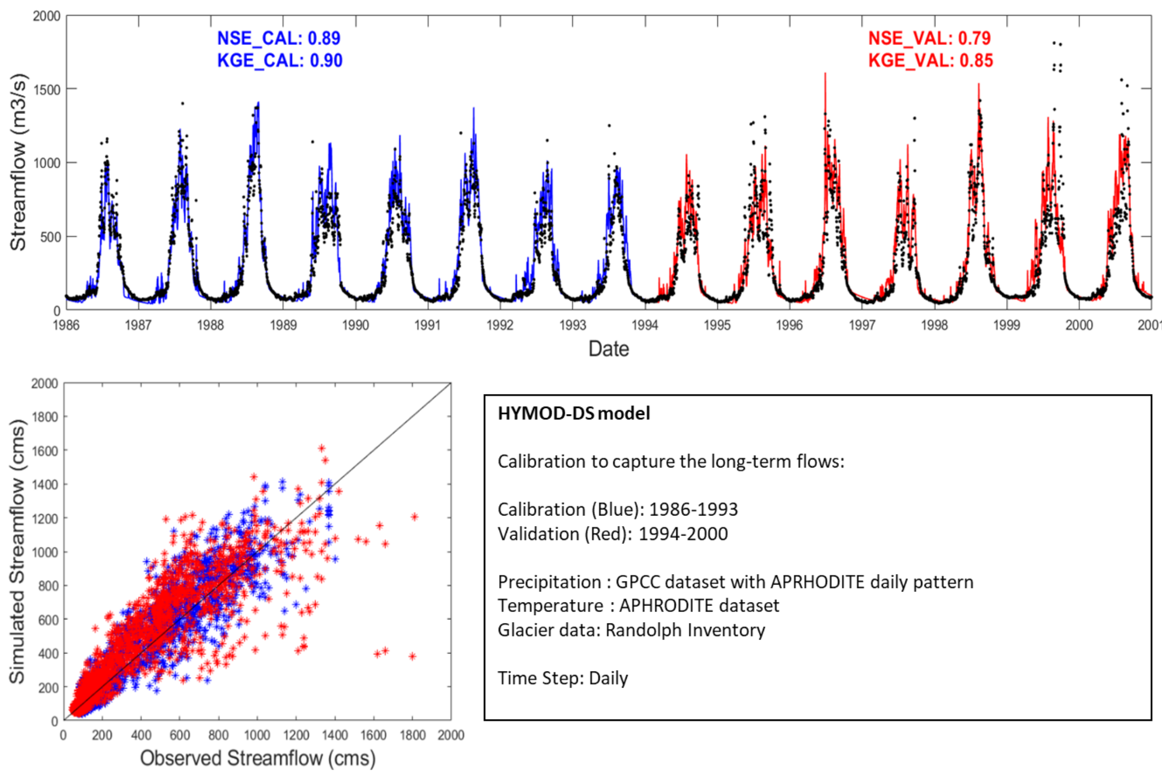


*Figure 9 Calibration and Validation of the hydrologic model. Model calibration and validation period along with precipitation and temperature dataset used in the hydrologic modeling*

The calibration and validation results of HYMOD-DS model is shown in Figure 9. Nash Sutcliffe Efficiency of 0.89 ad 0.79 indicates that the model is well-calibrated and well-validated. The model captures the underlying hydrologic processes in the basin and its relative contribution to the streamflow well. This calibration captures the long-term flow process and is used for evaluating the effect of climate change in the basin.

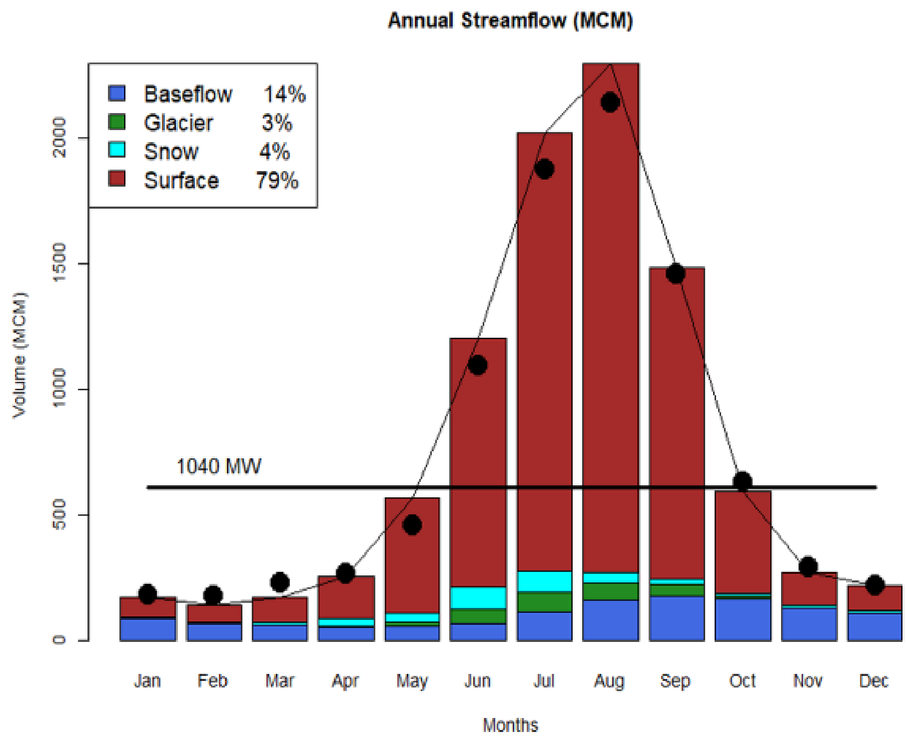


*Figure 10 Breakdown of the hydrologic model into components by months. The black dots indicate the historical observations, and the black line indicates the volume corresponding to the design discharge. The months Nov-Mar is dry season with high-value electricity selling rate (NRs. 8.80/KWh), the months Apr-Oct are wet season with low-value electricity selling rate (NRs 4.80/KWh).*

The breakdown of the simulation into components is illustrated in Figure 10. The bar-graph represents the simulated flow in different months, the colors in the bar represent contribution of different components to the flow: deep blue, baseflow; light blue, snowmelt; green, glaciermelt; maroon, direct precipitation runoff. The black dots on each month over the barplots represent the mean historical observed discharge. The black horizontal line shows the design discharge of the power plant, i.e., only the streamflow below the black line contributes to the hydropower generation by the power plant.

The Upper Arun basin lies roughly in the central Himalayas and is located in the Upper Ganges Basin. The summer monsoon advancing from the southeast is the main source of precipitation. Although a large portion of the upper catchment lies in the dry and arid Tibetan Plateau in the north of the Himalayas, the lower catchment enjoys heavy rain during summer. The moisture carried by the monsoon clouds precipitates as it hits the southern slopes of Himalayas in Nepal.

In the dry winter (November-March), it receives less than 200 mm of rainfall per year from the westerlies. Based on the results of the hydrologic model, we estimate that the snowfall contributes to about 4% of the streamflow. The hydrograph continues to rise as the monsoon advances. The peak flow and the floods in the streamflow occur in late July to August in the basin when the monsoon is at its peak. The hydrograph sharply recedes after August through October. We estimate that the direct runoff from the monsoon precipitation contributes to about 79% of the discharge. The groundwater recharge and release play a significant role in this basin. The monsoon rainfall is stored and released steadily throughout the year. The groundwater release contributes to provide baseflow all year round. We estimate that the baseflow contributes 14% of the total annual streamflow volume in the basin. Although there are numerous glaciers especially along the Himalayas and in the Tibetan plateau on the north of the Himalayas, their contribution in the streamflow is small relative to that of monsoonal precipitation. We estimate that with the current climate, the glacier melt contributes to less than 5% of the flow. The glacier melt occurs in the summer coinciding with the monsoon peaks.

**Caveat:** The hydrologic model is made with the best understanding of the basin with limited measurement of precipitation and temperature. We also do not have ground observations of the snow volumes, or availability of groundwater or its depth. The glacier volume was estimated using a relationship based on the glacial area derived from Randolph Glacier Inventory (RGI) 3.2 (Please refer to Annex 3: Data Analysis for further details). The model was built with the best available knowledge of the basin and seems to capture the process pretty well as we see it is calibrated.

### 5.2.3 The Energy Model

The energy generated by the UAHEP was estimated at an hourly time scale considering the reservoir and turbine operation using Equation 1.

$$Energy_{daily} = \sum_{o}^{24} \eta\gamma \, Q_{net,daily} \, H_{net,t} \, \Delta t$$

*Equation 1*

Where,

$\eta$ is the efficiency (0.8869), and $\gamma$ is 9.81 (acceleration due to gravity), $Q_{net, daily}$ is the daily discharge in MCM/hour, available after allowing for the environmental flow of 2.41 MCM/hour.

$H_{net,t}$ is the net hourly head that depends on the reservoir level fluctuating between Minimum Operating Level (1625 masl) and Full Supply Level (1640 masl), and also considers the headloss associated with the number of turbine units in operation.

The peak energy occurs when the hours (t) are [17:22], and non-peak energy occurs when the hours (t) are [1:16 &23, 24].

The model was provided by Dr. Peter Meier in excel and was translated into R programming language by the research team at UC. It is run on an hourly time scale. A sample of reservoir and turbine operation in dry and wet season is presented in Figure 11.

#### *5.2.3.1 Reservoir and turbine operation*

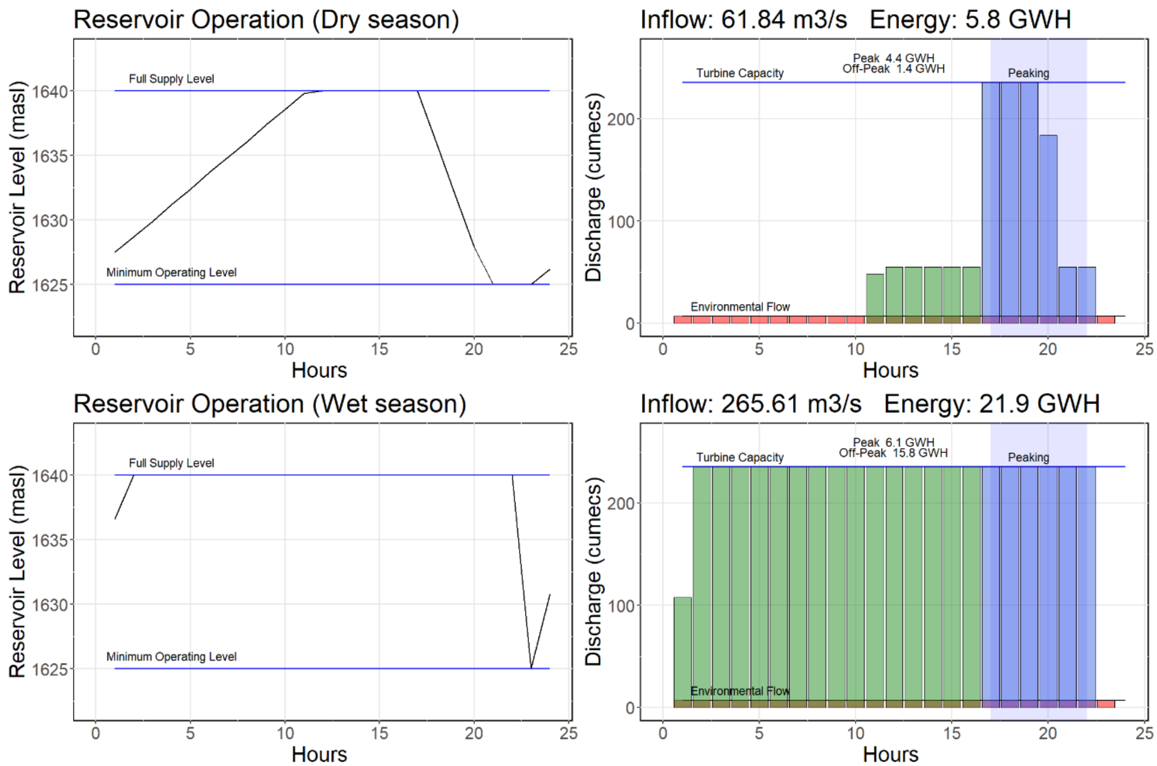


*Figure 11 Reservoir operation (left) and energy generation (right) scheme of the Upper Arun Hydroelectric Project run at an hourly time scale. In the reservoir operation graph, the water level fluctuates between the minimum operating level and the full supply level to allow for six hours peaking storage. In the energy generation graph, the discharge (after allowing for a minimum environmental flow and limited at the maximum by the turbine capacity), is used along with the reservoir head is used to estimate the off-peak energy (green) and the peak energy (blue). The top row represents a typical dry season operation, and the bottom row represents a typical wet season operation.*

#### *5.2.3.2 Sediment Flushing Regime*

The following rules were considered for sediment flushing:

- **Partial flushing mode:** 575 < Q < 1050 $m^3s^{-1}$
  Gates fully open for 48 hours, during which time no power generation. Units resume power generation for 7 days. If flow still above 575 $m^3s^{-1}$, flushing for 48 hours repeated.
- **Full flushing mode**: Q > 1050 $m^3s^{-1}$
  No power generation during that time. Sediment bypass tunnel is close. Low level outlet fully open (1590 masl). Dam gates are fully open for flushing.

The model was provided by Dr. Peter Meier in excel and was used in R programming language by the research team at UC. It is run on a daily time scale.

With climate change as the discharge increases, the number of power plant shutdown days required for sediment flushing also increases. The shift in the distribution of the annual power plant shutdown days as the climate shifts towards a wetter or a drier future is presented in Figure 12. To prevent overcrowding we only present the shift in some scenarios representing drier and wetter future.

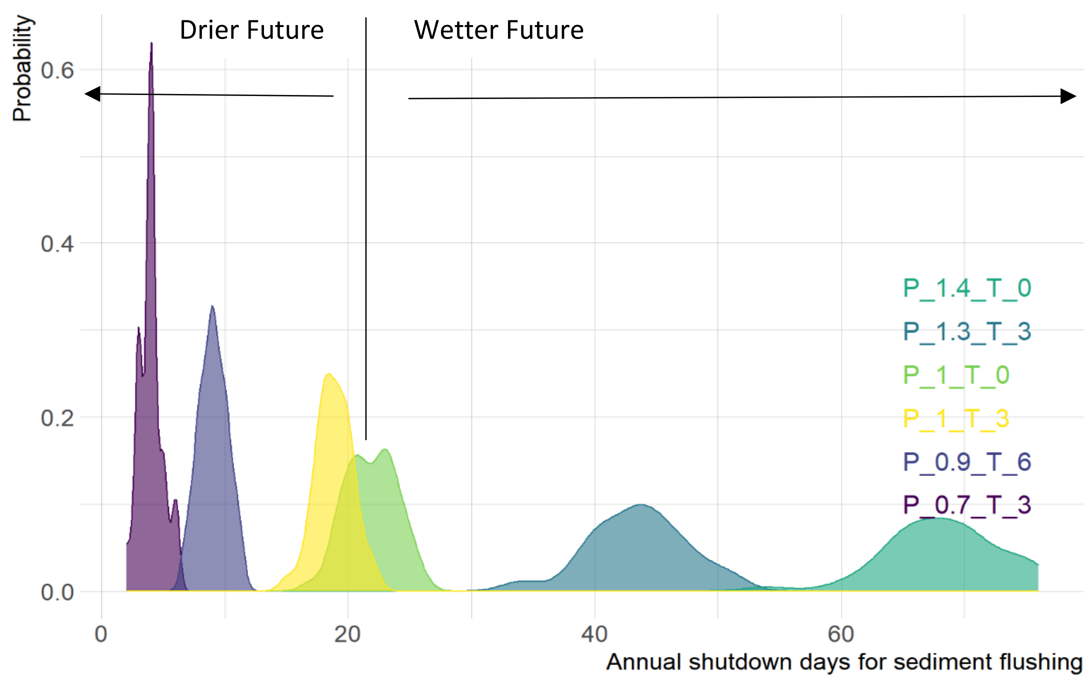


*Figure 12 Frequency distribution of annual power plant shutdown days for sediment flushing. The distribution becomes flatter with increased mean as for a scenario that is wetter than the current climate. The distribution becomes sharper with lower mean for a scenario that is drier than the current climate. Only a few climate scenarios are presented here to prevent overcrowding.*

This calculation of the number of power plant shutdown days is incorporated in the estimation of the annual energy under climate change.

### 5.2.4 The Financial Model

The financial model is summarized in Table 5 and Equation 2.

*Table 5 Variables in estimation of NPV of the project*

| S/No | Inputs | Units | Values |
|---|---|---|---|
| 1 | Selling Rate (r) | NPR/KWh | Wet season (Jun-Nov): 4.80<br>Dry season (Dec-May): 8.40 (Off-peak); 10.55 (Peak) |
| 2 | Capital Cost (C) | USD | 1337 Million USD |
| 3 | Annual O&M Cost (O) | USD/year | 1.5% of Cap Cost/year |
| 4 | Discount Rate (i) | % | 10 |
| 5 | Time Period (t) | Year | 50 |
| 6 | Conversion Rate | USD/NPR | 1/110 |

$$\textit{Annual Revenue} = \sum \boldsymbol{Energy}_{wet} * \boldsymbol{r}_{wet} + \boldsymbol{Energy}_{dry,peak} * \boldsymbol{r}_{dry,peak} + \boldsymbol{Energy}_{dry,off-peak} * \boldsymbol{r}_{dry,off-peak}$$

$$\boldsymbol{NPV} = \sum \frac{\textit{Annual Revenue} - \textit{Annual OM}}{(1+i)^t} - \boldsymbol{C}$$

*Equation 2*

### 5.2.5 Sediment-Discharge Relationship

Sediment is sampled at different time of the year using manual sampling techniques and instruments such as Swedish handheld sampler to estimate the sediment concentration in the Upper Arun River. Samples collected in 1990-1991 in the Feasibility Report (FSR-1991), UAHEP project intake site in 2018-2019 (UAHEP), and Arun-4 dam intake site further downstream of the project location in April-December 2018 (Arun-4) are compiled to derive seasonal sediment rating curves for Upper Arun Project. The seasonal sediment-discharge relationship used in the interim report was updated with a single all-year relationship.

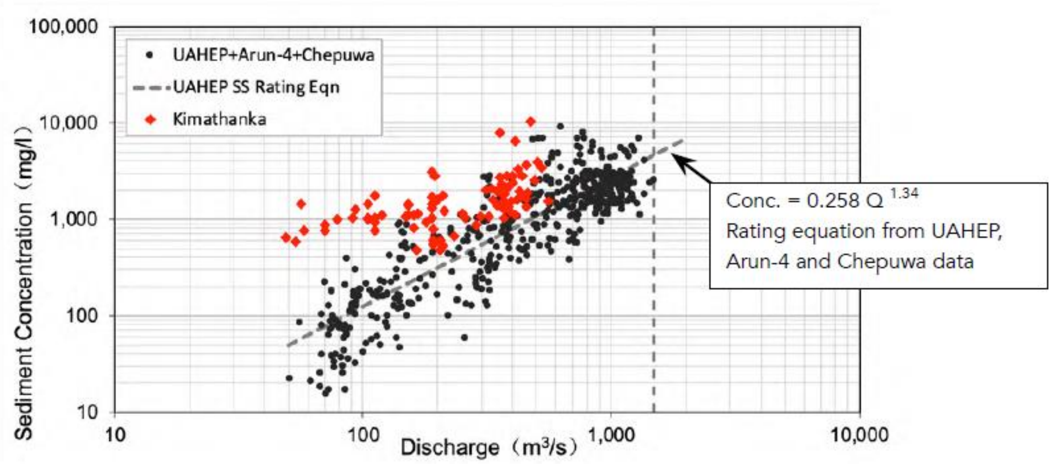


*Figure 13 Updated Sediment-Discharge rating curve established for UAHEP. Suspended concentration-discharge data from Kimathanka dam site (red), compared to the combined data from Chepuwa, UAHEP and Arun-4 datasets, and the rating equation resulting from these last 3 datasets.*

Since the interim report, the sediment-discharge relationship has been updated as presented in Figure 13 (Sediment concentration(S) = 0.258 $Q^{1.34}$). Instead of having seasonal relationships, now we have a single rating curve applicable throughout the year.

## 5.3 Response Surface: Changes in mean precipitation and temperature

The extent of climate perturbation is informed by the projected changes in the future climate by the GCMs. The GCMs are used only to inform the ranges of possible future climate, and not for the climate data itself (unlike the top-down approaches, which downscale GCM output for direct use in the modelling chain). A change of -40% to +40% with an increment of 10% each was applied to the daily precipitation time series. A change of warming by 0°C to 6°C with an increment of 1°C was applied to the daily temperature time series. Daily streamflow values were computed with the hydrologic model for each combination of perturbed precipitation and perturbed temperature.

### 5.3.1 Streamflow Generation

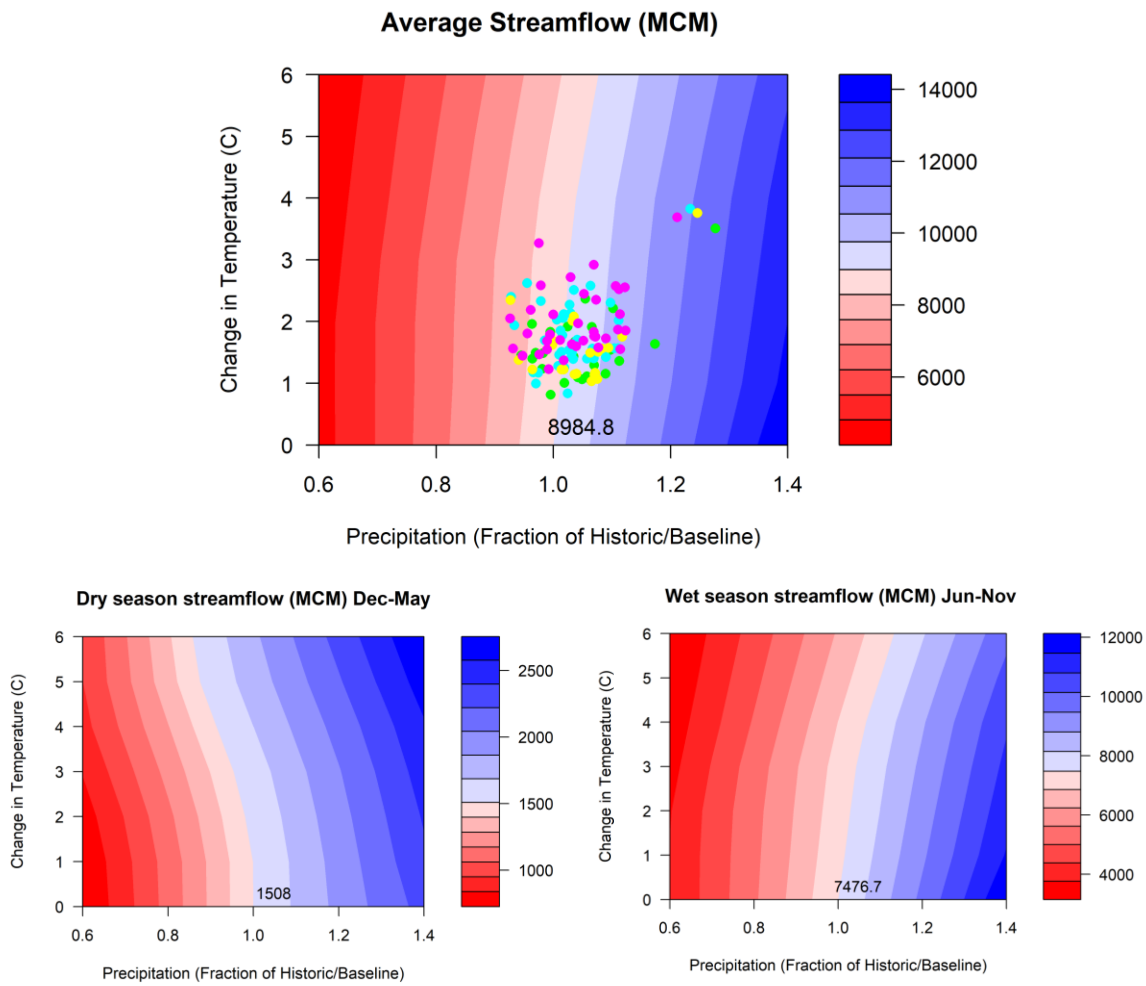


*Figure 14 Response surface for total annual, dry season, and wet season streamflow with changes in mean precipitation and temperature. The dots on the response surface represent the CMIP5 climate change projection (centered on year 2036). Representative concentration pathway (RCP) Green: RCP 2.6; Cyan: RCP 4.5; Yellow: RCP 6.0; Magenta: RCP 8.5.*

The following are the major findings of the study:

a) As the temperature increases, we see that the dry season flow is predicted to increase. With earlier snowmelt and glacier melt, the flow in the river pre-monsoon months, the dry season flow can be expected to increase.

b) The wet season flow on the other hand will decrease with increasing temperature as the snow and glacier melts earlier. The overall effect of increasing temperature is observed as an increase in the total annual flow in the river.

### 5.3.2 Energy and Financial Analysis:

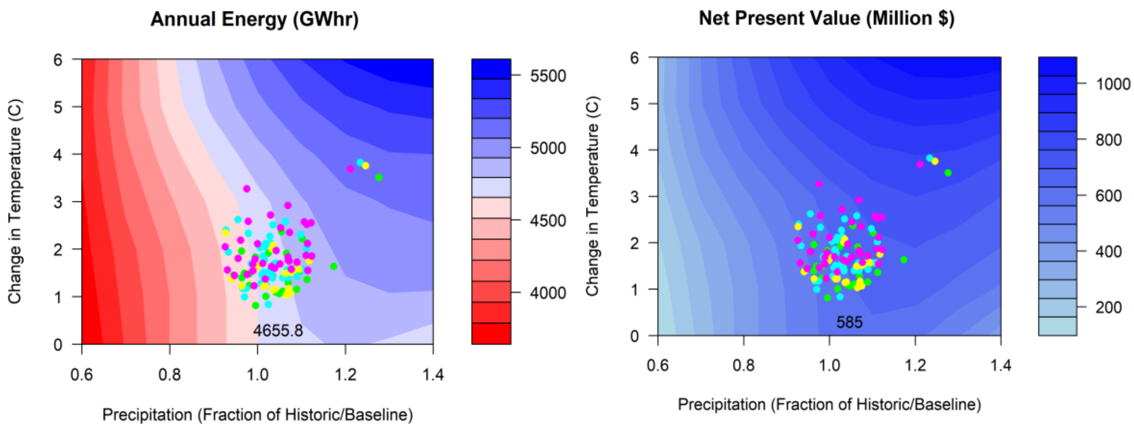


*Figure 15 Response surface for Annual Energy and Net Present Value. The dots on the response surface represent the CMIP5 climate change projection (centered on year 2036). Representative concentration pathway (RCP) Green: RCP2.6; Cyan: RCP 4.5; Yellow: RCP 6.0; Magenta: RCP 8.5*

Results and Discussion:

**Energy Response Surface**

a) According to the project design, the estimated annual energy of UAHEP project is 4492 GWhr. According to our simulation (using traces from weather generator, hydrologic model, simulation of hourly reservoir and turbine operation), our estimation of the energy under no climate change is 4655.8 GWhr which lies within 3% error and provides confidence on the use of modeling sequence for analyzing the system under climate change. -20% to +18% changes in the energy is predicted under precipitation perturbation (-40% to +40%) and temperature perturbation (+0 C to +6 C).

b) We observe that the annual energy is predicted to increase with increasing temperature. This is likely because, as temperature increases, the dry season flow increases which translates into an increase in the dry season energy. The response surface of the annual energy also takes into account the number of power plant shutdown days required for sediment flushing due to excessive sediment load.

**Net Present Value Response Surface**

a) The NPV of the project under current design is estimated in the economic analysis against the competitive energy option (oil in this case). The NPV is estimated as 580 million USD. In our analysis we used the selling price of electricity established by Nepal Electricity Authority (NEA), and the NPV value under no climate change was estimated as 585 million USD.

b) The response surface of NPV closely follows the pattern of the annual energy. The color of the surface is all blue indicating that the NPV remains positive even under the worst climate change scenario analyzed in this study.

c) Some of the climate models predict a decrease in the precipitation by up to 10% by mid-century. Such a reduction in the precipitation can cause between 1%-5% decrease in energy and a corresponding to 2%-10% decrease in the NPV values.

### 5.3.3 Sediment Analysis:

The response surface of the annual sediment load was obtained by coupling the Sediment-Discharge rating curve with the Hydrologic model, and perturbed climate traces from the weather generator (Figure 16). This analysis assumes that the relationship between sediment and discharge is stationary i.e., this relationship can be extrapolated for changes in the streamflow with changing temperature and precipitation. Further, this is a continuous simulation. It does not take into account, a sudden change in the sediment load with a one-time event such as a landslide or avalanche.

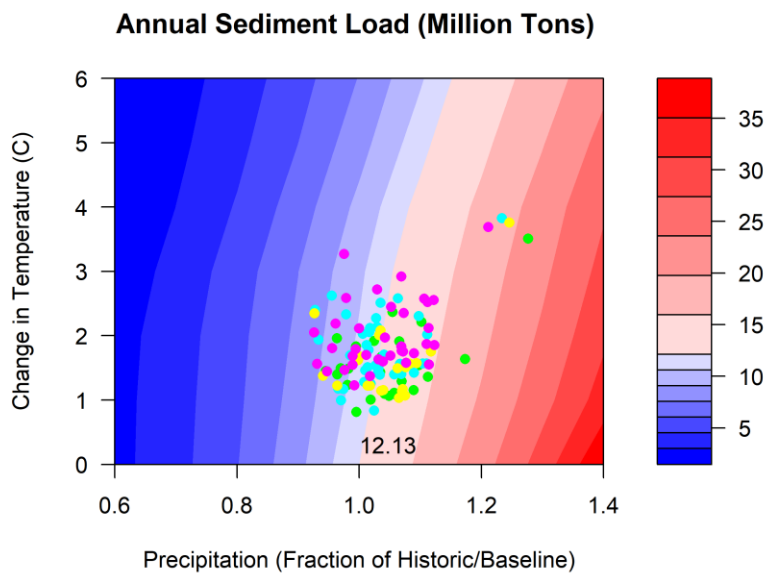


*Figure 16 Response surface for annual sediment load. The dots on the response surface represent the CMIP5 climate change projection (centered on year 2036). Representative concentration pathway (RCP) Green: RCP 2.6; Cyan: RCP 4.5; Yellow: RCP 6.0; Magenta: RCP 8.5.*

**Results and Discussions**

It is observed that the sediment load can be expected to increase in the basin with increase in precipitation and does not depend very much on the change in temperature. At this stage of project development, the type of turbine and its final design is not yet decided. We recommend that the hydropower planners to closely follow the IHA Sediment Management Guide in their design (https://www.hydropower.org/publications/hydropower-erosion-and-sedimentation-how-to-guide). Some recommendations are presented below:

a) For the UAHEP project, considering a high sediment load and the possibility of an increase in the sediment in the future, a real time sediment monitoring system is recommended. This system not only monitors the sediment concentration but automatically shuts down the power plant when the sediment concentration reaches a threshold value to prevent excessive damage to the electromechanical components. The recommended threshold (based on the values adapted by similar power plants in the Himalayan region) is between 4000-6000 PPM. Detailed economic tradeoff analysis between the loss due to electricity generation in the shutdown duration and added benefit with reduction in the operation and maintenance costs is required to find the suitable threshold for the power plant. It is beyond the scope of the Climate Risk Assessment analysis. It is strongly recommended to the detailed design team.

b) Consider installing coated turbines: Since the project is located in a steep geography and glacier-fed catchment, in the upper part of the catchment, the particles are sharp and are capable of eroding the turbines with high concentration of minerals above Moh's hardness of 5. Detailed economic tradeoff analysis between the additional costs of installing coated turbine and added benefit with reduction in the operation and maintenance costs is required to determine the type, thickness and frequency of coating. It is beyond the scope of the Climate Risk Assessment analysis.

## 5.4 Study of possible changes in the design flood in the UAHEP under climate

The UAHEP design flood is a conservative design. The project was designed to be safe against the PMF, which is generally larger than the 10,000-year return period flood. Moreover, the project is also vulnerable to the risks of Glacial Lake Outburst flood. As the estimated GLOF magnitude were larger than the estimated PMF, the design flood is governed by the GLOF estimate. The current design flood of the UAHEP project is based on the GLOF estimates (Dam: 7576 $m^3/s$, Powerhouse: 8478 $m^3/s$), which are larger than the PMF estimates (Dam: 4990 $m^3/s$, Powerhouse: 6060 $m^3/s$,), and the 1:10,000-year return period flood estimates by CSPDR (Dam: 4,870 $m^3/s$, Powerhouse: 5,550 $m^3/s$).

The purpose of this study is to evaluate if the project is safe against future flood. To achieve this goal, the research team at UC, followed the following steps:

a) Estimated the 10,000-year return period flood, evaluated if the estimates have changed in the past 30 years, and reported the uncertainty around such estimates.
b) Estimated the PMP and PMF values for the basin using the historical precipitation estimates and the hydrologic model. Estimated the projected changes in the extreme precipitation and the corresponding PMP and PMF in the future. Much of the research effort was spent in this section.
c) Compared the future PMF with the GLOF magnitude on which the design is based currently.

**a) 10,000-year return period flood**

The UC estimate with 10,000-year return-period flood at the Uwagaon Station is 2673 $m^3/s$. This estimate was obtained by fitting a Gumbel distribution to the annual maximum discharge at Uwagaon and estimating the 10,000-year return period flood. This is relatively much lower than the CSPDR estimate, and we would recommend that the CSPDR revisit the fit of the distribution and the estimated flood. Further details on the choice of the distribution, and the uncertainty associated with the estimated value is presented in Figure 39 through Figure 41 in Annex 3: Data Analysis.

**b) PMP and PMF estimation: Past and Future**

The current design is conservative (based on PMF and GLOF) considering high risks to the cumulative basin. This estimate is much higher than the estimate with 10,000-year return period flood. The PMF approach is usually selected for the design when the catastrophic consequences are possible and structural failure cannot be tolerated (ICOLD, 2014). Since the Arun basin has several other projects planned downstream of the UAHEP project, the failure of one UAHEP could result in catastrophe in the other projects as well.

The general process adopted in this study for PMP and PMF estimation are:

Step-1: Estimate the PMP using the historical data in the basin.

Step-2: Estimate the PMP using the outputs of different climate models in the basin. Calculate the changes in the PMP estimates in near future and far future with respect to the historical observations (from the climate models).

Step-3: Develop a hydrologic model that captures the major storms and floods in the basin.

Step-4: Estimate the PMF in the basin using the PMP and the hydrologic model. Calculate the changes in the PMF under climate change by supplying the alternate PMP to the hydrologic model.

Each of these steps is elaborated in the sub-headings 5.4.1-5.4.4 in this study.

### 5.4.1 Historical PMP estimates (Hershfield method)

An empirical formula for calculating the PMP is given by the Hershfield method (Hershfield, 1965). This empirical method is useful for quick analysis in data poor regions or where detailed study is not feasible. The previous works in this basin (CSPDR, 2020) used the Hershfield method to estimate the PMP and PMF in the basin. In this study, we also use the Hershfield method with the ARHO-GPCC dataset (same data used in the calibration and validation of the hydrologic model) for estimating the PMP and PMF values.

$$PMP = X_n + K_m * S_n$$

*Equation 3*

$$K_m = (R_{max} - X_{n-1})/S_{n-1}$$

*Equation 4*

Where,

*Xn* and *Sn*, are, respectively, the mean and standard deviation of the annual series of 3-day precipitation. $K_m$ is the frequency factor, $R_{max}$ is the maximum of the series, $X_{n-1}$ and $S_{n-1}$ are the mean and the standard deviation estimated by excluding $R_{max}$ from the series.

The frequency factor was estimated using precipitation data for each grid cell of the APHRO-GPCC dataset lying within the UAHEP catchment area. A maximum value of 12 was set as the threshold of $K_m$ following standard literature practices. We calculated the largest 3-day precipitation per year and estimated the PMP using Equation 3 and Equation 4. The results are presented in Figure 17.

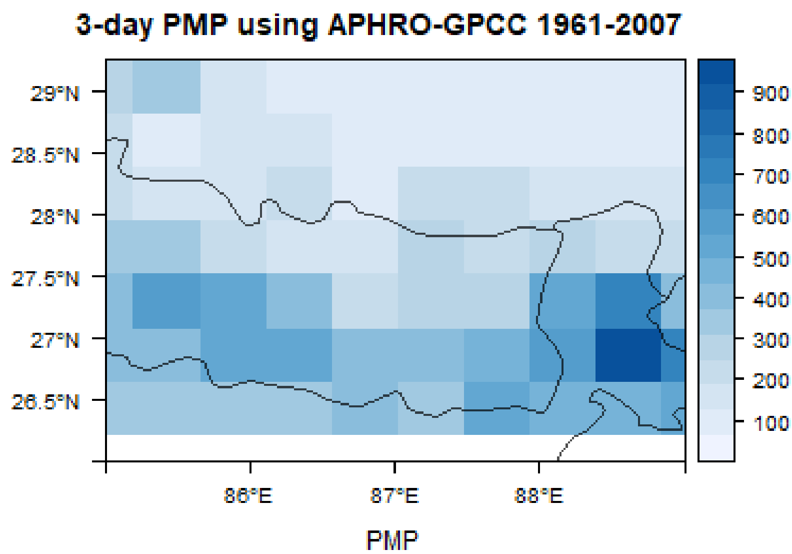


*Figure 17 Probable Maximum Precipitation was estimated using the 3-day precipitation following the statistical method developed by Hershfield.*

### 5.4.2 PMP under climate change (Moisture maximization approach)

We know with high confidence that global surface-level temperature will continue to increase with increasing atmospheric greenhouse gas concentration. Other meteorological changes are predicted as a function of the change in temperature and are known with less confidence. For instance, the Calusius-Clapeyron equation explains the variation of saturation vapor pressure with temperature (Koutsoyiannis, 2012). This equation is used to estimate the increase in atmospheric moisture holding capacity with increase temperature (roughly 7% per 1°C) and predict intensification of extreme precipitation under climate change globally (Allen & Ingram, 2002; O'Gorman & Muller, 2010). However, upper extreme precipitation (99.9$^{th}$ percentile events) is observed to scale significantly faster (between 5.7-15% per °C) depending on model parameters and details (Bao et al., 2017). Furthermore, the increase in storm runoff extremes is higher than that predicted using the Calusius-Clapeyron scaling for intensification of precipitation extremes (Yin et al., 2018). All these studies suggest that increasing temperature causes an intensification of precipitation and streamflow extremes.

To better understand the possible changes under climate change on extreme precipitation and PMP, we evaluated the changes in PMP using the moisture maximization method. Moisture maximization is the process of adjusting the moisture factors of high-efficiency storms to their maximum (World Meteorological Organization, 2009), and can be calculated with Equation 5.

$$PMP = P_{obs} \times \frac{PW_{max}}{PW_{obs}} = P_{obs} \times r$$

*Equation 5*

Where,

$P_{obs}$ is observed rainfall depth (mm), PW is the precipitable water (mm), $PW_{max}$ and $PW_{obs}$ are the maximum and observed PW (mm) of storm to be maximized. The ratio (r) is the maximization ratio.

Here, we used CORDEX data to estimate the future PMP values. The details of CORDEX data are presented in the section 4.2.2 of this report. The monthly distribution of daily rainfall events illustrates that the wet season rainfall (June-October) is driven by the Indian Summer Monsoon, and the rest of the months are dry with little precipitation (Annex 3: Data Analysis). Only a part of west Nepal receives some rainfall, which is driven by a westerlies jet (a different process than the summer monsoon). To ensure that we capture the ISMR process, we considered the daily data of only the wet season (June, July, August, September, and October) in this study.

The precipitable water (PW) in a moisture maximization technique that can be estimated using the dew point temperature. The CORDEX data unfortunately did not have the dew point temperature as an available output. Thus, the dew point temperature was estimated using Equation 6 and Equation 7, and was used to calculate the precipitable water following the procedure described in Rouhani & Leconte (2020).

$$T_d \approx T - \frac{100-RH}{5}$$

*Equation 6*

$$ln(PW) = A + B \times T_{dF}$$

*Equation 7*

Where,

$T_d$ is dew point temperature ($^0$C), RH is relative humidity (%), T is air surface temperature ($^0$C), $T_{dF}$ is dew point temperature in degrees Fahrenheit (F), and A and B are constants, A = −1.288; and B = 0.0384 (Smith, 1966).

The analysis was done for three different periods: 1971-2005 (35 years of historical simulations), 2021-2055 (35 years of near future projection) and 2056-2085 (30 years of far future projection). The procedure used for the estimation of PMP from the CORDEX data is summarized in a step-by-step fashion in Box 1.

Figure 18 summarizes the changes in the temperature, 3-day precipitation, relative humidity and the dew point temperature derived using Equation 6.

Figure 19 presents the derived values of precipitable water using Equation 7 and the maximum precipitable water.

Following the procedure described in Box 1 we calculated the PMP values for all the different future climate models. The results for each of the climate model individually is presented in Table 6, and spatial distribution of the ensemble mean is presented in Figure 21.

**Box 1: Stepwise process PMP estimation with CORDEX data**

Step-1 From the South Asia CORDEX dataset, retrieve daily time series of

1. Precipitation(P)
2. Surface Temperature (T)
3. Relative Humidity (RH)

Step-2 Calculate daily precipitable water (PW) from T and RH (Relative Humidity) using Equation 6 and Equation 7

Step-3 For each year (yr)

3.1 Calculate the 3-day cumulative precipitation ($P_{3day}$) and precipitable water ($PW_{3day}$).

3.2 Calculate the 3-day maximum precipitation ($P_{obs, yr}$) at max ($P_{3day}$).

3.3 Find the precipitable water ($PW_{obs, yr}$) corresponding to the event $P_{obs, yr}$.

3.4 Calculate the maximum precipitable water ($PW_{max, yr}$).

Step-4 Calculate the following:

$P_{obs}$ = max ($P_{obs, yr}$)

$PW_{obs}$ = Value of ($PW_{obs, yr}$) corresponding to $P_{obs}$.

$PW_{max}$ = $PW_{100}$ (100-yr PW from a GEV distribution fitted to annual max PW i.e., $PW_{max, yr}$

Step-5 Calculate maximization ratio (r) and PMP with $P_{obs}$, $PW_{obs}$, and $PW_{max}$ using Equation 5.

Step-6 Repeat Steps-1 through Step-6 for all climate models for historical, near future and far future.

Step-7 Evaluate the changes in PMP in the near future and far future compared to the historical

*Box 1 Procedure for PMP estimation using the CORDEX dataset.*

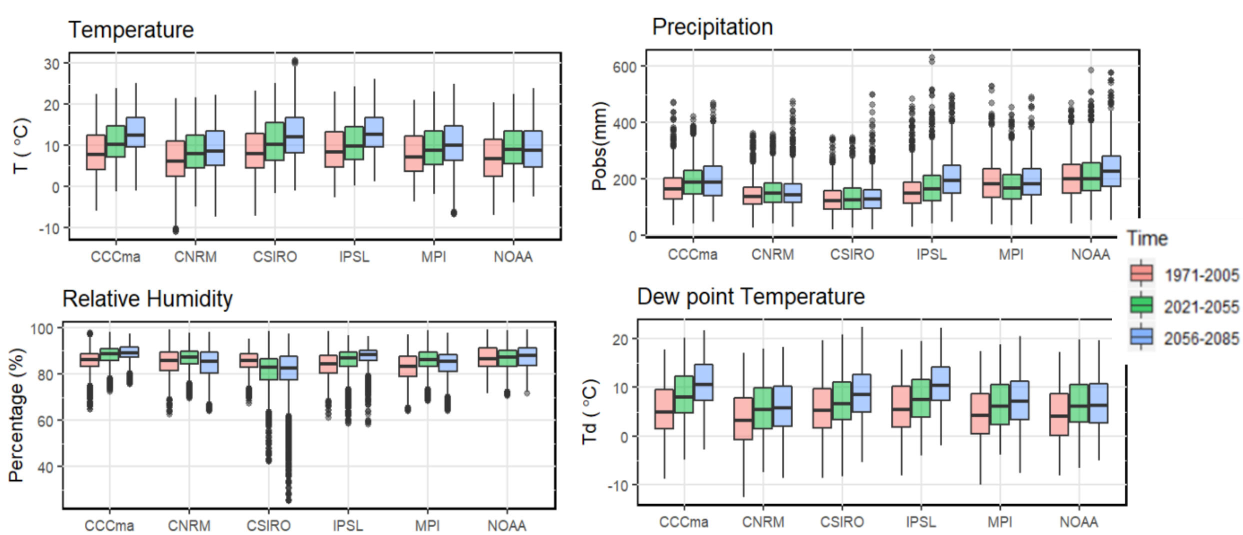


*Figure 18 CORDEX results of the extremes from CORDEX dataset for temperature, precipitation, relative humidity and dew point temperature for historical (1971-2005), near future (2021-2055), and far future (2056-2085). The points in the boxplot are the values for CORDEX grids laying within the catchment area.*

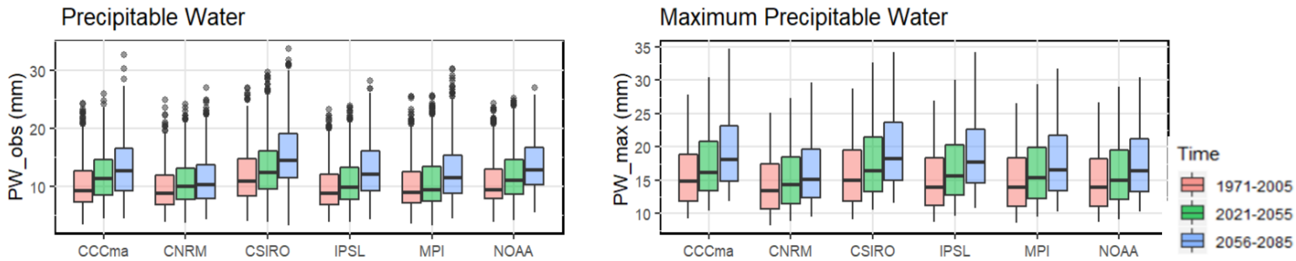


*Figure 19 Derived values of CORDEX results of precipitable water, and the annual maximum precipitable water for historical (1971-2005), near future (2021-2055), and far future (2056-2085). The points in the boxplot are the values for CORDEX grids laying within the catchment area.*

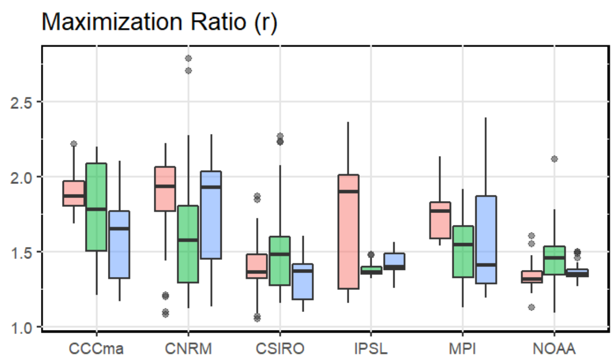


*Figure 20 Maximization ratio ($PW_{100}$/ $PW_{obs}$) projected by CORDEX climate models for historical (1971-2005), near future (2021-2055), and far future (2056-2085).*

*Table 6 The $P_{obs}$, and PMP (mean of all the grids) for all the climate models and near-future and far-future. These are the values averaged over the basin.*

| Model Name | $P_{obs}$ 1971-2005 | $P_{obs}$ 2021-2055 | $P_{obs}$ 2056-2085 | PMP 1971-2005 | PMP 2021-2055 | PMP 2056-2085 |
|---|---|---|---|---|---|---|
| CCCma-CanESM2 | 369 | 356 | 382 | 695 | 624 | 590 |
| CNRM-CERFACS-CNRM-CM5 | 314 | 307 | 345 | 576 | 486 | 608 |
| CSIRO-QCCCE-CSIRO-Mk3-6-0 | 297 | 295 | 356 | 408 | 451 | 470 |
| IPSL-IPSL-CM5A-LR | 376 | 456 | 428 | 639 | 626 | 608 |
| MPI-M-MPI-ESM-MR | 395 | 367 | 425 | 693 | 554 | 656 |
| NOAA-GFDL-GFDL-ESM2M | 401 | 414 | 485 | 537 | 606 | 659 |
| CCCma-CanESM2 | 369 | 356 | 382 | 695 | 624 | 590 |
| Ensemble Mean | 359 | 366 | 403 | 591 | 558 | 598 |
| **Percentage Increase for Ensemble Mean** | | **2%** | **12%** | | | |

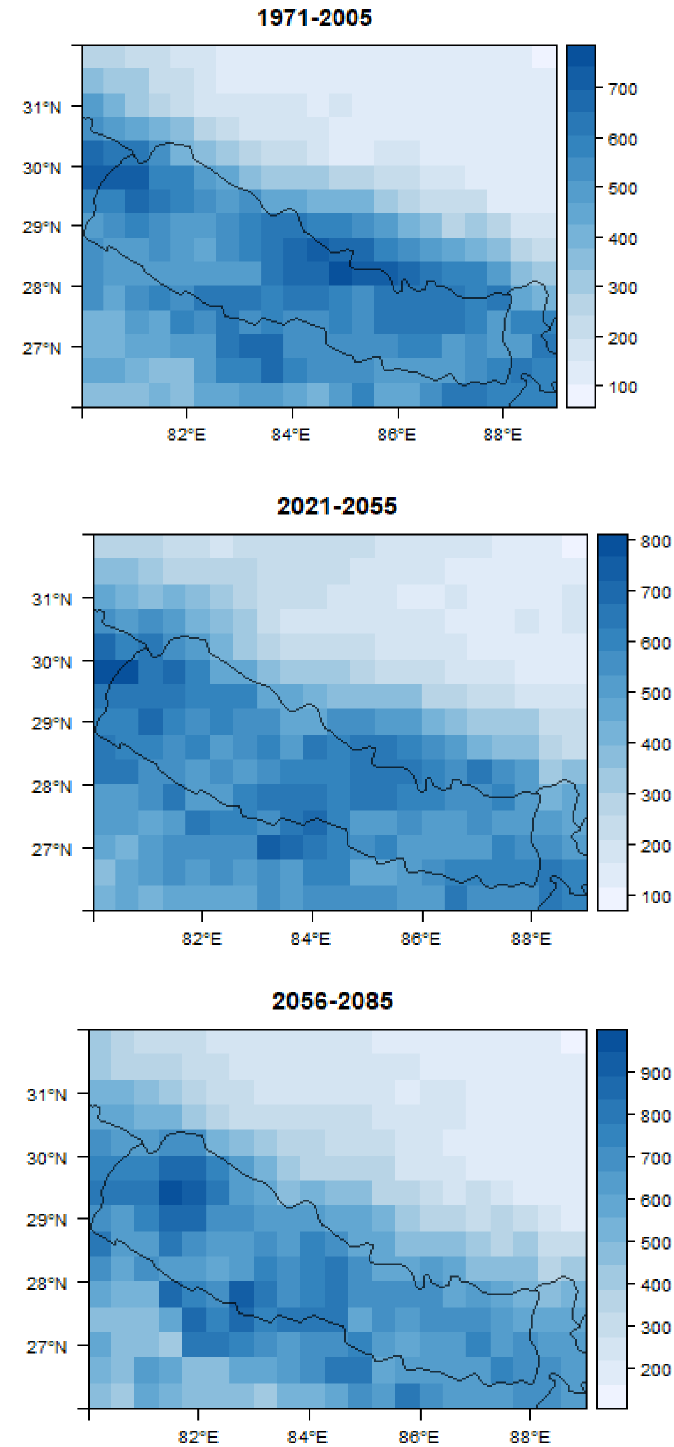


*Figure 21 Probable Maximum Precipitation (PMP) estimates for historical (1971-2005), near future (2021-2055), and far future (2056-2085). Ensemble mean is presented here. The units are in mm.*

**Results and Discussion**

1. The temperature, relative humidity, and the dew point temperature are projected to increase in the basin in the near future (2021-2055), and far future (2056-2085), compared to the historical (1970-2005) for different climate models in the CORDEX experiment for the grids laying within the catchment area (Figure 18).
2. The estimates of precipitable water, and the annual maximum precipitable water are projected to increase in the basin in near future (2021-2055), and far future (2056-2085), compared to the historical (1970-2005) for different climate models in the CORDEX experiment for the grids lying within the catchment area (Figure 19).
3. The 3-day maximum precipitation ($P_{obs}$) is projected to increase in the basin in the near future (2021-2055), and far future (2056-2085), compared to the historical (1970-2005) for different climate models in the CORDEX experiment in the catchment area (Table 6).
4. The behavior of the maximization ratio ($r = PW_{100}: PW_{obs}$) under warmer climate (for near future as well as far-future) is very erratic, and inconsistent amongst different climate model (Figure 20). This is a very strange and possibly an errant figure. While we are alternate approaches to estimate the maximization approach, we do not see any reason to believe that it would decrease in the future.
5. Thus, the PMP estimates ($PMP = P_{obs}*r$) are projected to increase only very slightly in the basin (Table 6 and Figure 21).

Although we observe an increase in the ensemble mean of the maximum 3-day precipitation by 12% by far future (Table 6), we do not see a corresponding increase in the PMP estimates as the maximization ratio (r) in Figure 20.

This analysis demonstrates that the current state of science in estimating the PMP under climate change is not mature enough to evaluate the possible increase in PMP with moisture maximization. We at the University of Cincinnati are researching alternate approaches to estimation of future flood risk, and advancement on estimation of the PMP, and PMF under climate change. The improved approach will reflect the estimated increase in the 3-day maximum precipitation in the basin. In the absence of analytical approaches capable of demonstrating this phenomenon, we submit this inferential statement: To our best understanding the PMP estimates in the future should be greater or equal to the estimated changes in the $P_{obs}$ as we have no reason to believe that the maximization ratio (r) would decrease in the future.

### 5.4.3 Development of Hydrologic Model to translate PMP to PMF

A HYMOD-DS hydrologic model (described in Section 5.2.2) was used to translate the PMP to PMF. The calibration parameters of the hydrologic model that was designed for the long-term flow were updated with new parameters that capture extreme events more accurately at the cost of the overall fit to the data. The updated model is presented in Figure 23 and Figure 24.

The daily precipitation of Num and Chepuwa station and the daily streamflow of Uwagaon station is presented in Figure 22. The downstream precipitation station Num receives high precipitation, which does not always appear in the upstream Chepuwa station. In addition, some spikes in the flow do not correspond to recorded precipitation in any of the stations, indicating either: a) there is a rainstorm that is not captured by either of the precipitation stations; or b) the flood was caused by some other event such as sudden snowmelt, or possibly a landslide.

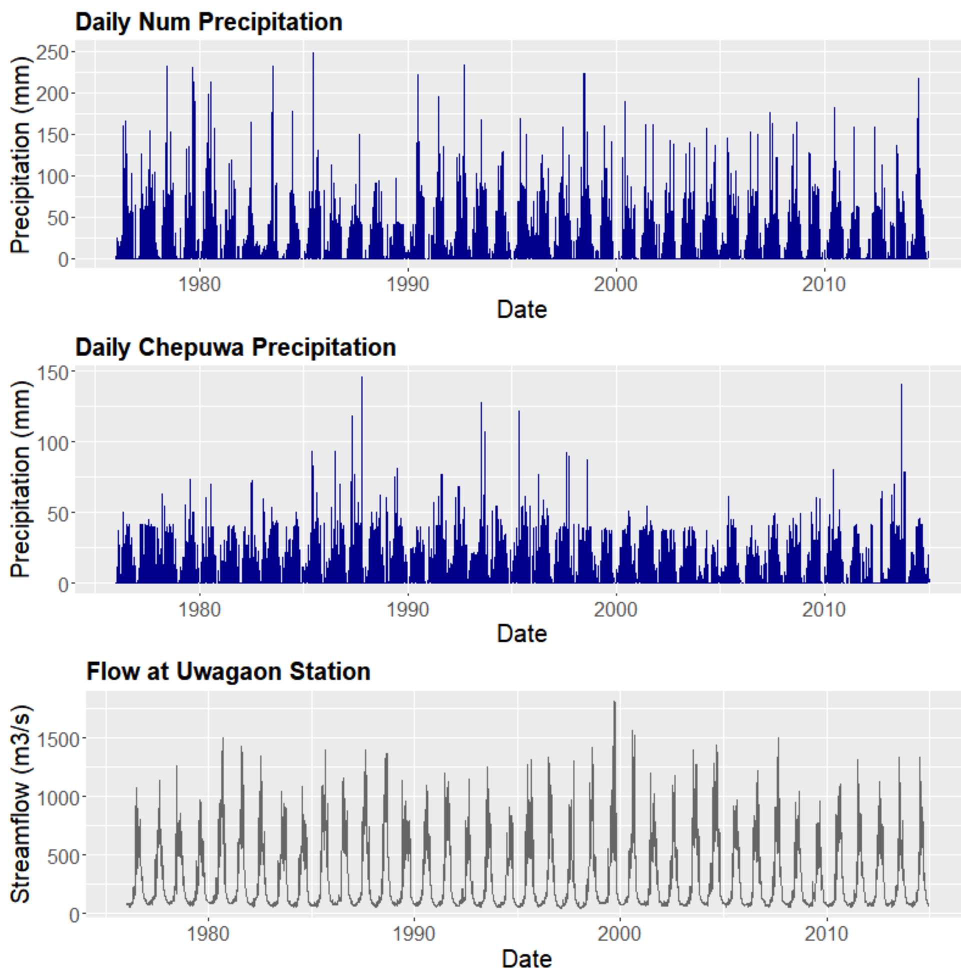


*Figure 22 Daily Precipitation at station Num (mm), and Chepuwa (mm) and the recorded flow at Streamflow station Uwagaon*

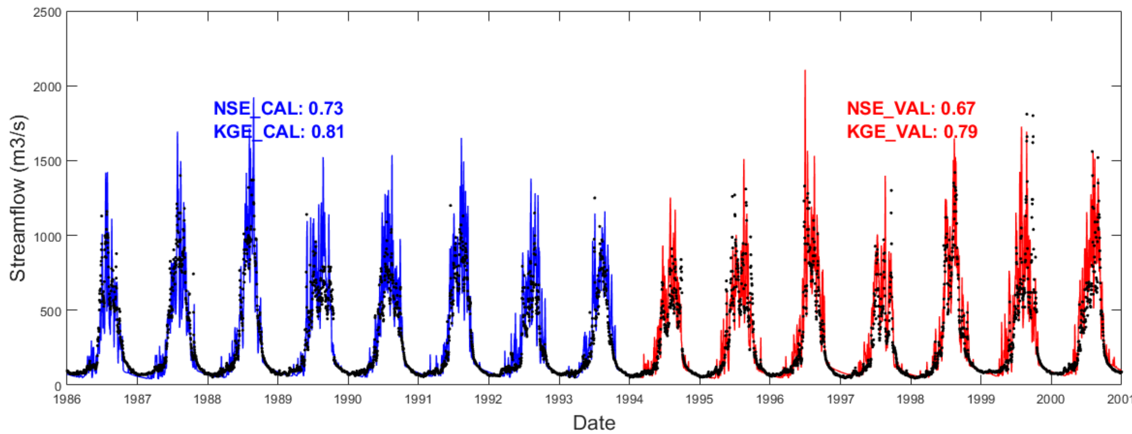


*Figure 23 Alternate calibration of the hydrologic model that captures the peak flows better to be used in the PMF estimation.*

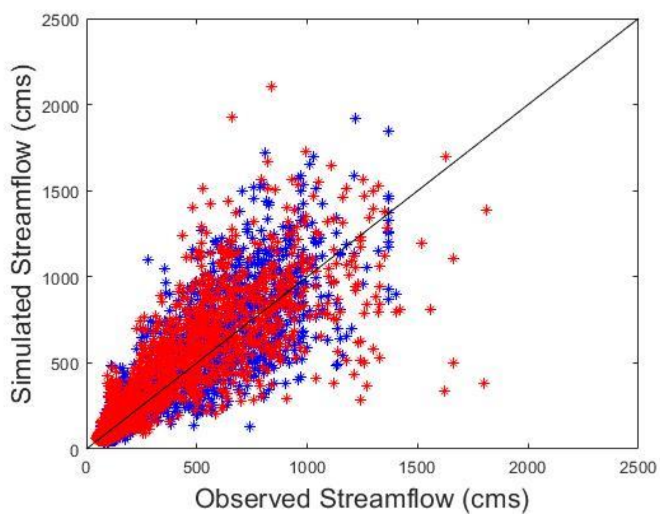


*Figure 24 Correlation plot for the calibration and validation of the hydrologic model that captures the peak flows better to be used in the PMF estimation.*

### 5.4.4 PMF estimation from PMP values

The PMF was estimated using two three different PMP scenarios (indicated by Scenario A, Scenario B, and Scenario C in this report). Scenario A and Scenario B w identified in the previous report (PMF Extract from Upper Arun FS 1991). An additional scenario (Scenario C) was added by the UC team.

Scenario A: The spillover effect of the PMP developed for the southern slopes of the Himalayas covering 150 km$^2$ of the Tibetan drainage area, which is located along the river valley close to the border and below the elevation of 3600 masl.

Scenario B: A second subbasin of 2150 km$^2$ from the Tibetan portion is taken as contributing to the PMP. This assumption takes account of the drainage area in Tibet up to an elevation of 4600 m.

Scenario C: The entire Upper Arun basin of 26,750 km$^2$ is taken as contributing to the PMP. This assumption takes account of the entire drainage area in Nepal and Tibet.

In this analysis, we implemented Scenario A, Scenario B, and Scenario C to estimate PMF. We ran the hydrologic model by replacing the precipitation in the area described in the scenarios with the PMP estimates. The rest of the catchment was assumed to receive normal precipitation during the PMF event. The largest of the PMF obtained from these alternate scenarios was taken as the PMP estimate under historical climate.

The previous report (Updated Feasibility Study and Detailed Engineering Design of UAHEP, CSPDR, 2019) had taken the ratio for allocation of 3-day PMP based on the precipitation recorded in Chepuwa station (375.5 mm) on 3-5 October 2012. The maximum precipitation in Chepuwa station (except this particular event) is close to 150 mm, and there was no storm recorded in the Num station downstream. Thus, this event was not used taken in our analysis. Instead, we chose the event of 19-21 October 1987 for the ratio allocation of 3-day PMP as shown in Table 7.

A suggestion was made to use a milder ratio to distribute the PMP values for the duration of 3-days to calculate the PMF values. We analyzed the distribution of 1-day and 3-day precipitation in Chepuwa and Num station (Figure 28 of Annex 3: Data Analysis) and proceeded with the ratio obtained in 19-21 October 1987.

The ratio-allocation in Table 7 was used to distribute the PMP values obtained as illustrated in Figure 17. This replacement was applied to the precipitation time series to simulate the flood of 26-28 August 1999 (the largest flood in the observed historical record). The hydrologic model was run, and the maximum value obtained between 1999 mid-August to mid-September was taken. The hydrologic simulation conducted to obtain the PMF estimates is presented in Figure 25.

The ratio of 1.1 was supplied by the client as an approximation of daily to instantaneous flow in the basin. Some literature suggests using a percentage as high as 25%, but the instantaneous flow is geography and local flow characteristics depended. Thus, the daily values are multiplied by 1.1 to obtain the instantaneous PMF estimate. It was observed that the PMF is highest when estimated with Scenario C.

*Table 7 Ratios for Allocation of the 3-day PMPs*

| Date | 1987-10-19 | 1987-10-20 | 1987-10-21 |
|---|---|---|---|
| Rainfall of Chepuwa Station (mm) | 22.0 | 146.2 | 12.5 |
| Ratio | .12 | .81 | .07 |

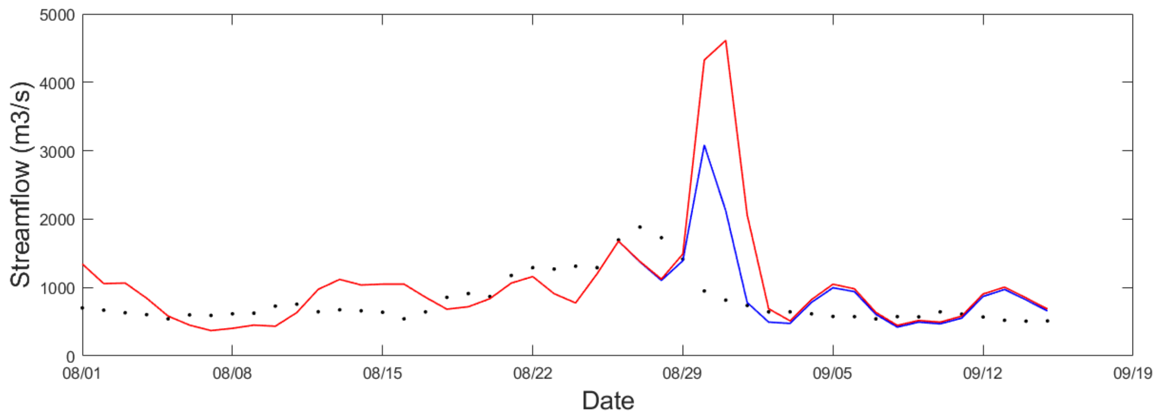


*Figure 25 PMF estimation. The black dots are historical observed flood in the basin. The blue is the PMF simulation under Scenario A and the red is the PMF simulation under Scenario C, Scenario B is not presented here.*

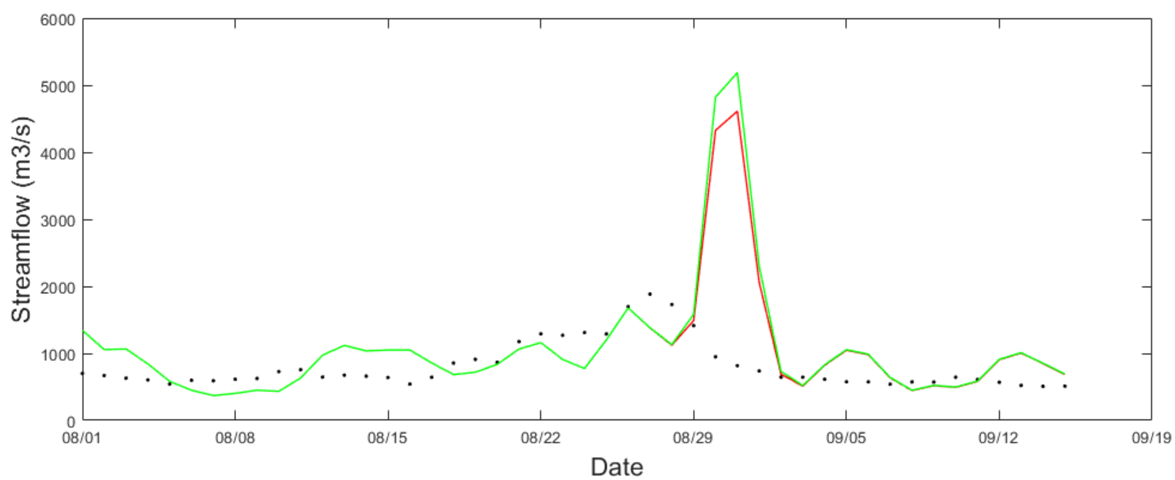


*Figure 26 PMF estimation under climate change. The black dots are historical flow in the basin. The red is the PMF calculated with the historical data (4612 $m^3s^{-1}$). The green represents the PMF calculated by increasing the 3-day precipitation by 12% in the far future (5186 $m^3s^{-1}$).*

To evaluate the changes in PMF under climate change, the PMP input to the hydrologic model was multiplied by the ratio of estimates for a) near-future/historical and b) far-future/historical obtained from Figure 21 for the catchment area defined by Scenario C. Since the near-future and far-future estimates of the PMP values from the CORDEX data are close to the historical estimates, almost no changes are found between the PMF calculated for the future and the PMF calculated for historical.

**What-if scenarios:**

As the erratic behavior of the maximization ratio under warmer climate in near-future and far-future is not well understood (Figure 20), a what-if scenario is run by increasing the PMP estimates by 12% based on the increase maximum 3-day precipitation by 12% in the far future (Table 6). Thus, the new PMF was estimated by increasing the PMP values by 12%. The results are presented in Figure 26. The projected future 3-day PMF in the basin is 5186 $m^3s^{-1}$.

**Results and Discussion**

1. The 3-day PMF was estimated in the basin to be 4612 $m^3$/s. When multiplied by 1.1, the instantaneous PMF estimated was 5073 $m^3$/s.
2. Despite an increase in the moisture availability in the atmosphere, the PMP values were almost same in the historical and future projection because of the maximization ratio. The results of the what-if scenario indicated that the 3-day PMF is projected to be 5186 m, corresponding to a 12% increase in 3-day max precipitation estimates in the far future. When multiplied by 1.1, the instantaneous PMF was estimated as 5704 $m^3$/s for far future.

**c) Comparison of future PMF and GLOF magnitude**

The GLOF in the basin is estimated as 7576 $m^3$/s at the Dam location and 8478 $m^3$/s at the Powerhouse location. There is a tributary joining the Arun River downstream of the intake site before the powerhouse. These estimates are higher than the PMF estimates not only for the historical climate but also for the future.

### 5.4.5 Final Comments on the current design flood under climate change.

1. Although the quantitative analysis indicates that the PMF is not likely to increase with climate change, we recommend an increase in the magnitude of the 3-day PMF by 12%-15% to account for an increase in the 3-day precipitation by 12% on average in the far future. Thus, the suggested design PMF is 5704 $m^3$/s.
2. The UAHEP faces GLOF risks and the current design is based on the dam break analysis of the glacial lakes. With increasing temperature, the probability of occurrence of GLOFs in the future may increase. The effect of climate change on GLOF behavior is not studied here and is beyond the scope of this assessment.
3. This study also does not consider the flood risks to the project due to a landslide, sudden avalanche, or earthquake-induced increase in water level or natural hazards. A detailed geo-hazard analysis and disaster planning is recommended to understand these risks to the project.

# 6 Phase 4 of the Climate Change Risk Assessment

**Suggested design modification or operational changes to improve climate resilience**

## 6.1 Low flow risks

The long-term performance of the project is robust to climate change, and no modification is recommended. Some climate models predict a decrease in the precipitation by 10% by mid-century. We estimate that such a reduction in the precipitation would decrease energy production by 1%-5%.

In our previous experience with Kabeli-A Hydroelectric Project, the terms and conditions defined in the power purchase agreement determined the financial success of the power plant. It was found that the PPA was restrictive with high penalties for failing to deliver the promised quantity of electricity and the project was vulnerable mostly during the months of April-June (Wasti and Ray, 2019). At this stage no PPA is available for UAHEP, which presents an opportunity to design the PPA with flexibility in the rising limb of the hydrograph.

## 6.2 Sediment risks

The UAHEP faces high sediment load, which is projected to increase in the next 30 years with climate change. We recommend the installation of coated turbines to increase sediment robustness. Timely sediment flushing schedule is designed for UAHEP to reduce the amount of sediment entering the turbine based on the input discharge. With increased sediment (as a function of increase in discharge), the powerplant shutdown time might increase. Under normal operation (i.e., in days with no flushing), the sediment particle abrade the turbines. For uncoated Francis turbine, Pradhan (2004) reported an efficiency reduction of 4 % at the best efficiency point and of 8 % at part load due to abrasion.

From experience in hydropower in Nepal (Kabeli A Hydroelectric Project), the turbine is replaced every 7 years, allowing the loss in efficiency to drop upto 15.5% before replacement. Due to climate change as the sediment concentration increases, thus the loss in efficiency of turbine per year is projected to increase. We estimate that the increase in sediment concentration by a 50% doubles the turbine replacement frequency and the replacement expenses during the project lifetime. For further details, see Wasti and Ray (2019). It is recommended that a do a cost-tradeoff analysis for turbine coatings.

## 6.3 High flow risks

The PMF is likely to increase with climate change, but the increased value estimated in this study is lower than the current design flood value, which was based not on a precipitation event, but on a GLOF event. If the PMF increases in the future by 15%-20% (not supported by calculations based on available methods and data), then the result would be an increase in projected extreme precipitation by 12% on average by 2056-2085. The 12% increase in current estimates of PMF would not exceed the value on which the design is now based, derived on the occurrence of a GLOF.

# 7 Phase 5 of the Climate Change Risk Assessment

**Monitoring and Evaluation**

Design of resilient infrastructure under an uncertain future climate remains incomplete without timely monitoring and evaluation of performance indicators. Monitoring and real-time detection of changes to stress indicators, and critical transitions of the tipping points, is essential to ensure success of the project and implementation of the adaptation plan if and when necessary (Haasnoot et al. 2018). Monitoring of the status and trends of the risk factors is essential to anticipate the potential costs and opportunities after the commission of the project.

The following monitoring is recommended:

a) Monitor the area and volume of upstream glaciers and glacier lake. Actively track the possibility of GLOF events and invest in an emergency response plan.
b) Continuously monitor the sediment concentration at the project location.
c) Establish continuous streamflow monitoring stations in the upstream catchment, if possible.
d) Carefully observe temperature in the basin and detect any shifts in the snowmelt season. The difference in dry season and wet season electricity pricing plays an important role in the financial performance of the project.

# 8 Summary of the findings of the Climate Change Impact Assessment Report

The results of this assessment are based on the climate change risk assessment to the UAHEP project conducted following the guidelines defined in the IHA Climate Resilience Guide. In general, the findings of this updated report reconcile with the findings of the AUS11077 report produced in 2015. The design of 1040 MW project seems to be robust to climate change and performs well under warmer and wetter climate scenarios. With increased temperature, early melting of snow is likely to increase the dry season energy generation.

**Comments on low flow risk:** The project appears to be robust to climate change-induced decreases in long-term average streamflow. With increased temperature the low flow during the dry months, especially February and March, is likely to increase with increased snow and glacier melt. Most of the GCMs agree on the likelihood of such warming by mid-century. The current estimation of the annual energy generation of 4492 GWhr appears to be a safe estimate. Some climate models predict a decrease in the precipitation by 10% by mid-century. Such a reduction in the precipitation would cause a decrease in energy production of 1%-5%.

**Comments on sediment risk:** The historical sediment load in the project location is high. Our analysis indicates that with an increase in precipitation, most likely the sediment load would increase. Furthermore, with increased glacier melt activities and possible avalanches, there is higher chance of increased sediment load in the basin. At this stage of the project with the turbine design and settling basins not yet finalized, it is recommended that a comprehensive sediment management strategy be implemented, including sediment-guided operations (closing the plant when concentration reach certain threshold values), and a detailed cost-benefit analysis be conducted to consider investing in hard-coated turbines.

**Comments on high flow risk:** The 10,000-year return period flood in the basin is lower than the PMF estimate. The streamflow in the basin is driven by monsoon precipitation. Under current climate, the models indicate that the 3-day maximum precipitation on the basin is likely to increase by 12% by 2056-2085. Thus, it is recommended that the design PMF be increased by 15%-20%. Both the 10,000-year flood and the climate-change-increased PMF are lower than the design flood for the UAHEP, which is based on GLOF risk, and therefore no change to project design flood is recommended.

**Comments on GLOF risk:** The GLOF risk, and the impact of climate change on GLOF risk is not evaluated quantitatively in this analysis. However, due to increasing temperature, glacier melt processes are likely to be increase. Regular monitoring of the glacial lake and establishment of early warning system is recommended. Furthermore, it is recommended to perform a detailed geo-hazard analysis and disaster risk assessment to quantify the flood risk associated with landslides, avalanches, and earthquakes.

References

Allen, M. R., & Ingram, W. J. (2002). Constraints on future changes in climate and the hydrologic cycle. Nature, 419(6903), 224-+. https://doi.org/10.1038/nature01092

Baidya, S. K., Shrestha, M. L., & Sheikh, M. M. (2008). Trends in daily climatic extremes of temperature and precipitation in Nepal. Journal of Hydrology and Meteorology, 5(1), 38-51.

Bao, J., Sherwood, S. C., Alexander, L. V., & Evans, J. P. (2017). Future increases in extreme precipitation exceed observed scaling rates. Nature Climate Change, 7(2), 128-+. https://doi.org/10.1038/NCLIMATE3201

Bohlinger, P., & Sorteberg, A. (2018). A comprehensive view on trends in extreme precipitation in Nepal and their spatial distribution. International Journal of Climatology, 38(4), 1833-1845. https://doi.org/10.1002/joc.5299

Eriksson, M., Xu, J., Shrestha, A. B., Vaidya, R. A., Santosh, N., and Sandström, K. (2009). The changing Himalayas: impact of climate change on water resources and livelihoods in the greater Himalayas. International centre for integrated mountain development (ICIMOD), .

G. Huffman, D. Bolvin, D. Braithwaite, K. Hsu, R. Joyce, P. Xie, 2014: Integrated Multi-satellitE Retrievals for GPM (IMERG), version 4.4. NASA's Precipitation Processing Center, accessed 21 January, 2020, ftp://arthurhou.pps.eosdis.nasa.gov/gpmdata/

G. Huffman, D. Bolvin, D. Braithwaite, K. Hsu, R. Joyce, P. Xie, 2014: Integrated Multi-satellitE Retrievals for GPM (IMERG), version 4.4. NASA's Precipitation Processing Center, accessed 25 February, 2020, ftp://arthurhou.pps.eosdis.nasa.gov/gpmdata/

Grinsted, A. (2013). "An estimate of global glacier volume." Cryosphere, 7(1), 141-151.

Hamed, K. H. and Rao, A. R. (1998). A modified Mann-Kendall trend test for autocorrelated data. Journal of Hydrology, 204(1–4): 182–196. <doi:10.1016/S0022-1694(97)00125-X>

Hershfield, D. M. (1965). Method for estimating probable maximum rainfall. Journal‐American Water Works Association, 57(8), 965-972.

Kendall, M. (1975). Rank Correlation Methods. Griffin, London, 202 pp.

ICOLD (International Commission on Large Dams) (2014). Integrated Flood Risk Management. ICOLD Bulletin 156.

Kamiguchi, K., Arakawa, O., Kitoh, A., Yatagai, A., Hamada, A., and Yasutomi, N. (2010). "Development of APHRO_JP, the first Japanese high-resolution daily precipitation product for more than 100 years." Hydrological Research Letters, 4 60-64.

Koutsoyiannis, D. (2012). Clausius-Clapeyron equation and saturation vapour pressure: simple theory reconciled with practice. European Journal of Physics, 33(2), 295-305. https://doi.org/10.1088/0143-0807/33/2/295

Kumar, K. K., Rajagopalan, B., & Cane, M. A. (1999). On the weakening relationship between the Indian monsoon and ENSO. Science, 284(5423), 2156-2159. https://doi.org/10.1126/science.284.5423.2156

Lohmann, D., Raschke, E., Nijssen, B., and Lettenmaier, D. P. (1998). "Regional scale hydrology: I. Formulation of the VIC-2L model coupled to a routing model." Hydrological Sciences Journal-Journal Des Sciences Hydrologiques, 43(1), 131-141.

O'Gorman, P. A., & Muller, C. J. (2010). How closely do changes in surface and column water vapor follow Clausius-Clapeyron scaling in climate change simulations? Environmental Research Letters, 5(2), 025207. https://doi.org/10.1088/1748-9326/5/2/025207

Pfeffer, W. T., Arendt, A. A., Bliss, A., Bolch, T., Cogley, J. G., Gardner, A. S., Hagen, J., Hock, R., Kaser, G., Kienholz, C., Miles, E. S., Moholdt, G., Moelg, N., Paul, F., Radic, V., Rastner, P., Raup, B. H., Rich, J., Sharp, M. J., Andeassen, L. M., Bajracharya, S., Barrand, N. E., Beedle, M. J., Berthier, E., Bhambri, R., Brown, I., Burgess, D. O., Burgess, E. W., Cawkwell, F., Chinn, T., Copland, L., Cullen, N. J., Davies, B., De Angelis, H., Fountain, A. G., Frey, H., Giffen, B. A., Glasser, N. F., Gurney, S. D., Hagg, W., Hall, D. K., Haritashya, U. K., Hartmann, G., Herreid, S., Howat, I., Jiskoot, H., Khromova, T. E., Klein, A., Kohler, J., Konig, M., Kriegel, D., Kutuzov, S., Lavrentiev, I., Le Bris, R., Li, X., Manley, W. F., Mayer, C., Menounos, B., Mercer, A., Mool, P., Negrete, A., Nosenko, G., Nuth, C., Osmonov, A., Pettersson, R., Racoviteanu, A., Ranzi, R., Sarikaya, M. A., Schneider, C., Sigurdsson, O., Sirguey, P., Stokes, C. R., Wheate, R., Wolken, G. J., Wu, L. Z., Wyatt, F. R., and Randolph Consortium. (2014). "The Randolph Glacier Inventory: a globally complete inventory of glaciers." J.Glaciol., 60(221), 537-552.

Pradhan PMS (2004) Improving sediment handling in the Himalayas:1-6
https://www.un.org/esa/sustdev/sdissues/energy/op/hydro_pratik_pradhan.pdf

Rouhani, H., & Leconte, R. (2020). Uncertainties of Precipitable Water Calculations for PMP Estimates in Current and Future Climates. Journal of Hydrologic Engineering, 25(3)https://doi.org/10.1061/(ASCE)HE.1943-5584.0001877

Sanjay, J., Krishnan, R., Shrestha, A. B., Rajbhandari, R., & Ren, G. (2017). Downscaled climate change projections for the Hindu Kush Himalayan region using CORDEX South Asia regional climate models. Advances in Climate Change Research, 8(3), 185-198.

Schneider, Udo; Becker, Andreas; Finger, Peter; Meyer-Christoffer, Anja; Rudolf, Bruno; Ziese, Markus (2011): GPCC Full Data Reanalysis Version 6.0 at 0.5°: Monthly Land-Surface Precipitation

Shrestha, A. B., Bajracharya, S. R., Sharma, A. R., Duo, C., & Kulkarni, A. (2017). Observed trends and changes in daily temperature and precipitation extremes over the Koshi river basin 1975-2010. International Journal of Climatology, 37(2), 1066-1083. https://doi.org/10.1002/joc.4761

Sigdel, M., & Ikeda, M. (2012). Summer monsoon rainfall over Nepal related with large-scale atmospheric circulations. J Earth Sci Climate Change, 3(112), 2.

Smith, W. L. (1966). Note on the relationship between total precipitable water and surface dew point. Journal of Applied Meteorology, 5(5), 726-727.

Suman, M., & Maity, R. (2020). Southward shift of precipitation extremes over south Asia: evidences from coRDeX data. Scientific Reports, 10(1), 1-11.

Wasti, A. and Ray, P., 2019. Kabeli-A Run-of-River Hydroelectric Project, Climate Change Risk Analysis for projects in Kenya and Nepal. Deltares, FutureWater and University of Cincinnati for the World Bank.

Weedon, G. P., Balsamo, G., Bellouin, N., Gomes, S., Best, M. J., and Viterbo, P. (2014). "The WFDEI meteorological forcing data set: WATCH Forcing Data methodology applied to ERA-Interim reanalysis data." Water Resour.Res., 50(9), 7505-7514.

Wi, S., Yang, Y. C. E., Steinschneider, S., Khalil, A., and Brown, C. M. (2015). "Calibration approaches for distributed hydrologic models in poorly gaged basins: implication for streamflow projections under climate change." Hydrology and Earth System Sciences, 19(2), 857-876.

Willmott, C. J., and Matsuura, K. (2001). "Terrestrial air temperature and precipitation: Monthly and annual time series (1950–1999) Version 1.02." Center for Climatic Research, University of Delaware, Newark, .

World Meteorological Organization. (2009). Manual on estimation of probable maximum precipitation (PMP). World meteorological organization.

Yin, J., Gentine, P., Zhou, S., Sullivan, S. C., Wang, R., Zhang, Y., & Guo, S. (2018). Large increase in global storm runoff extremes driven by climate and anthropogenic changes. Nature Communications, 9, 4389. https://doi.org/10.1038/s41467-018-06765-2

Yasutomi, N., Hamada, A., and Yatagai, A. (2011). "Development of a long-term daily gridded temperature dataset and its application to rain/snow discrimination of daily precipitation." Global Environ.Res, 15(2), 165-172.

Yatagai, A., Kamiguchi, K., Arakawa, O., Hamada, A., Yasutomi, N., and Kitoh, A. (2012). "APHRODITE Constructing a Long-Term Daily Gridded Precipitation Dataset for Asia Based on a Dense Network of Rain Gauges." Bull.Am.Meteorol.Soc., 93(9), 1401-1415.

Yue, S., Pilon, P., Phinney, B., and Cavadias, G. (2002). The influence of autocorrelation on the ability to detect trend in hydrological series. Hydrological Processes, 16(9): 1807–1829. <doi:10.1002/hyp.1095>

# Updated Schedule of Task

| c | Activity[1] | Months[2] | | | | | | | | | | | | | | | | |
|---|---|---|---|---|---|---|---|---|---|---|---|---|---|---|---|---|---|---|
| | | **1 Oct** | **2 Nov** | **3 Dec** | **4 Jan** | **5 Feb** | **6 Mar** | **7 Apr** | **8 May** | **9 Jun** | **10 Jul** | **11 Aug** | **12 Sep** | **13 Oct** | **14 Nov** | **15 Dec** | **16 Jan** | **17 Feb** |
| 1 | **Task 1: Training in Wuhan** | | | | | | | | | | | | | | | | | |
| | Preparation of training materials | | | | | | | | | | | | | | | | | |
| | Training | | | | | | | | | | | | | | | | | |
| | Data/reports/models collection | | | | | | | | | | | | | | | | | |
| | Inception Report | | | | | | | | | | | | | | | | | |
| 2 | **Task 2: DTF Application UAHEP** | | | | | | | | | | | | | | | | | |
| | Rapid Scoping | | | | | | | | | | | | | | | | | |
| | Definition of main parameters | | | | | | | | | | | | | | | | | |
| | Models developments/adaptation | | | | | | | | | | | | | | | | | |
| | Climate Stress Test | | | | | | | | | | | | | | | | | |
| | Analysis proposed design/operational modification (if any) | | | | | | | | | | | | | | | | | |
| | Interim Report | | | | | | | | | | | | | | | | | |
| 3 | **Revisions** | | | | | | | | | | | | | | | | | |
| | Hydrologic Model | | | | | | | | | | | | | | | | | |
| | Energy Model and power plant shutdown regimes | | | | | | | | | | | | | | | | | |
| | Training CSPDR on the use of hydrologic model | | | | | | | | | | | | | | | | | |
| | Other revisions | | | | | | | | | | | | | | | | | |
| 4 | **Task 3: Future flood and its affects** | | | | | | | | | | | | | | | | | |
| | Data identification and download | | | | | | | | | | | | | | | | | |
| | Literature Review | | | | | | | | | | | | | | | | | |
| | Development of techniques | | | | | | | | | | | | | | | | | |
| | Draft final report | | | | | | | | | | | | | | | | | |
| | Revisions | | | | | | | | | | | | | | | | | |
| | Executive Summary and major findings | | | | | | | | | | | | | | | | | |
| | Final Report | | | | | | | | | | | | | | | | | |

Note: The red boxes indicate the submission of the report. The blue/silver are the major milestones.

# Annex 1: Terms of Reference

## TERMS OF REFERENCE FOR CLIMATE CHANGE RISK ASSESSMENT (CCRA) FOR THE UPPER ARUN HYDROPOWER PROJECT IN NEPAL

### A. Background

The World Bank is supporting the feasibility study, detailed design and the environmental and social impact assessment of the Upper Arun Hydropower Project in Nepal. The current climate risk assessment needs to be revised, the method used by the consultants is far off of best practice, and one might say is dangerously dismissive of the risk of climate change. Because they do not yet detect a statistically significant trend in annual total streamflow, they disregard the need to look into any climate change scenario more severe than RCP 2.6, which is widely regarded as very likely to be exceeded. Secondly, they choose to use only a single GCM – the polar opposite of the best practice embraced by the bottom-up, robustness-based decision support community (and advocated by the International Hydropower Association in the 2019 Hydropower Sector Climate Resilience Guide https://www.hydropower.org/publications/hydropower-sector-climate-resilience-guide).

The WBG is therefore seeking consultant services to undertake this assignment closely aligned with the in accordance with the Hydropower Sector Climate Resilience Guide, as per the scope of work described below.

### B. Methodology and Scope of Work

The Consultant shall apply the following bottom-up methodology as pertinent to the characteristics of the Upper Arun run-of-river hydroelectric project study, according to the tasks described for each one in sections below:

a) Review of existing information:

   i. Available reports and information on the project including pre-feasibility or feasibility studies, pre-designs, detailed designs, etc.;

   ii. Review of other proposed developments in the river basin;

   iii. Other data and information available that may be useful for the consultant's assignment.

b) Data collection:

   i. Available hydrological/meteorological data including station type and location, historical station data series, global meteorological datasets, existing hydrologic and system models available for the project's watershed and model/data assimilation products, as well as aquifer and water quality data series as pertinent to the present studies;

   ii. Available data on the contributing watershed such as vegetation cover, land-use patterns, existing and proposed water-use developments, inter alia;

   iii. Available socioeconomic data (energy use, demographic data, etc.);

iv. Analysis of local hydro-climatological and other relevant socio-economic historical data;

v. Compilation of a database and other items, as needed.

c) Data and model development and analysis:

i. Conduct an analysis of the available hydro-meteorological and other data, assessing their key characteristics such as adequacy, accuracy, representativeness, and trends;

ii. Use regression analysis (or other suitable technique) to assess potential influences of climatic and non-climatic factors (such as changes in water policy, water quality, groundwater use, population, vegetation cover and/or land-use) in the contributing watershed that may be useful in explaining trends in stream flows that may have been discovered in the analysis;

iii. Assess the adequacy of existing hydrologic models available for the basin. If none are available, determine whether development of hydrologic models is necessary based on the project's magnitude of potential regrets, and its risk and opportunity register (for hydropower, see Hydropower Sector Climate Resilience Guide [1] for details). If development of hydrologic models is warranted, perform and present satisfactory calibration and validation for the Project's basin.

iv. If development of hydrologic models is deemed unnecessary, identify and present a detailed methodology for evaluation of the sensitivity of the project to climate changes. One example methodology (offered for illustrative purposes only) useful for exploring the sensitivity of the project to climate change in the absence of a hydrologic model is direct perturbation of streamflow (if an approximate relationship can be drawn between streamflow and contributing climate conditions).

v. Assess the adequacy of existing water resources system models applicable to the Projects and select (or develop, if necessary) a model for the analysis that accounts for the necessary water withdrawals.

vi. Within the limits of the available data, analyze the secondary effects of climate change on sediment load.

vii. Develop advanced statistical tools to identify the physical climate drivers responsible for the occurrence of extreme streamflow events in region including the Upper Arun River.

i. Review the climate risk assessment conducted by CSPDR, the design consultants for Upper Arun Hydropower Project based in Wuhan, China. The review is included in CSPDR's updated feasibility study for Upper Arun Hydropower Project.

d) Stakeholder consultation:

[1] Link to Hydropower Sector Climate Resilience Guide in eConsultant

ii. The Consultant will work closely with CSDPR, especially their hydrology, sediment and design engineers to understand the design parameters that CSPDR has used for Upper Arun Hydropower Project.

iii. With the aid of the Project Team and other pertinent entities, the consultant shall identify the key stakeholders of the project;

iv. Perform consultations with the stakeholders to identify the key non-climate risk factors and to define and select the project performance indicators including those for robustness/ resilience and their thresholds to be used in the robustness analysis.

e) Relative importance of potential climate and non-climate sensitivities

i. Based on the project's magnitude of potential regrets, and its risk and opportunity register (for hydropower, see Hydropower Sector Climate Resilience Guide for details), define a detailed plan to perform a rapid project scoping of its sensitivity to climate change, using streamflow perturbation methods (mentioned as an example for indicative purposes only) to evaluate the elasticity of runoff to precipitation and temperature changes and the elasticity of the selected performance indicators to runoff changes. The rapid scoping methodology should also include the project's sensitivity to the identified key non-climate risks to allow comparison of both climate and non-climate potential sensitivities.

ii. The rapid scoping plan should also include a detailed methodology to do a robustness analysis should the scoping show that the non-climate potential sensitivities are dominant or significant.

iii. Present the rapid scoping plan and methodologies for WBG's no-objection;

iv. Apply the rapid scoping plan's climate and non-climate rapid scoping methodology and discuss with the Project Team and key stakeholders the results to jointly decide on which factors the detailed robustness analysis on the project should be performed.

f) Climate robustness analysis:

i. Usually, unless the climate sensitivity of the project is very small or the sensitivity for any other non-climate factor is very large, a climate robustness analysis should be performed. The climate robustness analysis is to be a stress test that systematically samples climate-related inputs to the modeling workflow in a controlled scientific experiment by which changes to system performance can be directly attributed to specific changes in climatic conditions. The likelihood of those changes is a question of secondary concern;

ii. A bottom-up approach (such as in the DTF[2]) should be followed (for hydropower, follow the Hydropower Climate Resilience Guide), i.e., emphasizing the vulnerability of project performance (based on the selected project performance indicators/metrics) by parametrically or stochastically

[2] https://openknowledge.worldbank.org/handle/10986/22544

varying the climate (precipitation and temperature) using a weather generator[3] plus a coupled hydrologic/system model to define the failure region, and then elaborating situations based on these vulnerabilities. For illustration purposes only, the selection of the anticipated range of changes in the climate parameters can be aided by portals such as the WBG Climate Change Knowledge Portal[4], the Nature Conservancy's Climate Wizard[5], the UNDP's Adaptation Learning Mechanism[6], or others.

iii. Other methods to evaluate the vulnerability of the water system to a wide range of climate futures may also be used that at least goes beyond the range indicated by the most current IPCC CMIP, to obtain insights applicable to those cases where development of a weather generator of sufficient complexity such as in g) ii., is not possible or not necessary.

iv. In-situ measured data will be superimposed and supplemented if necessary, with existing, and appropriate public domain data and paleo-data. GCM projections[7] within a plausible range of climate changes relevant to the economic life of the project will also be superimposed to explore the risk to the system, in terms of the filling of a reservoir, the yield, meeting the required water-use demands, and other selected metrics. Such projections provide insight into the likelihood of the changes in climate conditions explored in the climate stress test. Modeling will be at the appropriate temporal resolution (e.g., finer resolution for flood concerns than for concerns related to long-term average power generation performance), but no coarser than monthly intervals;

v. Obtained results of impact/probability in the spectrum between a low-risk situation (low impact and few indications from GCM projections, historical occurrences and trends, expert opinion, etc., that future conditions might fall within the failure domain) and high risk (high impact and many indications of the likelihood of future conditions within the failure domain) will be analyzed;

vi. In the case of flood concerns, the consultant will present a climate-informed likelihoods of changes in the design flood, and other floods of interest to the Project Team or stakeholders. The impact of floods of various magnitudes will be evaluated only if data relating flood stage to estimated flood damages are available.

vii. Define robustness/resilience indicators and evaluate the feasibility design. If the thresholds are not met, determine if robustness/resilience can be achieved by direct feasibility design modifications by repeating the analysis of the project

[3] Weather generators are models developed to provide controlled experiments in the sensitivity to specific climate variabilities.

[4] http://sdwebx.worldbank.org/climateportal/index.cfm

[5] http://www.climatewizard.org/

[6] http://www.adaptationlearning.net/

[7] Downscaled output of the most-current ensemble of Intergovernmental Panel on Climate Change (IPCC) Coupled Model Intercomparison Project (CMIP) General Circulation Models (GCMs) can provide insight into physically-based, nonlinear relationships between climate parameters responsive to large-scale oceanic and atmospheric climate processes useful for understanding the likelihood of the various climate changes explored using the weather generator.

with the proposed modifications and propose those modifications for a robust/resilient design; if the project is deemed too risky, uncertainty is too great, or options for design modifications are limited, discuss other project options with the WBG Team, as well as the application of advanced tools for decision making under uncertainty such as Robust Decision Making, Dynamic Adaptive Policy Pathways, Robust Optimization, Real Options Analysis, inter alia.

viii. The consultant shall prepare a climate change action / adaptation plan, and related costs, in compliance with the requirements of the WBG.

ix. The Consultant shall work closely with CSPDR and provide training to both CSPDR and NEA.

**C. Duration of the assignment and place of work**

The contract will be from October 1st, 2019 to May 30th, 2020. It is expected that the work will be performed in the Consultant's place of residence as well as in China, Nepal and Washington, DC. Frequent communication by e-mail, fax, text messaging, telephone or video-conference with the Bank's Project Teams will be maintained for the duration of the assignment.

**D. Qualifications of the Consultant**

The principal personnel of the selected Consultant shall have a strong background in Hydrology/Meteorology/Water Resources and at least one member of the team shall have a strong background in water resources economics. Additionally, at least one member of the team shall have engineering experience in hydropower development. Knowledge about alternative methods on risk-based decision making and adaptation of vulnerable water systems considering the effect of uncertain information, especially the effects of climate change, is a must. Knowledge and previous experience in using methods such as decision scaling and in applying such methodologies will be beneficial. Previous experience in working with the Bank will be an asset. The Consultant should have experience in compilation and analysis of hydrometeorological and water resources economic data and in using hydrologic and water resources systems models. An academic degree, preferably at the PhD level of its principal personnel to be assigned to the study is also required, as well as fluent spoken and written English. The consultant should have some experience of conducting a climate risk assessment and familiarity with using the *Hydropower Sector Climate Resilience Guide*

**E. Travel**

The Consultant should be willing to make at least two trips to Nepal and Wuhan, China (where CSPDR the design consultant is based) during the period of the consultancy (one visit to Nepal and one trip to China of approximately 5 days each, dates to be agreed). The first trip is mainly to present and discuss the work plan with stakeholders and the Project Team during launch workshops, and to compile additional information, as needed. The second trip is mainly to discuss and validate the results of the study with stakeholders and the Project Team and complete closing workshops. Slide presentations during these trips may be required. During these trips, the consultant should visit the WBG Nepal country offices and/or client offices to coordinate its work and discuss progress and preliminary results with the teams and interested staff. The visit to China is aimed at having discussions with CSPDR, the design consultants for the Upper Arun Hydropower Project.

The Consultant should also be willing to visit the Bank's HQ in Washington, DC (at least two visits of approximately 2 days each, dates to be agreed). It may also be necessary for the Consultant to participate in at least one BBL during the visits to DC, organized by the Bank in dates to be agreed.

**F. Reports**

The Consultant shall prepare the following set of reports described in section I:

a) Inception report;

b) Interim advance report;

c) Draft final report;

d) Final report;

e) PowerPoint (or other slideshow software) presentations, as directed;

**G. Contract type**

The contract will be a fixed lump sum contract for 49,000 US dollars. The trips to Nepal, China and DC not to exceed 10,000 US dollars covering flights, hotels and accommodation should be included in the 49,000 US Dollars.

**H. Schedule of Payments**

The Consultant shall present a Financial Proposal for the total contract, disaggregated and subcategorized to align with the task described in section J.

As indicated in the General Conditions of Contract for Operational Consulting Services (GTC), an amount not to exceed the Contract Price proposed in Annex B of the Financial Proposal, shall be paid to the Consultant as a lump sum basis pursuant to the Contract Type and the Schedule of Payment agreed at negotiation.

An illustrative schedule of payment for remuneration would be as follows:

10% on Consultant's submission and Bank acceptance of inception report;

50% on Consultant's submission and Bank acceptance of interim report;

40% on the Consultant's submission and Bank acceptance of the Final report, including the comments and observations from the Bank as well as the Executive Summary.

The Consultant may also propose a payment schedule for the remuneration component of the financial proposal.

Notwithstanding the contract type and schedule proposed by the Consultant, the contract shall be based on the type and scheduled agreed by the Parties at negotiation and confirmed by the Bank's Corporate Procurement.

**I. Supervision**

The Consultant will report to Pravin Karki (pkarki@worldbank.org), will also receive copies of the deliverables. Others may be added to this list at the discretion of the Task Team.

## ANNEX 1 TERMS OF REFERENCE

### SUMMARY OF THE UPPER ARUN HYDROELECTRIC PROJECT, NEPAL

Nepal is a land-locked country, with a population of 27.5 million and a per capita income of US$ 717. About 24.8 percent of the Nepali population lives on less than US$ 1.25 per day, and 82 percent live in rural areas. Poverty is much more severe in rural areas (27%) compared to urban areas (15%) and particularly severe in mountainous areas (42%). Despite a decade-long armed insurgency and protracted political transition, Nepal has made exemplary progress in poverty reduction and human development. Nepal has halved extreme poverty, and thus attained the first Millennium Development Goal ahead of time. While 75 percent of the population of Nepal is estimated to have access to electricity, service is not necessarily available due to shortage of supply, with load shedding of up to 18 hours per day in grid-covered areas in the dry season. A significant disparity in access to electricity exists between urban (90%) and rural areas (30%). Average annual consumption remains very low at about 70 kWh per capita.

The country is endowed with a huge theoretical hydropower potential of about 84,000 MW and economically viable potential of 43,000 MW. However, the installed hydropower generation capacity as of July 2013 was merely 746 MW. To deal with the energy crises and eventually achieve reliable, affordable and sustainable electricity supply in Nepal, the strategy of the Government of Nepal (GON) is to (a) reduce NEA's system losses and adding generation capacity that can be quickly installed in the short term; (b) reach supply-demand balance in the medium term through the commissioning of hydropower under construction and power imports from India; and (c) develop its huge hydropower resources to sustain domestic growth and earn export revenues in the long term. In line with the strategy are actions, including: (a) investing in system loss reduction and pilot of grid-connected solar power generation; (b) enhancing planning, feasibility studies and construction of a transmission system, including construction of a high-voltage cross-border line for up to 1,000 MW of power import from India; and (c) facilitating private investment in large hydropower projects, with several projects (about 4,000 MW) under negotiations for Project Development Agreements (PDAs), most of them with large export components to India.

The Arun river is one of the major tributaries of the Sapt Kosi River basin located in the east of Nepal. The river originates from the Qingkangjiale Glacier on the North Slope of Mt. Xixabangma Feng, in the Nyalam County, of Tibet, China. The total length of the Arun river is about 510 km, and the total drainage area of the river is about 30,400 km². The dam site, of the Upper Arun HEP, is near the confluence of Chepuwa Khola with the Arun river. The catchment area, at the dam site, is 25,700 km², accounting for 84.5% of the total area of the Arun river basin.

The Upper Arun Hydroelectric Project (UAHEP) is one such project in the Eastern Development Region, which has a very high head and stable river flow. The Government of Nepal has also decided to implement the Project through NEA.

The UAHEP draws water discharge from Arun River. The Project site is located in the Sankhuwasabha District of Koshi Zone in the Eastern Development Region of Nepal. The Project is located about 70 km north of Khandbari, the district headquarters, and about 200 km east of Kathmandu. The proposed dam site is located in a narrow gorge about

150 m downstream of the Chepu Khola the in Chepuwa Village. The proposed powerhouse will be located in the Hatiya Village, which is about 500 m upstream from the confluence of the Arun River with Leksuwa Khola. The Project area is situated within Longitude 87°20’00” to 87°30’00” East and Latitude 27°38’24” to 27°48’09” North.

The Project area is located within the Middle and High Mountains Region. The elevation ranges from about El.1,100 m at the powerhouse site to over El.1,600 m at the headworks site, along the ridgeline separating the powerhouse and the dam site. Topographically, the outgain slopes of the Project area are very steep and the Arun river forms a deep and narrow gorge at the dam site, and a wider valley at the powerhouse site.

The annual average discharge, at the dam site of UAHEP, has accordingly been calculated to be approximately, 217 m³/s. The annual suspended sediment load is approximately 13,810,000 t. The bed load is estimated to be approximately 2,430,000 t. The annual average suspended sediment concentration is about 2.013 kg/ m³.

**Table A2.1: Salient Features of the Upper Arun Hydroelectric Project**

| SN | Item | Unit | Value | Remark |
|---|---|---|---|---|
| **1** | **HYDROLOGY** | | | |
| (1) | Catchment Area | | | |
| | Arun River Basin | km² | 30,400 | |
| | Catchment area above damsite | km² | 25,700 | |
| (2) | Length of Flow Series | Year | 39 | |
| (3) | Annual Average Runoff | billion m³ | 6.85 | |
| (4) | Representative Flow | | | |
| | Annual average flow | m³/s | 217 | |
| | 2-year return period flood | m³/s | 1,050 | |
| | Probable Maximum Flood(PMF) (dam site/powerhouse site) | m³/s | 4,990/6,060 | |
| | Glacial Lakes Outburst Flood(GLOF) (dam site) | m³/s | 7,822 | |
| (5) | Sediment | | | |
| | Annual average suspended Sediment | T | $1.381\times10^7$ | |
| | Annual average sediment concentration(suspended sediment) | kg/m³ | 2.013 | |
| | Annual average bed load | T | $2.43\times10^6$ | |
| **2** | **RESERVOIR** | | | |
| (1) | Water Levels | | | |
| | Maximum water level | El.m | 1,642.59 | At GLOF |
| | Full supply level | El.m | 1,640 | |

| | | | | |
|---|---|---|---|---|
| | MOL during peak | El.m | 1,625 | |
| | Sediment sluicing level | El.m | 1,625 | |
| (2) | Reservoir Surface Area at FSL | km² | 0.201 | |
| (3) | Reservoir Storage | | | |
| | Storage under FSL | MCM | 5.07 | |
| | Peaking pondage (live Storage) | MCM | 2.41 | |
| | Storage under MOL duringpeak | MCM | 2.66 | |
| (4) | Pondage Factor (Pondage storage/Annual runoff volume) | % | 0.04 | |
| (5) | Regulation Performance | | Daily | |
| (6) | Water Utilization Rate | % | 53 | |
| **3** | **POWER GENERATION BENEFIT** | | | |
| | Installed capacity | MW | 1,040 | 6 Units |
| | Firm capacity | MW | 697.2 | Under Q95 inflow conditions, daily peaking for 6 hours during the dry season from December to May of following year |
| | Average energy output | GWh | 4,492 | |
| | Dry season peak energy | GWh | 835 | |
| | Dry season off-peak energy | GWh | 422 | |
| | Dry season /total energy ratio | % | 28% | |
| | Wet season peak energy | GWh | 942 | |
| | Wet season off-peak energy | GWh | 2,294 | |
| | Plant factor | % | 49.3 | |
| **4** | **MAIN STRUCTURES** | | | |
| (1) | Dam | | | |
| | Dam type | | concrete gravity dam | |
| | Foundation Rockmass | | slightly weathered and fresh gneiss | |
| | Dam crest elevation | El.m | 1,644 | |
| | Minimum Foundation level | El.m | 1,553 | at dam heel |
| | Maximum dam height | M | 91 | |
| | Downstream face slope ratio | - | 1:0.8 | |
| | Dam crest width | M | 10 | |
| | Dam crest length | M | 184 | |
| (2) | Flood and Sediment Discharge Facilities | | | |
| i) | Low-level Outlet | | | |
| | Number of low-level outlets | Pc | 3 | |
| | Sill elevation | El.m | 1,590 | |
| | Size of the orifice | M | 9×10 | |
| | Maximum discharge capacity at GLOF | $m^3/s$ | 6,750 | |
| | Energy dissipation | | ski-jump | |

| | | | | |
|---|---|---|---|---|
| | Service gate type | | radial gate | |
| | Number of service gates | No. | 3 | |
| | Number of lifting equipment for service gate | | 3 | Hydraulic hoist |
| | Capacity of lifting equipment for service gate | kN | 4,000/800 | opening capacity/ push capacity |
| | Emergency Gate type | | wheel gate | |
| | Number of Emergency Gate | No. | 1 | |
| | Number of lifting equipment for Emergency Gate | | 1 | Gantry crane |
| | Capacity of lifting equipment for Emergency Gate | kN | 2×1,250 | |
| | Stoplog type | | slide type | |
| | Number of Stoplog | No. | 1 | |
| | Number of lifting equipment for Stoplog | | 1 | Rotating crane of Gantry crane |
| | Capacity of lifting equipment for Stoplog | kN | 1,000 | |
| ii) | Ungated Spillway | | | |
| | Crest elevation | El.m | 1,640.0 | |
| | Length | M | 30 | |
| | Maximum discharge capacity at GLOF | $m^3/s$ | 265 | |
| | Energy dissipation | | Stepped+ski-jump | |
| iii) | Sediment Bypass Tunnel (SBT) | | | |
| | Type | | Pressurized tunnel | |
| | Number of SBT | No. | 1 | |
| | Length of SBT | M | 1,321.50 | |
| | Sill elevation of inlet | El.m | 1,610 | |
| | Size of the orifice at service gate | m×m (W×H) | 7×6.5 | |
| | Cross section of pressurized Tunnel | | circle | |
| | Diameter of tunnel | M | 8.5 | |
| | Design discharge capacity (at EL.1625) | $m^3/s$ | 815 | |
| | Type of lining | | Concrete | |
| | Service gate type | | Radial gate | |
| | Number of service gate | No. | 1 | |
| | Number of lifting equipment for service gate | | 1 | Hydraulic hoist |

| | | | | |
|---|---|---|---|---|
| | Capacity of lifting equipment for service gate | kN | 1,200/800 | opening capacity/ push capacity |
| | Emergency Gate type | | wheel gate | |
| | Number of Emergency Gate | No. | 1 | |
| | Number of lifting equipment for Emergency Gate | | 1 | |
| | Capacity of lifting equipment for Emergency Gate | kN | 800 | Bridge crane |
| | Stoplog type | | slide type | |
| | Number of Stoplog | No. | 1 | |
| | Number of lifting equipment for Stoplog | | 1 | Bridge crane |
| | Capacity of lifting equipment for Stoplog | kN | 2×250 | |
| (3) | Waterway | | | |
| i) | Rated discharge | m³/s | 235.44 | |
| ii) | Intake type | NA | Intake integrated with Dam | |
| | No. | Pc | 1 | |
| | Sill elevation | M | 1,606.80 | |
| | Type of Emergency gate | NA | Wheel gate | |
| | Number of Emergency gate | Pc | 1 | |
| | Size of the orifice | m×m | 6.7×8.64 | |
| | Type of lifting equipment for Emergency gate | NA | Hydraulic Hoist | |
| | Number of lifting equipment for Emergency gate | Pc | 1 | |
| | Capacity of lifting equipment for Emergency gate | KN | 1,200/800 | |
| iii) | Low pressure steel lining Conduit | | | |
| | No. | Pc | 1 | |
| | Diameter | M | 8.40 | |
| | Length | M | 108 | |
| | Center elevation | M | 1,611.00 | |
| | Flow velocity | m/s | 4.29 | |
| iv) | Low pressure headrace tunnel | | | |
| | No. | Pc | 1 | |
| | Surrounding rock characteristic | NA | Gneiss/schist | |
| | Length | M | 8362 | |
| | Section net diameter | M | 8.40 | |

| | | | | |
|---|---|---|---|---|
| | Center elevation | M | 1,611.00 | |
| | Lining type | NA | Concrete lining | |
| | Flow velocity | m/s | 4.29 | |
| v) | Surge tank | | | |
| | Type | NA | Restricted orifice surge Tank, Open surge tank | |
| | No. | Pc | 1 | |
| | Surrounding rock characteristic | NA | Gneiss/schist | |
| | Inner diameter | M | 20.0 | |
| | Lining type | NA | Concrete lining | |
| | Top elevation | El.m | 1,674.50 | |
| | Bottom elevation | El.m | 1,584.00 | |
| | Maximum upsurge | El.m | 1,671.56 | |
| | Maximum downsurge | El.m | 1,587.84 | |
| | Diameter of restricted orifice | M | 4.3 | |
| vi) | Pressure drop shaft | | | |
| | No. | Pc | 1 | |
| | Surrounding rock characteristic | NA | Gneiss/schist | |
| | Length | M | 558 | |
| | Elevation | El.m | 1,095~1,577.80 | |
| | section diameter | M | 7.3 | |
| | lining type | NA | Concrete lining | |
| vii) | Main high pressure headrace Tunnel | | | |
| | No. | Pc | 1 | |
| | Surrounding rock characteristic | NA | Gneiss | |
| | Length | M | 39 | |
| | Diameter | M | 6.0 | |
| | Center elevation | El.m | 1,095 | |
| | Lining type | NA | Steel lining | |
| viii) | Branch high pressure headrace Tunnel | | | |
| | No. | Pc | 8 | |
| | Surrounding rock characteristic | NA | Gneiss | |
| | Length | M | 31~69 | |
| | Diameter | M | 4.2,3.5,2.5 | |
| | Center elevation | El.m | 1,095 | |
| | Lining type | NA | Steel lining | |
| ix) | Branch tailrace tunnel | | | |
| | No. | Pc | 6 | |
| | Surrounding rock characteristic | NA | Gneiss | |

| | | | | |
|---|---|---|---|---|
| | Section type | NA | Inverted D-shape | |
| | Dimension(W×H) | m×m | 3.80×6.53 | |
| | Length | M | 127~161 | |
| | Lining type | NA | Concrete lining | |
| | Sill elevation | El.m | 1,084.84~1,085 | |
| x) | Main tailrace tunnel | | | |
| | No. | Pc | 2 | |
| | Section type | NA | Inverted D-shape | |
| | Surrounding rock characteristic | NA | Gneiss/Schist | |
| | Dimension(W×H) | m×m | 9.00×7.20 | |
| | Length | M | 602/605 | |
| | Lining type | NA | Concrete lining | |
| | Sill elevation | El.m | 1,084.2~1,084.84 | |
| xi) | Tailrace outlet | | | |
| | No. | Pc | 2 | |
| | Plane dimension（L×W） | m×m | 15.0 ×6.50 | |
| | Sill elevation | El.m | 1,084.20 | |
| | Top elevation | El.m | 1,104.00 | |
| | 0.1% tailwater elevation | El.m | 1,091.52 | |
| | GLOF tailwater elevation | El.m | 1,097.42 | |
| | Type of Emergency gate | NA | Wheel gate | |
| | Number of Emergency gate | Pc | 2 | |
| | Size of the orifice | m×m | 9.0×7.2 | |
| | Type of lifting equipment for Emergency gate | NA | Hydraulic Hoist | |
| | Number of lifting equipment for Emergency gate | Pc | 2 | |
| | Capacity of lifting equipment for Emergency gate | KN | 2×630/2×400 | |
| (4) | Powerhouse | | | |
| | Type | NA | Underground | |
| | Dimension of main powerhouse cavern (L×W×H) | m×m×m | 230.05×25.7×59.43 | |
| | Surrounding rock characteristic | NA | Gneiss | |
| | Installed elevation of turbine | El.m | 1,095 | |
| | Unit bay length | M | 28.80 | |
| (5) | Main transformer cavern | | | |
| | Dimension of main transformer cavern(L×W×H) | m×m×m | 238.2×16.70×37.18 | |
| | No. main transformer | Pc | 19 | |

| | | | | |
|---|---|---|---|---|
| (6) | Potyard | | | |
| | Base characteristic | NA | Gneiss | |
| | Surface elevation | El.m | 1,425 | |
| | Plane dimension of Potyard | m×m | 120 ×42 | |
| | Plane dimension of administration building | m×m | 26.3×17.4 | |
| | Stories of administration building | NA | 2 | |
| (6) | Eco-flow power station | | | |
| | Type | | Powerhouse at the dam-toe | |
| | Design discharge | m³/s | 10.82 | |
| | Sill elevation of intake | El.m | 1,615.6 | |
| | Diameter of penstock | M | 1.5/1.0 | main pipe/branch pipe |
| | Dimension of powerhouse (L×W×H) | m×m×m | 31×16.4×19.3 | |
| | Installed elevation of turbine | El.m | 1,585.20 | |
| | Number of units | Set | 2 | horizontal Francis turbine units |
| | Installed capacity | MW | 4.2(2×2.1) | Maximum output of 5.0MW |
| | Average annual energy | GWh | 22.64 | |
| (7) | Diversion during construction | | | |
| i) | Diversion Approach During Construction | | Dry season：Cofferdams for water retaining and the diversion tunnel for water release. Flood season: the overflow cofferdams in combination with the diversion tunnel are proposed for flood discharging | |
| ii) | Diversion tunnel | | | |
| | Design flood | m³/s | 257 | 20-year flood from November to April |
| | Section type | | Inverted D-Shape | |
| | Length of tunnel | M | 490.41 | |
| | No. | Pc | 1 | |

| | | | | |
|---|---|---|---|---|
| | Dimension(W×H) | m×m | 7×8 | |
| iii) | Upstream Cofferdam | | | |
| | Type | | earth-rock fill overflow cofferdam | |
| | Crest elevation | El.m | 1,586.00 | |
| | Height | M | 12 | |
| iv) | Downstream cofferdam | | | |
| | Type | | earth-rock fill overflow | |
| | | | Cofferdam | |
| | Crest elevation | El.m | 1,568.00 | |
| | Height | M | 5 | |
| **5** | **E&M EQUIPMENT** | | | |
| (1) | Turbine | | | |
| | NO. | Set | 6 | |
| | Unit capacity | MW | 173.33 | |
| | Runner diameter | M | 3.62 | |
| | Rated speed | r/min | 250 | |
| | Rated head | M | 508.26 | |
| | Rated flow | m³/s | 39.24 | |
| (2) | Generator | | | |
| | NO. | Set | 6 | |
| | Generator capacity | MVA | 213 | |
| | Power factor | | 0.85 | |
| | Rated voltage | kV | 15.75 | |
| (3) | Lifting Equipment in the Powerhouse | | | |
| | Type 1 | | Single trolley bridge crane | Main bridge crane |
| | NO. | Set | 1 | |
| | Capacity | T | 500t/50t | |
| | Type 2 | | Single trolley bridge crane | Construction bridge crane |
| | NO. | Set | 1 | |
| | Capacity | T | 125t/25t | |
| (4) | Main transformer | | | |
| | 400kV single phase booster transformer | Set | 19 | 18 work 1 stand by |
| **6** | **ROADS** | | | |
| | Access road | Km | 23 | Including a 80m long bridge and a 2km long tunnel |

| | | | | |
|---|---|---|---|---|
| | Project roads | Km | 16.647 | |
| | Project bridges | m/set | 140/2 | bailey bridge |
| | Adits | m/set | 1,490/7 | |

# Annex 2: Inception Visit

Inception Visit
Venue: CISPDR, Wuhan, Hubei, China
Date: 21-24 October 2019

Participants:

- Patrick Ray, Asphota Wasti, Zhipeng Zhu (University of Cincinnati)
- Cui Yazhu, Lila N. Bhandari, Li Liping, Yan Linlu (CSPDR)
- Ayog Basnyat (The World Bank)

**Day 1 (Monday October 21)**

- Morning:
    - Introductions
    - Dr. Ray presented previous work on Climate Change Impact Assessment in Upper Arun Hydroelectric Project (World Bank Report, Previous Publications, Decision Tree Framework, IHA Guide)
    - CISPDR presented recent work on design update of headwork (desander replaced with reservoir)
    - UC and CISPDR discussed their roles and plan ahead for the climate change impact assessment of Upper Arun. The roles are:
        - CISPDR provides reports, and data used in UAHEP assessment.
        - UC presents and trains CISPDR on Climate Resilience Analysis (CRA) approach with hands on training.
        - UC summarizes the previous work and defines the additional work required for an updated CRA of UAHEP
        - UC performs CRA on UAHEP upon returning to Cincinnati. CISPDR will be available for information exchange as required in the process.
- Afternoon:
    - Asphota discussed the overview of the approach and requested the data and models required for analysis to Dr. Li
    - Dr. Li shared hydrological and meteorological data used by CISPDR (additional to the previous Upper Arun Report)

**Day 2 (Tuesday October 22)**

- Morning:
    - Dr. Ray presented Introduction to Climate Change and Hydropower project
    - Dr. Ray presented extremes and climate change
- Afternoon:
    - Asphota conducted hands on training in data analysis

  - Asphota conducted hands on training in R
  - Dr. Li provided additional data for economic analysis and explanation of the flood analysis
  - Dr. Li provided sediment data and reports and flood data and reports including GLOF report via email.

**Day 3 (Wednesday October 23)**

- Morning:
  - Visit by UC team and Ayog and Mr. Ciu to CISPDR exhibition of the previous projects and its history
  - Visit by UC team and Ayog and Mr. Ciu to CISPDR physical model of the Upper Arun Hydroelectric Project
- Afternoon:
  - UC summarizes the meetings
  - Video call meeting planned with UC, CISPDR, and World Bank (Pravin Karki)

# Annex 3: Data Analysis

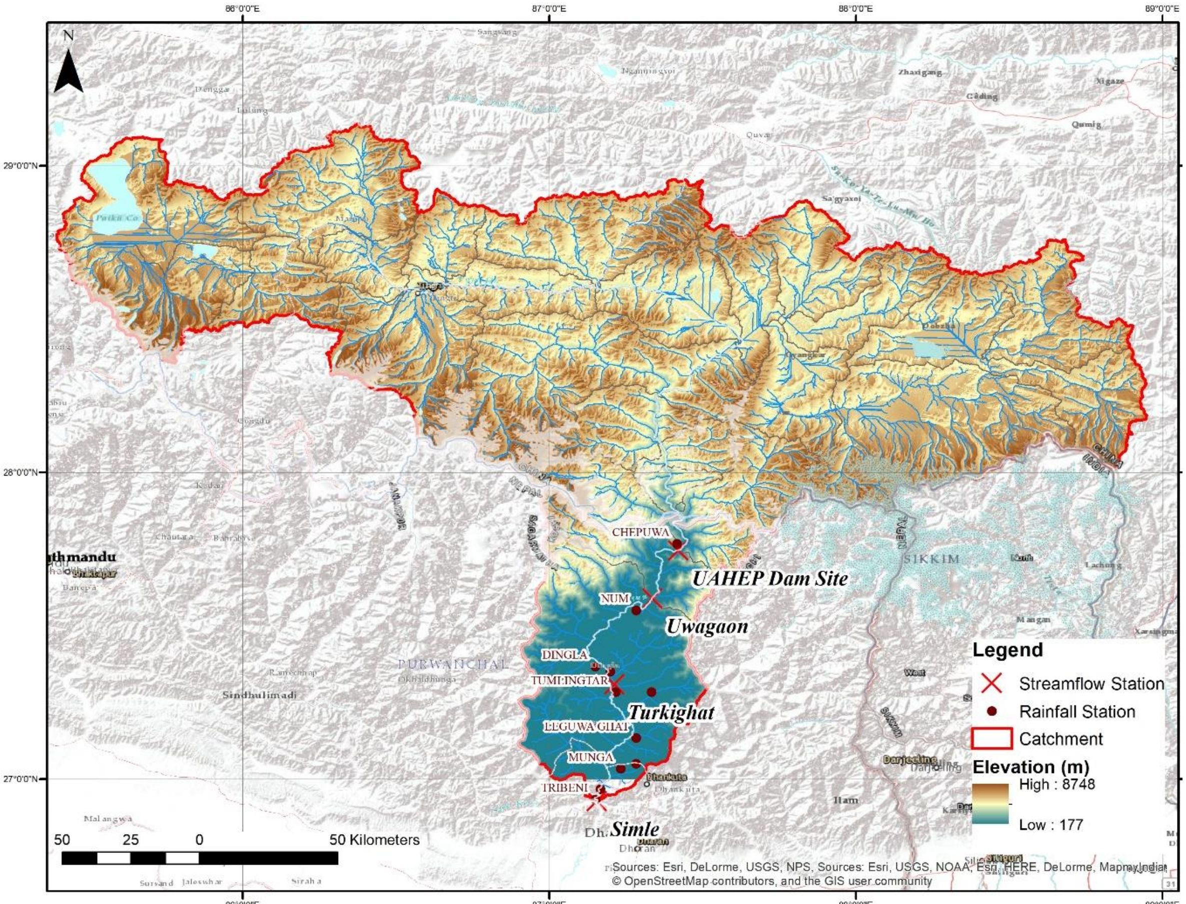


*Figure 27 Location map of project catchment area illustrating the hydrological and meteorological station in the basin. A recently established stream gage station at the provides a year long record of data (15- minutes interval) at the Dam Site. The Uwagaon station is the closest hydrological station downstream of the project site. The Chepuwa rainfall station is the only precipitation station that lies in the catchment delineated at Uwagaon. Num is the precipitation with the highest rainfall in Nepal. There are no ground observations for temperature measurements within the basin.*

**Data Analysis: Precipitation**

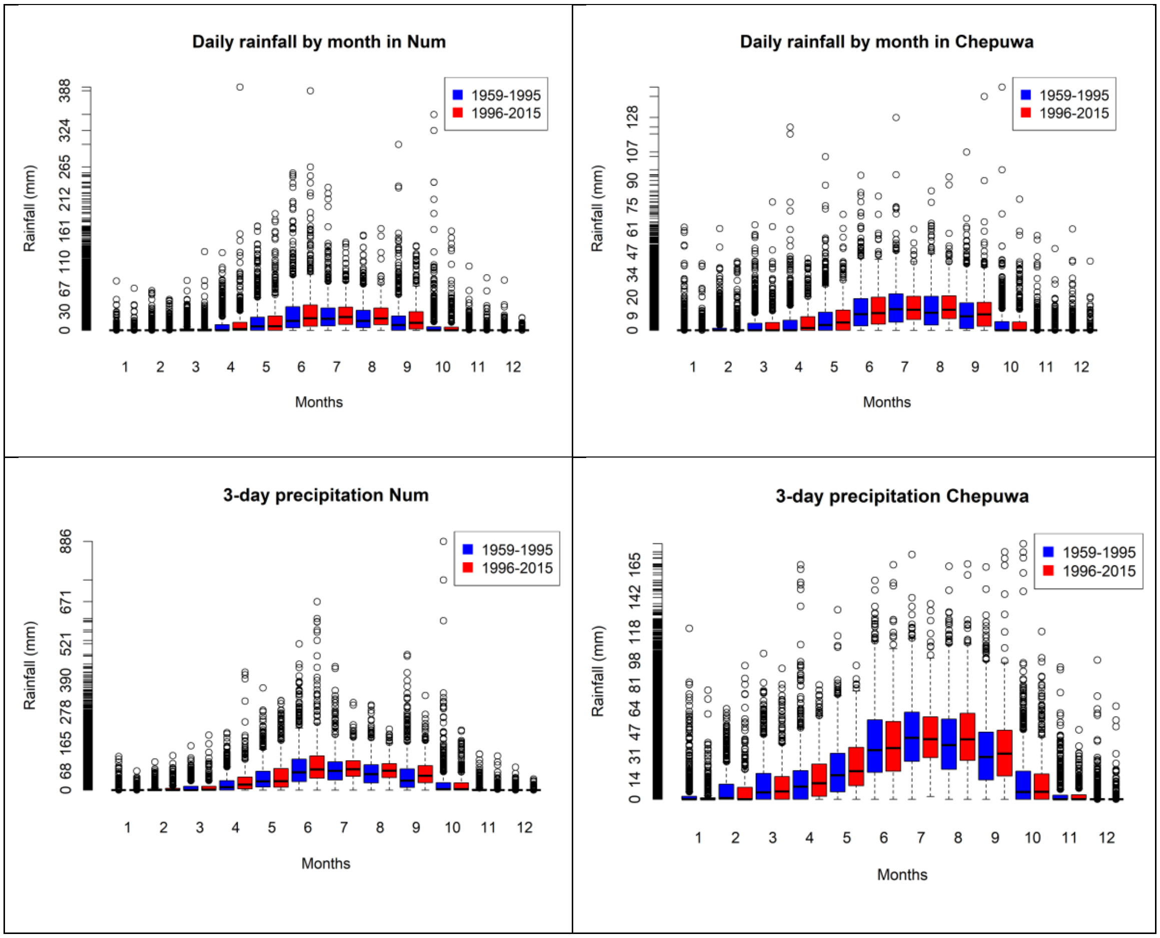


*Figure 28 Precipitation pattern in Num and Chepuwa (1-day and 3-day). 3-day precipitation is used to estimate the 3-day PMP in the basin.*

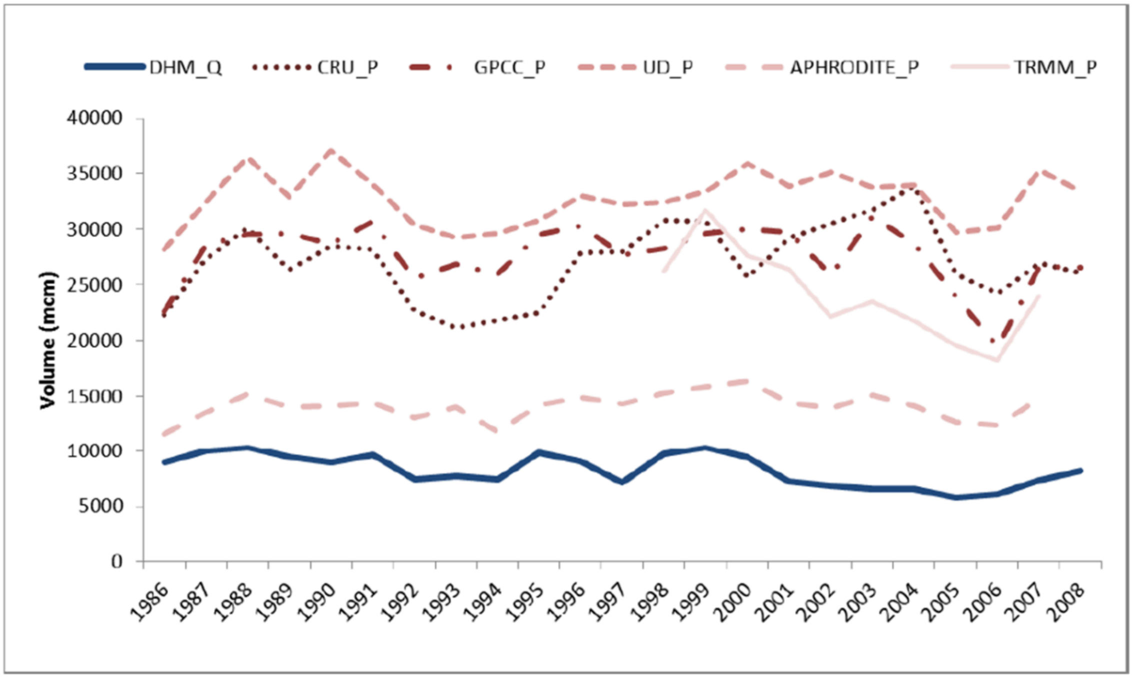


*Figure 29 Extracted from AUS11077: "Figure 53: APHRODITE, when converted to streamflow, is much lower than other gridded data. GPCC most closely follows TRMM, which uses satellite observations, and tends to be most trusted (with record only from 1998). The choice is then to use GPCC data, "downscale" it using ratios from APHRODITE data (and distribute it into daily values)" The APHRO_GPCC data is compared with other gridded datasets. This generated data is denoted as APHRO_GPCC in rest of the analysis.*

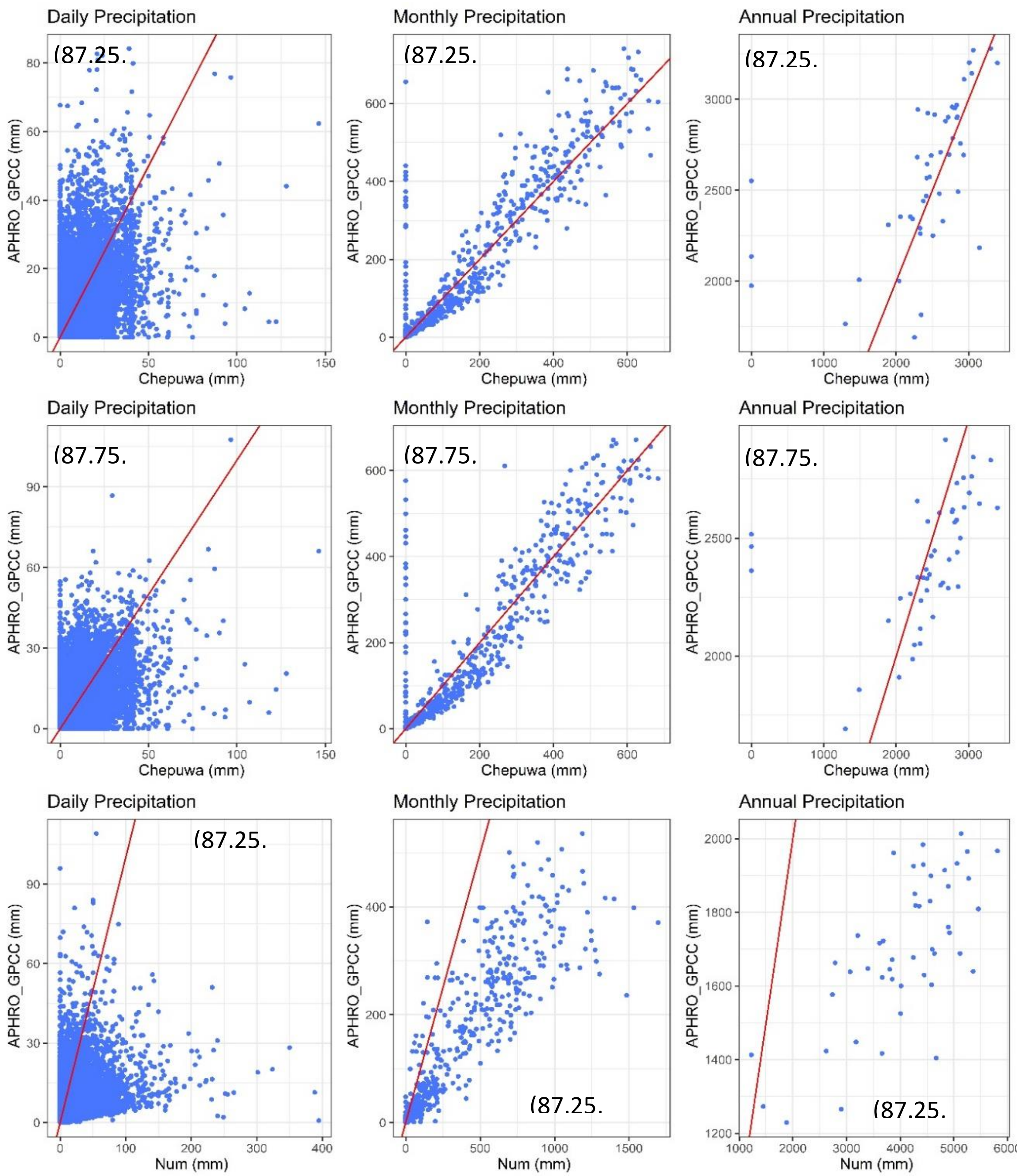


*Figure 30 Comparison of Num and Chepuwa ground station observation to the nearest APHRO_GPCC grid. The grid coordinates are indicated in the graph. The APHRO GPCC dataset captures the rainfall processes around Chepuwa station but understimates the rainfall process in Num.*

Figure:

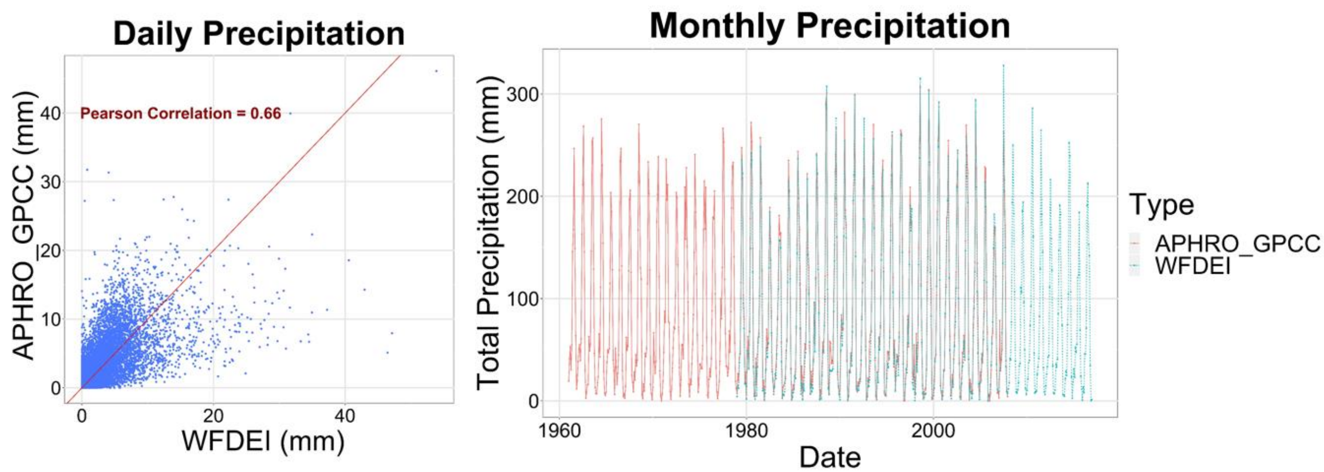


*Figure 31 Comparison of WFDEI (blue) and APHRODITE bais corrected with GPCC i.e. APHRO_GPCC (red) data precipitation (used in AUS11077). Correlation of Daily Precipitation (left); Time Series of Monthly Precipitation (right). The characteristics of WFDEI precipitation and APHRO_GPCC agree fairly well.*

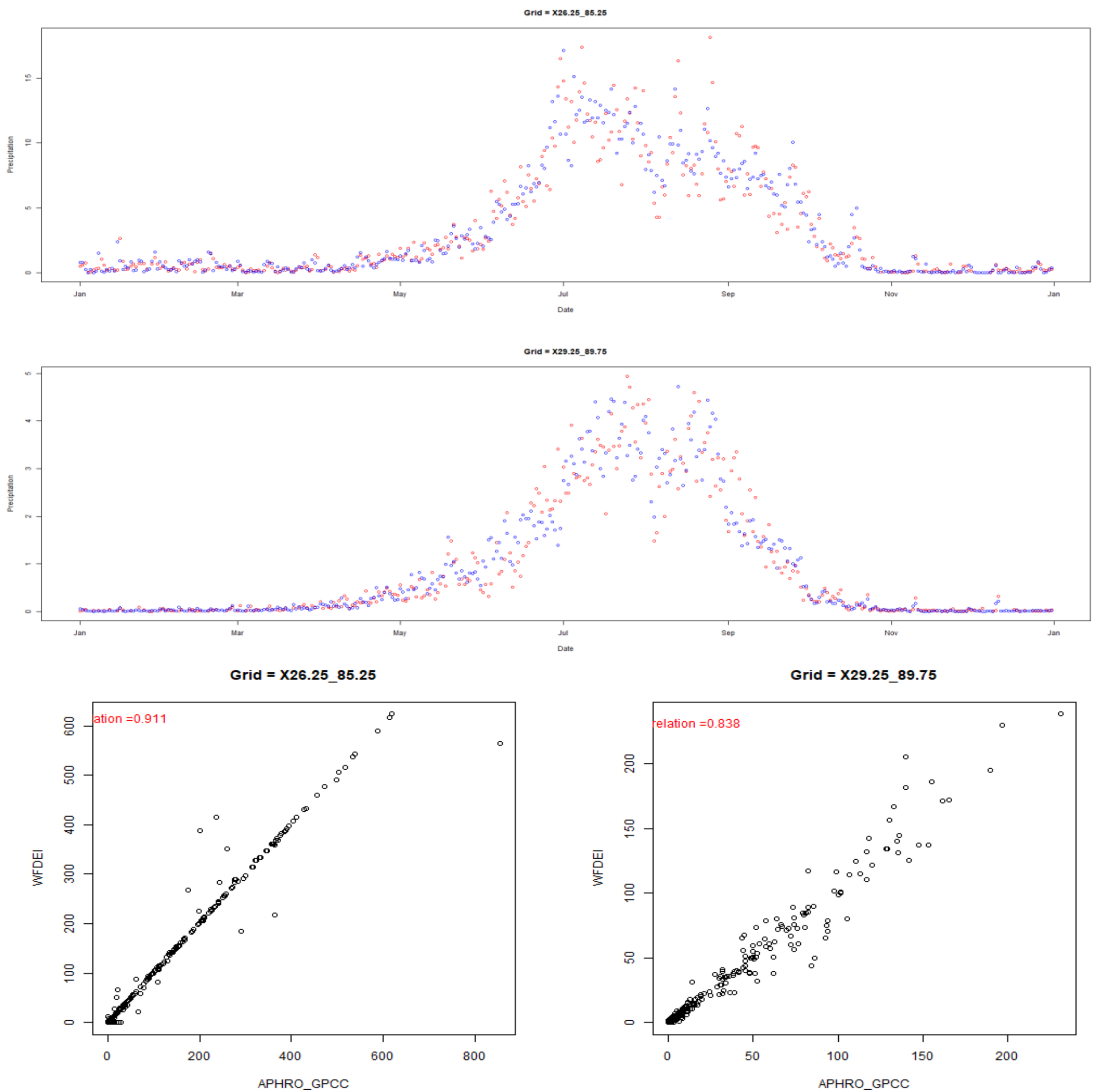


*Figure 32 Comparison of WFDEI (blue) and APHRO_GPCC (red) precipitation dataset presented for two grids that represents different topographic features. The figure indicates that precipitation pattern estimates from the two datasets are similar. The analysis adds supports the suitability of APHRO_GPCC dataset for precipitation. Analysis of WFDEI time series indicates that there is no significant change in precipitation post 2007 (not shown here). APHRO_GPCC data 1961-2007 represents the historical precipitation in the basin and its use is suitable for the development of the hydrologic model.*

**Data Analysis: Temperature**

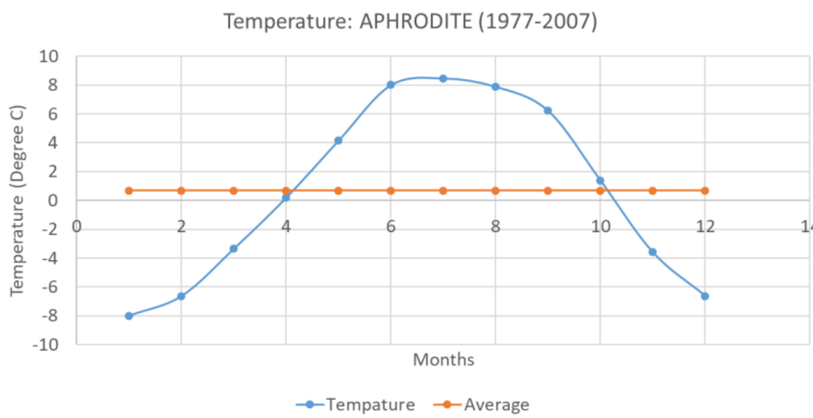


*Figure 33 Monthly basin average temperature in Upper Arun Basin APHRODITE data (1997-2007)*

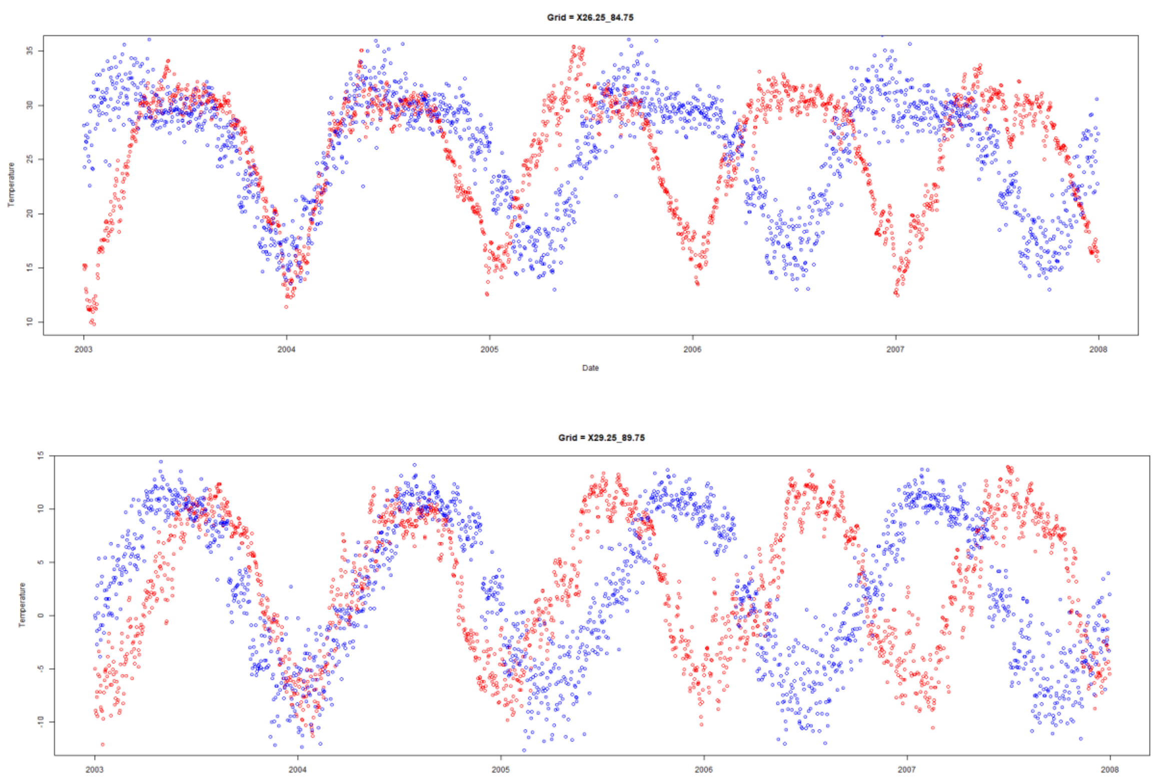


*Figure 34 Comparison of WFDEI (blue) and APHRO_GPCC (red) temperature dataset presented for two grids that represents different topographic features indicate that the WFDEI dataset does not capture the temperature variation and seasonality in the basin.*

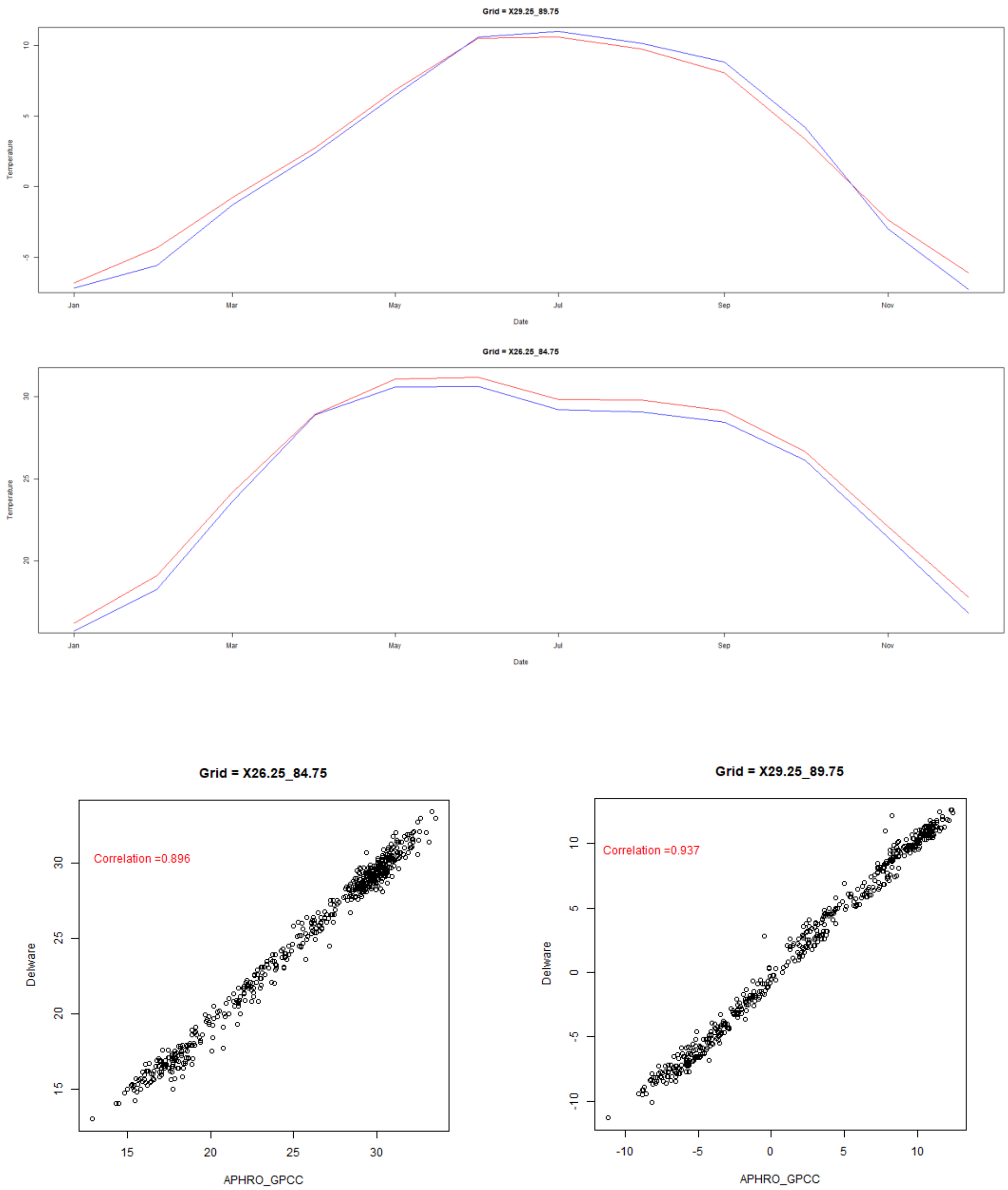


*Figure 35 Comparison of Delaware (blue) and APHRODITE (red) temperature dataset presented for two grids that represents different topographic features indicate that the pattern is similar. The analysis adds supports the suitability of APHRO_GPCC dataset for temperature. Analysis of Delaware monthly time series indicates that there is no significant change in precipitation post 2007 (not shown here). APHRODITE data 1961-2007 represents the historical temperature in in the basin, and its use is suitable for the development of the hydrologic model.*

## Data Analysis: Glacier

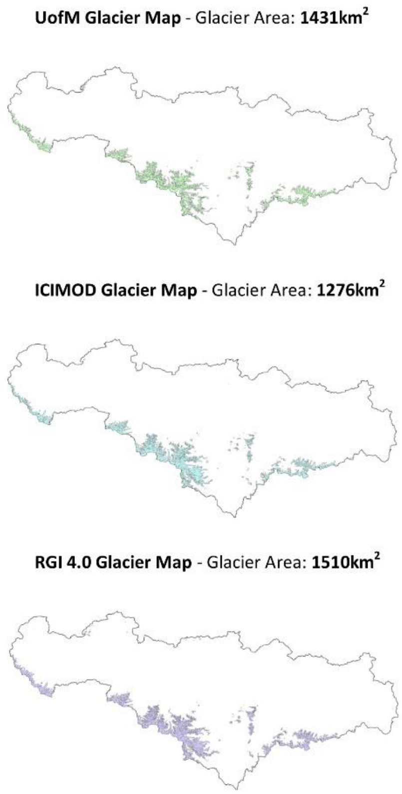


Glacier volume scaling relationship (Grindsted, 2013)

| | Scaling relationships |
|---|---|
| Ice caps | $V = 0.0552\,R^{0.124}\,A^{1.20}$ |
| | $V = 0.0432\,A^{1.23}$ |
| Glaciers | $V = 0.0413\,R^{-0.0565}\,A^{1.3}$ |
| | $V = 0.0433\,A^{1.29}$ |

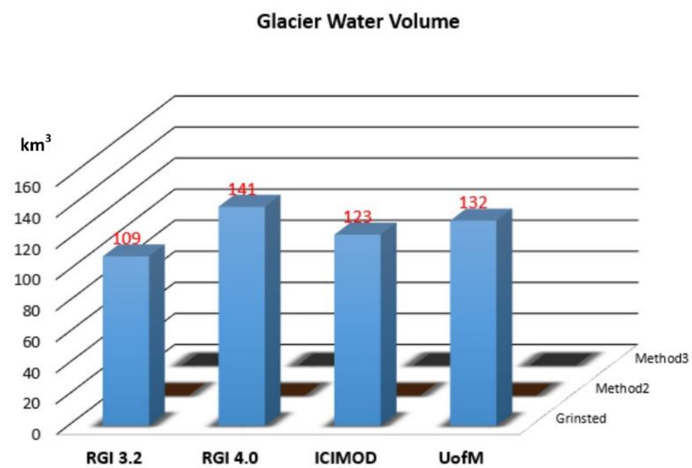


*Figure 36 Comparison of different glacier data and methods for estimation of Glacier Volume (Credit: Sungwook Wi). These methods provided different glacier area estimates. Randolph Glacier Inventory 3.2 was chosen to be the most suitable for the basin and is used in this analysis.*

**Data Analysis: Streamflow**

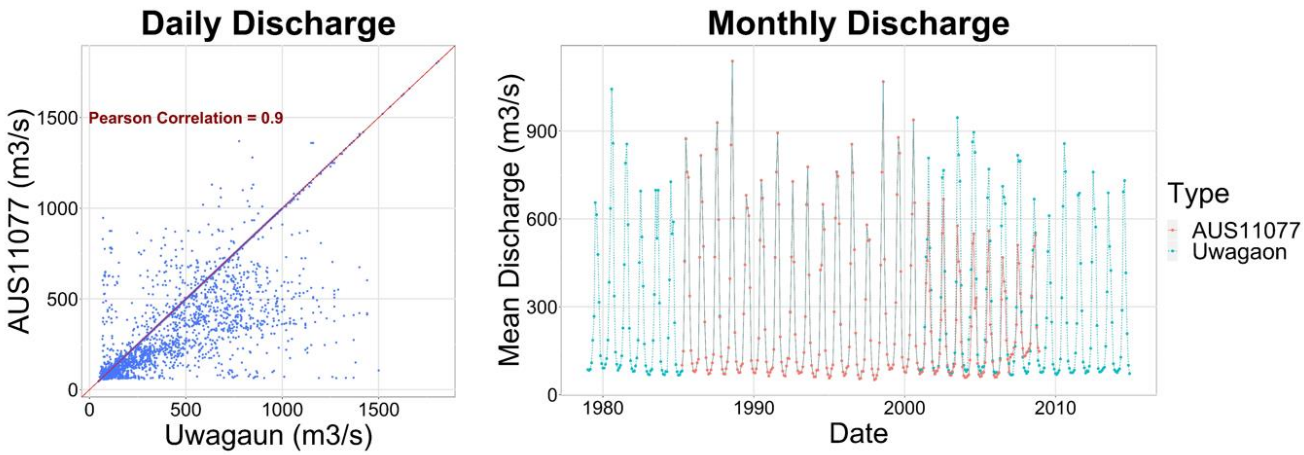


*Figure 37 Comparison of the discharge data used in AUS11077 (red), and the Uwagaon data (blue). Correlation of Daily discharge (left) and Time Series of monthly discharge (right). The streamflow data used in AUS11077 seems to be decreasing gradually after 2001. The Uwagaon data is used in throughout this analysis.*

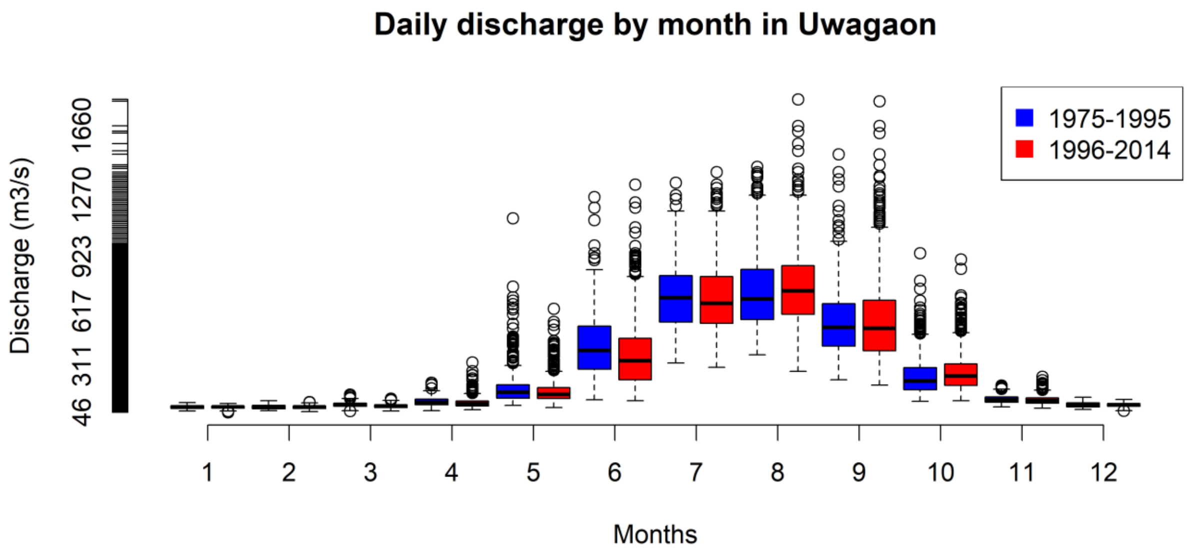


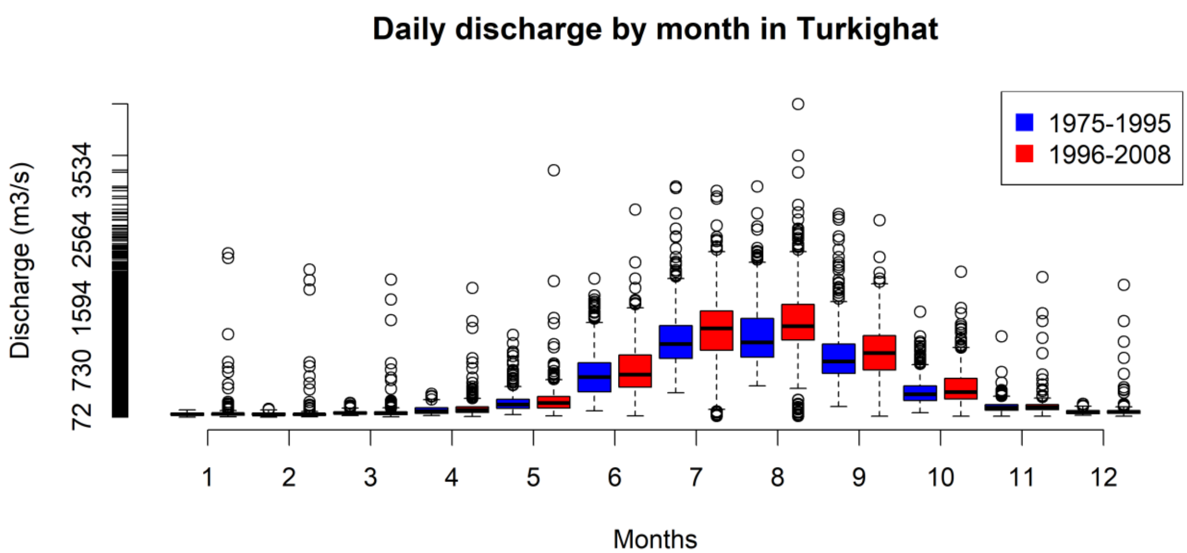


*Figure 38 Comparison of hydrographs of Uwagaon and Turkighat Station in the Upper Arun basin before and after 1995. We observe high flows responding to the Indian Summer Monsoon rainfall between July-October. A prominent increase in the flows during September and October is observed in Uwagaon station. A similar increase in observed in Turkighat station (although not as prominent). As such pattern is not observed in the precipitation stations (Figure 28), the changes in hydrographs could be because of changes in snow and glacier melt patterns.*

*Table 8 Trend analysis of maximum annual discharge in Uwagaon and Turkighat stations*

| | |
|---|---|
| 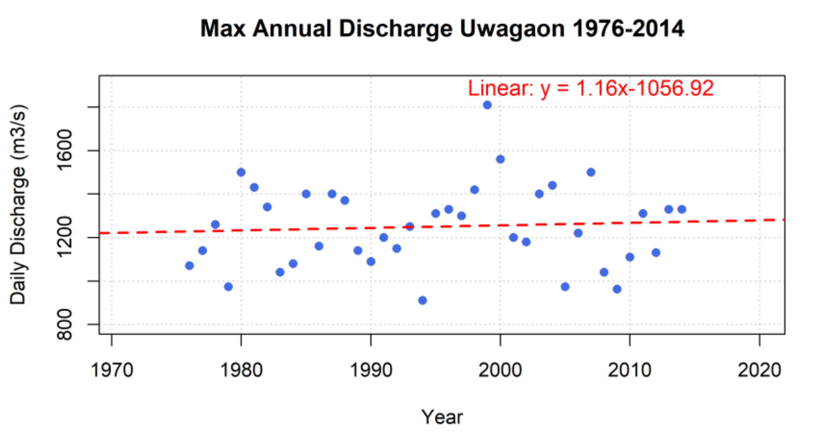 | Mann-Kendal trends in the annual maximum discharge<br><br>Sen's Slope[1]: 1.67<br>P-value[1]: 0.61<br><br>Sen's Slope[2]: 1.67<br>P-value[2]: 0.54<br><br>Sen's Slope[3]: 0.95<br>P-value[3]: 0.68 |
| 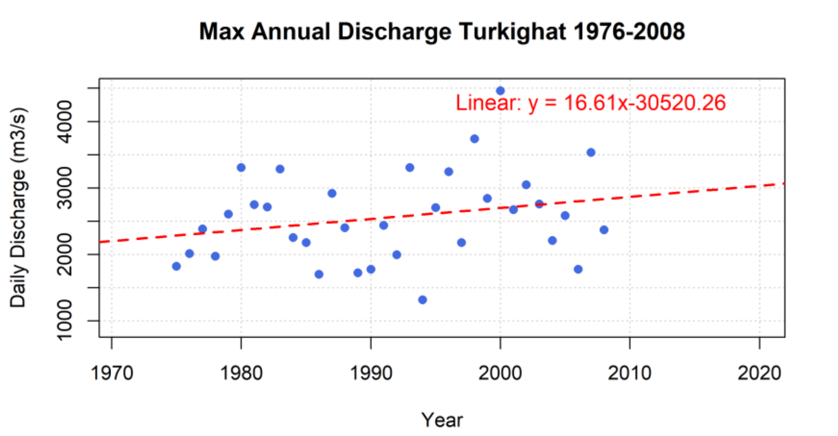 | Sen's Slope[1]: 16.15<br>P-value[1]: 0.23<br><br>Sen's Slope[2]: 16.15<br>P-value[2]: 0.23<br><br>Sen's Slope[3]: 10.82<br>P-value[3]: 0.34 |
| 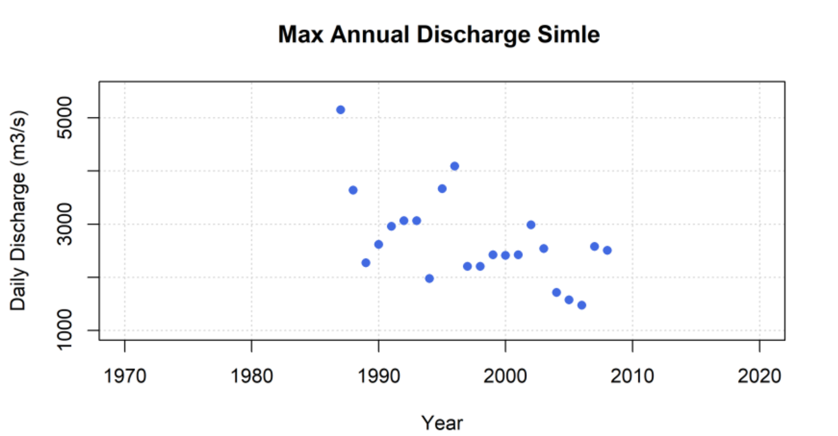 | Poor Data Quality |

[1] MK test: Mann Kendall Test **(Kendall, 1975)**
[2] MK test: Mann Kendall Test with modification to the variance **(Hamed and Rao 1998)**
[3] MK test: Mann Kendall Test with trend free pre-whitening **(Yue et al. 2002)**
**No significant trend is detected in the hydrologic time series.**

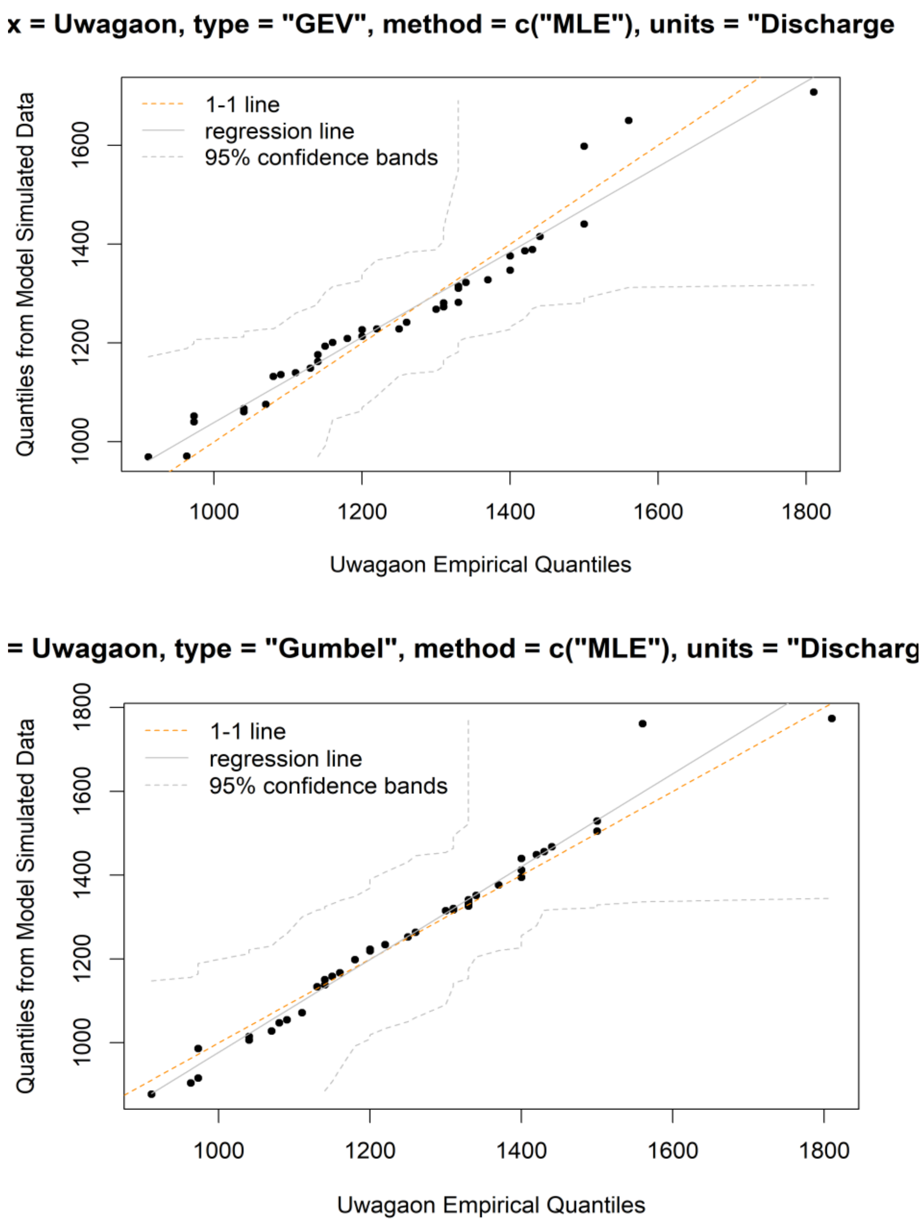


*Figure 39 Fitting a GEV distribution and Gumbel distribution using the maximum likelihood estimation method to the annual maximum flows at Uwagaon station (left and right). AIC of the Gumbel fit and GEV fit was 522.46, and 523.23. Thus, the Gumbel distribution was found to be suitable for estimating the flood frequency in the basin.*

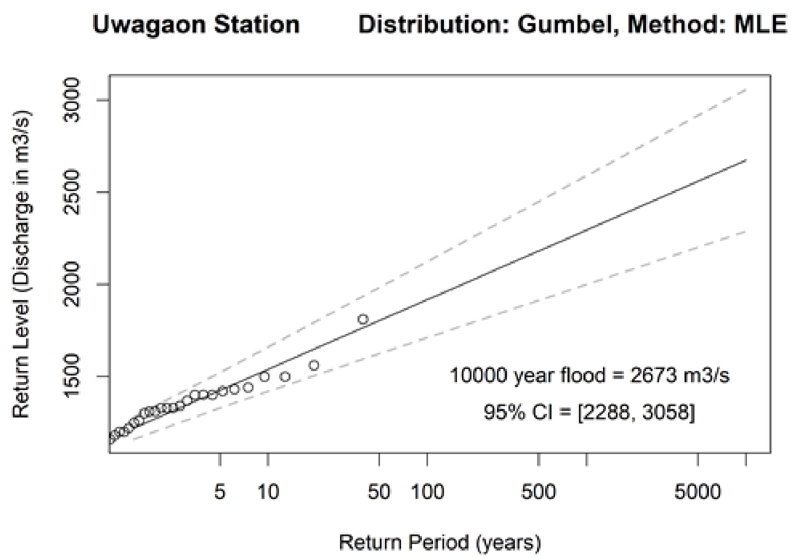


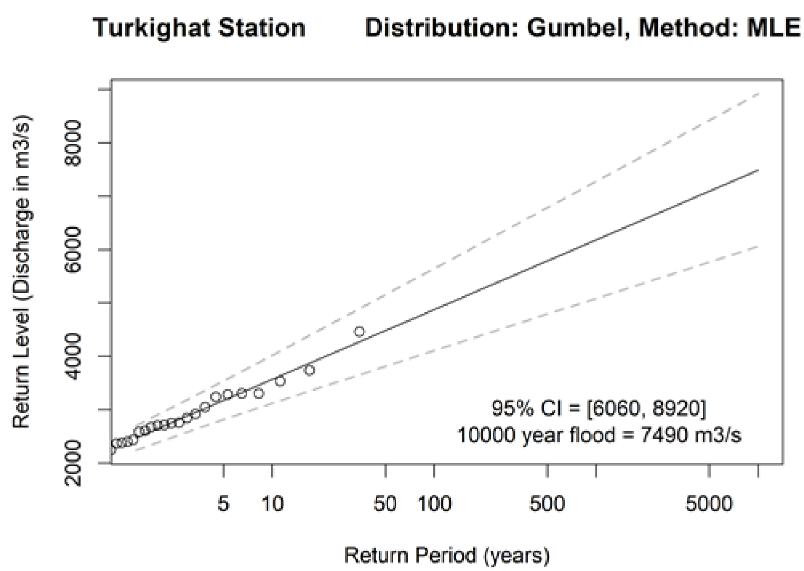


*Figure 40 Fitting Distribution to the annual maximum flood in Uwagaon and Turkighat station. The 10,000 year flood estimates using a Gumbel distribution and the associated uncertainty is highlighted. The 10,000 year flood estimate in Uwagaon station is 2673 m3/s.*

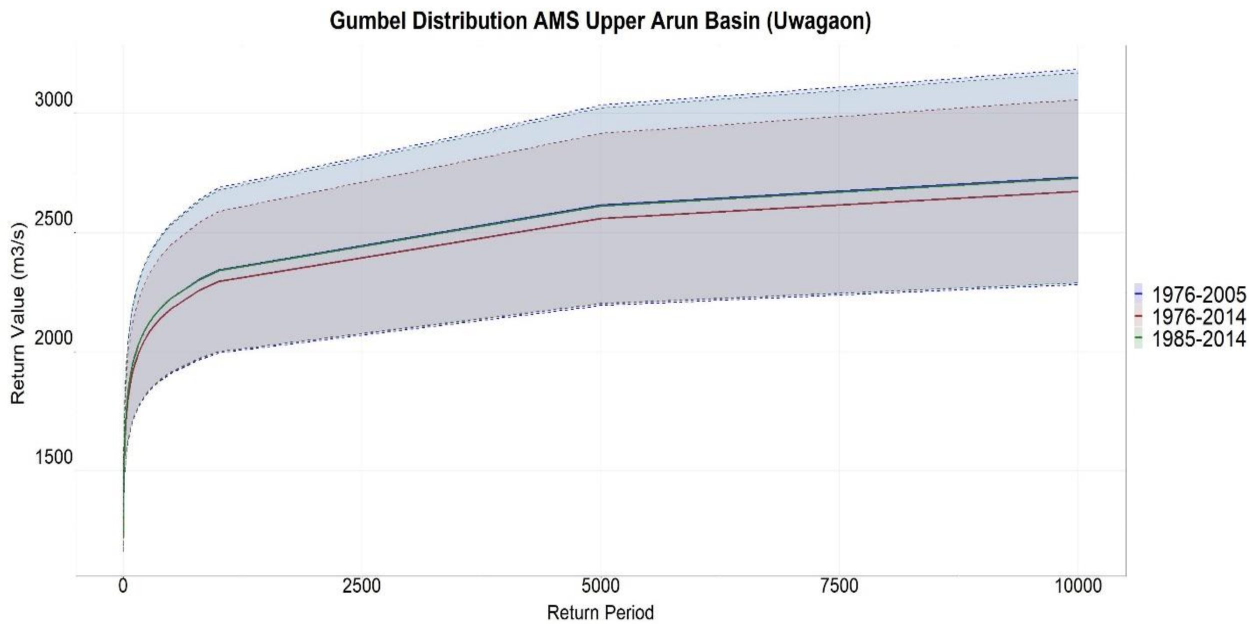


*Figure 41 10,000-year return period of Upper Arun Project (fitted with Gumbel Distribution). We observe an increase in the magnitude of 10,000-year return period flood; however, the uncertainty in the estimates of 10,000-year return period is huge. Hence, is not conclusive if the floods magnitude is increasing in the basin.*

*References:*

1. Yue, S., Pilon, P., Phinney, B., and Cavadias, G. (2002). The influence of autocorrelation on the ability to detect trend in hydrological series. Hydrological Processes, 16(9): 1807–1829. <doi:10.1002/hyp.1095>
2. Hamed, K. H. and Rao, A. R. (1998). A modified Mann-Kendall trend test for autocorrelated data. Journal of Hydrology, 204(1–4): 182–196. <doi:10.1016/S0022-1694(97)00125-X>
3. (Kendall, M. (1975). Rank Correlation Methods. Griffin, London, 202 pp.)

# Annex 4: Evaluation of CORDEX dataset for the Upper Arun Basin (For extreme precipitation)

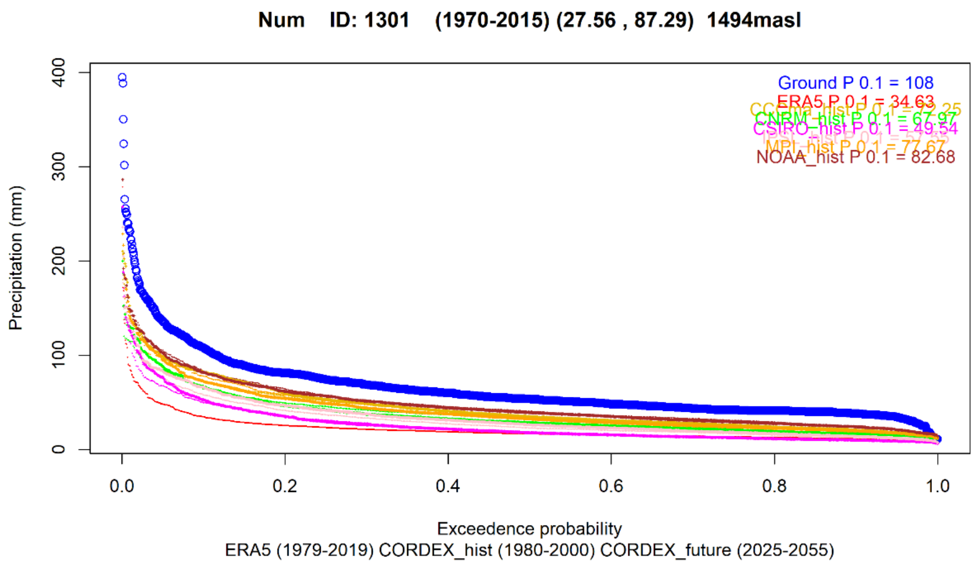


*Figure 42 Comparison of the top 10% precipitation per year between the CORDEX climate projection (multicolored lines) and the ground station Num (Dark blue line) indicate that the CORDEX does not capture the extremes recorded in station Num.*

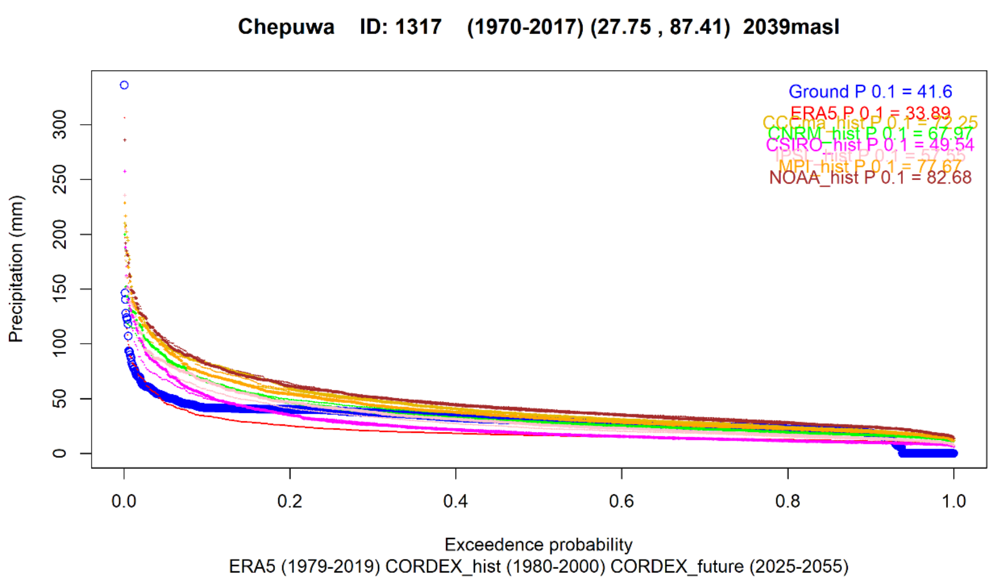


*Figure 43 Comparison of the top 10% precipitation per year between the CORDEX climate projection (multicolored lines) and the ground station Chepuwa (Dark blue line) indicate that the CORDEX captures the extremes recorded in station Chepuwa.*